THESIS

COMPUTATIONAL METHODS FOR DETERMINING EFFECTIVE DISCHARGE IN THE YAZOO RIVER BASIN, MISSISSIPPI

SUBMITTED BY

CHRISTOPHER LEE HOLMQUIST-JOHNSON

DEPARTMENT OF CIVIL ENGINEERING

In partial fulfillment of the requirements for the

Degree of Master of Science

Colorado State University

Fort Collins, Colorado

Spring 2002

TC
175.8
.H67
2002

Colorado State University

NOVEMBER 15, 2001

We hereby recommend that the thesis prepared under our supervision by Christopher Lee Holmquist-Johnson entitled Computational Methods for Determining Effective Discharge in the Yazoo River Basin, Mississippi be accepted as fulfilling in part requirements for the degree of Master of Science.

Committee on Graduate Work

Dr. Chester C. Watson, Advisor

Dr. Christopher I. Thornton

Dr. Ellen E. Wohl

Dr. Sandra L. Woods, Department Head

ABSTRACT OF THESIS

COMPUTATIONAL METHODS FOR DETERMINING EFFECTIVE DISCHARGE IN THE YAZOO RIVER BASIN, MISSISSIPPI

The Demonstration Erosion Control (DEC) project was established to develop, test, and monitor methods and structures used to control flooding, sediment transport, and bank failure in the Yazoo River Basin, located in central Mississippi. Primary methods utilized by the DEC project include grade control structures and flow control reservoirs. Hydrologic data are extremely important in stable channel design, as well as the design of grade control structures.

Prior to the 1960's, it was widely believed that infrequent flow events were responsible for channel formation. In 1960, Wolman and Miller presented evidence against the concept of infrequent events and presented the idea of an effective force. This concept was later termed effective discharge by Andrews in 1980. The definition and determination of effective discharge is often disputed. Bankfull discharge and the two-year discharge have also been associated with the effective discharge. As a result, the determination of effective discharge includes frequency analysis, bankfull analysis, and flood frequency analysis. Determination of effective discharge for the DEC sites would be an important aspect in the design of these methods and structures.

Data obtained from thirteen gauged sites in the Yazoo River Basin were instrumental in the determination of effective discharge. Based on these limited hydrologic records, several methods were developed to determine the effective discharge

at twenty-three study sites within the Yazoo River Basin. Procedures and data were developed to analyze and create flow-duration relationships. Sediment transport relationships were developed for total sediment load and total bed material load for thirteen USGS gauging stations within the DEC watersheds. Effective discharge calculations were made using the following data: 15-minute discharge data, total suspended load, and bed material load.

Calculated effective discharges transported a range of 47% to 67% of the total sediment yield and were within the published error range of $\pm$ 44% of the two-year discharge. The Q_{eff}/Q_2 ratio ranged from 0.4 to 1.2 (μ=0.8, σ=0.4). From the results of this study a general set of guidelines for determining a design discharge for the Yazoo River Basin, Mississippi was developed.

Christopher Lee Holmquist-Johnson
Civil Engineering Department
Colorado State University
Fort Collins, CO 80523
Spring 2002

Acknowledgments

Sincere appreciation and thanks are extended to those who assisted in this study. Special thanks are extended to my advisor, Dr. Chester Watson, for his continuous guidance and technical support throughout the preparation of this thesis. Special thanks and appreciation are extended to my committee members, Dr. Christopher Thornton and Dr. Ellen Wohl, for their insight and critical review of this document

I would also like to thank: Brian McCaig and Alejandro Flores for their assistance in developing the effective discharge program, Jason Christensen and Dana Buchwald for their numerous hours of data collection and analysis, and David Mooney for his friendship and assistance when I needed it most. I thank Ms. Gloria Garza for her assistance on compiling this document. Many thanks are extended to my fellow colleagues at the Engineering Research Center for their support and friendship.

I also would like to thank my family for encouraging me to pursue a higher education and sincerely appreciate their support throughout this study. Finally, a special thanks to my wife, Helen Holmquist-Johnson, for her encouragement, love, and understanding.

TABLE OF CONTENTS

1 Introduction 1
2 Literature Review 5
2.1 Channel-forming Processes 5
2.2 Channel-forming Events 9
2.2.1 Bankfull 10
2.2.2 Frequency 13
2.2.3 Effective Discharge 15
2.3 Effective Discharge Determination using Magnitude-Frequency Analysis 19
2.3.1 Frequency and Bin Size Determination 20
2.3.2 Sediment-rating Curves 25
2.3.3 Product – Effective Discharge 27
2.4 Recent Developments 28
2.5 Previous Effective Discharge Determination for DEC Sites 31
2.6 Summary of Literature Review 32
3 Methods for Determination of Effective Discharge 34
3.1 Yazoo River Basin (DEC) 34
3.1.1 Site Locations 35
3.1.2 Site Characteristics 35
3.2 Analytical Effective Discharge Calculation 38
3.3 Discharge Computations using Regionalized Equations 39
3.4 Effective Discharge Computation using Magnitude Frequency Analysis 41
3.4.1 Flow-frequency Distributions 41
3.4.2 Sediment Rating Curves and Yang's equation 45
3.4.3 Sediment Load Histogram – Effective Discharge 51
3.4.4 Summary 62
3.5 Effective Discharge Program 62
3.5.1 Inputs and Execution of the Program 62
3.5.2 Outputs of the Program 68
4 Analysis of Results 76
4.1 Analytical Effective Discharge Calculations 76
4.2 Sediment Traps 80
4.3 Magnitude Frequency Analysis – Effective Discharge 82
4.3.1 Classification of Problematic Computations 83
4.3.2 Cumulative Sediment Discharge 89
4.4 Effective Discharge Comparison 90
4.4.1 MFA - Logarithmic vs. Arithmetic Distribution 90
4.4.2 Effective Discharge versus Q2 93
4.5 Annual Sediment Yield 94
5 Conclusions and Recommendations 98
5.1 Summary 98
5.2 Conclusions 99
5.3 Recommendations for Further Research 103
6 References 104
Appendix A 109

Appendix B 112
Appendix C 114
Appendix D 137
Appendix E 141

List of Figures

Figure 1.1 – Map of the sixteen DEC watersheds 4

Figure 2.1 – Relationship between discharge, sediment transport, and frequency of occurrence 8

Figure 2.2 – Stream channel cross section (Williams 1978) 12

Figure 2.3 – Flow and sediment frequency distributions for Delaware River at Trenton, New Jersey. 30

Figure 3.1 – Site locations for analysis indicated by numbered pin markers 37

Figure 3.2 – Flow chart for generating flow-frequency distributions (after Soar 2000) .. 42

Figure 3.3 – Flow chart for generating sediment rating curves (after Soar 2000)..... 47

Figure 3.4 – Sediment-discharge data for Abiaca 21 near Cruger..... 49

Figure 3.5 – Comparison of sediment-discharge rating curves for Abiaca 21 near Cruger 51

Figure 3.6 – Flow chart for generating sediment load histograms (after Soar 2000)..... 52

Figure 3.7 – Arithmetic effective discharge plot for Abaica 21 near Cruger (50 bins).... 56

Figure 3.8 – Logarithmic effective discharge for Abiaca 21 near Cruger (50 bins)..... 57

Figure 3.9 – Arithmetic sediment CDF plot for Abaica 21 near Cruger (50 bins)..... 58

Figure 3.10 – Bed material load sediment trap 60

Figure 3.11 – Example input screen for effective discharge program 64

Figure 3.12 – Input screen for sediment transport equation option 66

Figure 3.13 – Input screen for Yang's sand d_{50} sediment transport equation..... 67

Figure 3.14 – Long Creek arithmetic effective discharge plot for 55 bins 69

Figure 3.15 – Long Creek logarithmic effective discharge plot for 55 bins..... 70

Figure 3.16 – Arithmetic percent exceedence plot for Long Creek (55 bins) 73

Figure 3.17 – Sediment yield versus number of bins for Long Creek. 75

Figure 3.18 – Effective Discharge versus number of bins for Long Creek 75

Figure 4.1 – Observed and calculated PDF for Abaica 21 Creek near Cruger 77

Figure 4.2 – Observed and calculated CDF for Abaica 21 Creek. 78

Figure 4.3 – Analytical effective discharge versus calculated 2-year recurrence discharge 80

Figure 4.4 – Plot of observed sediment transport at low flow for Abiaca 6 82

Figure 4.5 – Effective Discharge vs. number of bins for Long Creek 83

Figure 4.6 – Type I sediment load histogram (USGS Long Creek) 84

Figure 4.7 – Type II sediment load histogram (Abiaca 6 near Seven Pines) 85

Figure 4.8 – Type III sediment load histogram (USGS Long Creek) 85

Figure 4.9 – Type IV sediment load histogram (DEC Hotopha Creek) 86

Figure 4.10 – Type V sediment load histogram 86

Figure 4.11 – Cross-section plot of effective discharge 87

Figure 4.12 – Sediment CDF versus Q/Q_2 for bed material load 89

Figure 4.13 –Sediment CDF vs. $EffQ/Q_2$. 90

Figure 4.14 – Discharge bin size vs effective discharge method 91

Figure 4.15 – Skew versus Effective discharge method 92

Figure 4.16 – Effective Discharge versus Q2 for all sites with 44% error band 93

Figure 4.17 – Skewness versus annual sediment yield 97

Figure 5.1 – Flow chart for interpreting the outputs of the effective discharge calculations 101

Figure C.1– Abiaca 21 near Cruger (arithmetic bins) 115

Figure C.2– Abiaca 21 near Cruger (logarithmic bins) 115

Figure C.3– Abiaca 6 near Seven Pines DEC (arithmetic bins) 116

Figure C.4– Abiaca6 near Seven Pines DEC (logarithmic bins) 116

Figure C.5– Abiaca 3 DEC (arithmetic bins) 117

Figure C.6– Abiaca 3 DEC (logarithmic bins) 117

Figure C.7– Abiaca 4 DEC (arithmetic bins) 118

Figure C.8– Abiaca 4 DEC(logarithmic bins) 118

Figure C.9– Batupan Bogue at Grenada (arithmetic bins) 119

Figure C.10– Batupan Bogue at Grenada (logarithmic bins) 119

Figure C.11– Fannegusha DEC (arithmetic bins) 120

Figure C.12– Fannegusha DEC (logarithmic bins) 120

Figure C.13– Halrland 1 DEC (arithmetic bins) 121

Figure C.14 – Harland 1 DEC (logarithmic bins) 121

Figure C.15 – Harland 23 DEC (arithmetic bins) 122

Figure C.16 – Harland 23 DEC (logarithmic bins) 122

Figure C.17 – Harland near Howard (arithmetic bins) 123

Figure C.18 – Harland near Howard (logarithmic bins) 123

Figure C.19 – Hickahala 11 DEC (arithmetic bins) 124

Figure C.20 – Hickahala 11 DEC (logarithmic bins) 124

Figure C.21 – Hickahala 22 DEC (arithmetic bins) 125

Figure C.22 – Hickahala 22 DEC(logarithmic bins) 125

Figure C.23 – Hickahala near Senatobia (arithmetic bins) 126

Figure C.24 – Hickahala near Senatobia (logarithmic bins) 126

Figure C.25 – Hotopha DEC (arithmetic bins) 127

Figure C.26 – Hotopha DEC (logarithmic bins) 127

Figure C.27 – Hotopha near Batesville (arithmetic bins) 128

Figure C.28 – Hotopha near Batesville (logarithmic bins) 128

Figure C.29 – Long DEC (arithmetic bins) 129

Figure C.30 – Long DEC (logarithmic bins) 129

Figure C.31 – Long near Pope (arithmetic bins) 130

Figure C.32 – Long near Pope (logarithmic bins) 130

Figure C.33 – Otoucalofa DEC (arithmetic bins) 131

Figure C.34 – Otoucalofa DEC (logarithmic bins) 131

Figure C.35 – Otoucalofa near Water Valley (arithmetic bins) 132

Figure C.36 – Otoucalofa near Water Valley (logarithmic bins) 132

Figure C.37 – Senatobia DEC (arithmetic bins) 133

Figure C.38 – Senatobia DEC (logarithmic bins) 133

Figure C.39 – Topashaw near Derma (arithmetic bins) 134

Figure C.40 – Topashaw near Derma (logarithmic bins) 134

Figure C.41 – Yalobusha near Derma (arithmetic bins) 135

Figure C.42 – Yalobusha near Derma (logarithmic bins) 135

Figure C.43 – Yalobusha near Vardaman (arithmetic bins) 136

Figure C.44 – Yalobusha near Vardaman (logarithmic bins) 136

Figure E.1 – Abiaca 21 near Cruger 142

Figure E.2 – Abiaca 6 near Seven Pines 142

Figure E.3 – Abiaca 3 143

Figure E.4 – Abiaca 4 143

Figure E.5 – Fannegusha Dec 144

Figure E.6 – Hickahala 11 144

Figure E.7 – Hickahala 22 145

Figure E.8 – Hotopha Dec 145

Figure E.9 – Long Dec 146

Figure E.10 – Senatobia at Senatobia 146

List of Tables

Table 2.1 – Bankfull definitions presented by Williams (1978) 13

Table 2.2 – Type of class interval and number of classes used to calculate effective discharge in a selection of studies (after Soar, 2000) 20

Table 2.3 – Classification of the total sediment load for a sand bed stream 25

Table 2.4 – Classification of the total sediment load for a gravel bed stream 25

Table 3.1 – USGS and DEC study site locations and site characteristics 36

Table 3.2 – Period of record for USGS and DEC sediment data 48

Table 3.3 – Arithmetic sediment load histogram for Abiaca 21 near Cruger 54

Table 3.4 – Logarithmic sediment load histogram for Abiaca 21 Creek near Cruger 55

Table 3.5 – Discharge input file for Senatobia Creek 63

Table 3.6 – Effective discharge data sheet for Long Creek (55 arithmetic bins) 71

Table 3.7 – Arithmetic percent exceedence data sheet for Long Creek 72

Table 3.8 – Summary data sheet for Long Creek 74

Table 4.1 – Discharge frequency distribution for Abiaca 21 Creek near Cruger 77

Table 4.2 - Analytical effective discharge for each site 79

Table 4.3 – Suspended and bed load concentrations for Fannegusha Creek 81

Table 4.4 – Results of effective discharge calculations using 50 bins 88

Table 4.5 – Qeff/Q2 ratio for each site 94

Table 4.6 – Annual sediment yield for each site 95

Table 4.7 – Average sediment yield characteristics for each site. 97

Table 5.1 –Effective discharge results for the Yazoo River Basin, Mississippi 102

Table A.1 – Logarithmic flow frequency class size computation for Abiaca21 110

Table A.2 – Arithmetic flow frequency class size computation for Abiaca21 111

Table B.1 – Sediment rating coefficients for each site 113

Table D.1 – Inputs for Effective Discharge Program 138

Table D.2 – Channel coefficients for use with SedTrans Program..... 140

1 INTRODUCTION

The United States Army Corps of Engineers (USACE) established the Demonstration Erosion Control (DEC) Project in 1984 to develop and test systems for controlling sediment, flooding, and general channel stability improvements for selected stream sites in the Yazoo River Basin in Mississippi. Since the beginning of the DEC Project, many features have been utilized to accomplish DEC goals, including: grade control structures, pipe drop structures, flow control reservoirs, and bank stabilization measures. Colorado State University currently monitors 33 DEC sites within 16 basins in the State of Mississippi. Figure 1.1 presents the locations of the watersheds presently being monitored. The majority of the DEC sites have limited hydrologic data available or are ungauged. Because of the limited availability of hydrologic data for the Yazoo River Basin, additional methods for the determination of project hydrology must be used in order to aid in the continued design of channel stability improvements.

Determination of project hydrology is an essential step for the design of stable channels and grade control structures. Design of these structures and the channel systems must be analyzed and constructed to withstand the hydrological elements and change in channel form. To design these systems, engineers must be able to understand system changes, such as variations in channel form; and causes of these changes, such as variations in the channel flow and resulting sediment transport. The concept of a channel-forming discharge is closely related to the concept of dynamic-equilibrium, which is characterized by fluctuations of channel form around an average condition

through time. Soar (2000) states that the channel-forming flow or dominant discharge is a geomorphological concept and not a measurable parameter. However, there are three definable flows that have been used to represent the dominant flow based on the application of repeatable geomorphological and hydrological techniques: bankfull discharge, flow of a specified recurrence interval, and effective discharge. The focus of this study is based on the third technique, effective discharge, and will use the other techniques for comparisons.

Effective discharge is defined as that increment of discharge that transports the largest fraction of sediment load over a given period of time (Andrews, 1980). The general procedure for determining the effective discharge incorporates a Magnitude-Frequency Analysis (MFA) based on the concepts and definitions presented by Wolman and Miller (1960) and Andrews (1980). Measurements of sediment discharge and water discharge are needed to develop frequency of occurrence and sediment transport curves. Ideally, gauge-defined water discharge and sediment discharge would exist at each site. However, most channel stabilization projects involve unstable stream sites; therefore, it is unlikely any gauges will exist. Effective discharge determination would aid in the design of these projects and features.

Objectives of this study are to present a computational procedure for further investigation and development of the effective discharge for each of the DEC monitoring sites based on the limited, available hydrologic data obtained from the U.S. Geological Survey (USGS) gauging stations within the Yazoo River Basin. The procedure would be applicable to the Yazoo River Basin and should be widely applicable as a necessary

component of stable channel design. The following tasks were developed to accomplish the project objectives:

- develop a computational procedure for determining effective discharge for the DEC monitoring sites based on limited available hydrologic data;
- determine the effective discharge at gauged sites in the Yazoo River Basin using various computational methods: MFA, two year recurrence interval (Q_2), and an analytical effective discharge equation (Nash 1994);
- investigate how the results of the effective discharge calculations change based on methods used, arithmetic vs. logarithmic, and number of bins used in classification;
- investigate flow duration and annual sediment yield when calculating effective discharge; and
- better define the type of sediment transported at low flows in the Yazoo River Basin and the effects that the type of sediment has on the effective discharge calculations.

Chapter 2 presents the literature review of effective discharge definitions and methods of effective discharge determination. Chapter 3 discusses the methodology used for determining effective discharge in this study. Chapter 4 presents the analysis of results. Conclusions and recommendations are discussed in Chapter 5.

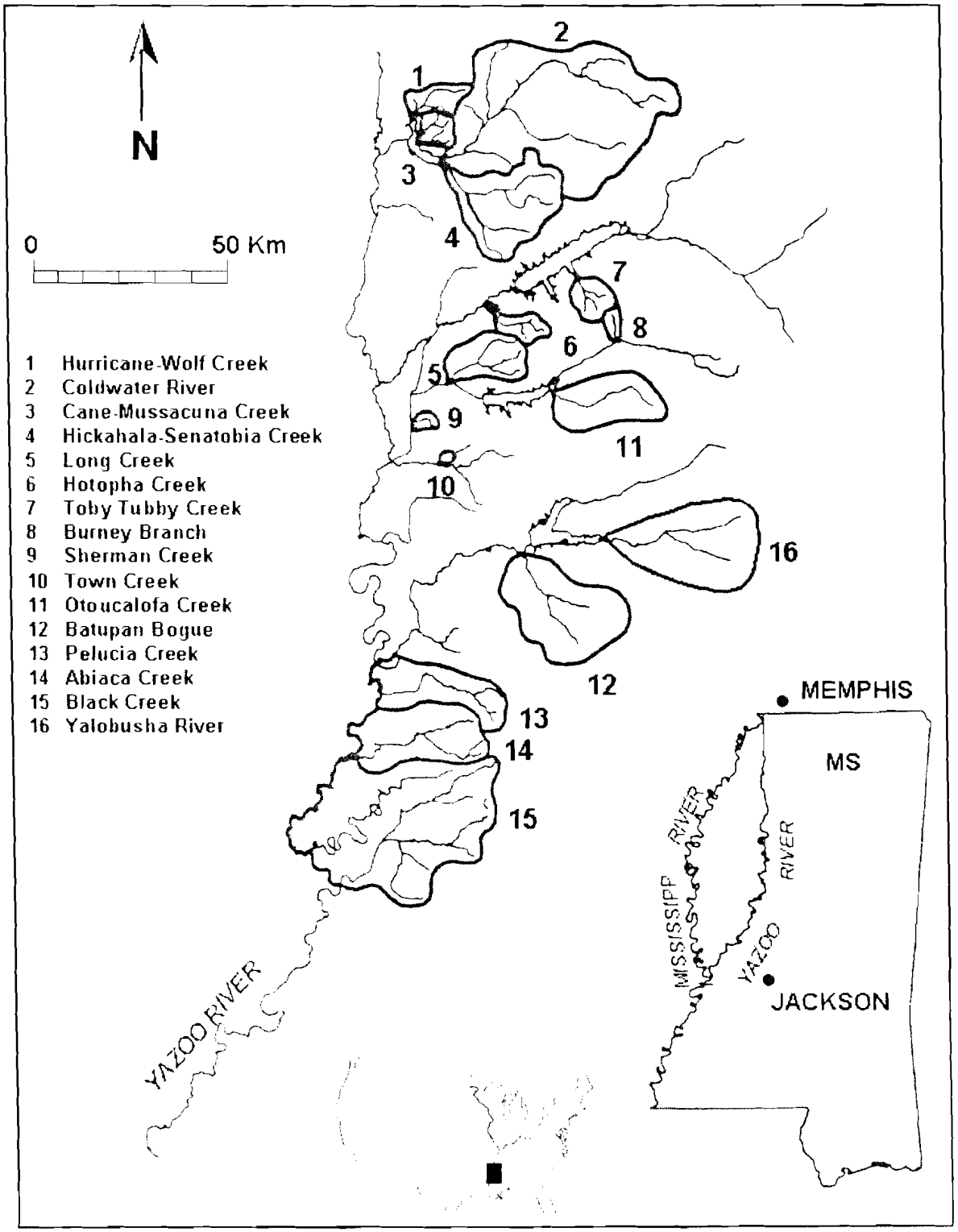

Figure 1.1 – Map of the sixteen DEC watersheds

COLORADO STATE UNIV LIBRARIES

2 LITERATURE REVIEW

A literature review was conducted to examine channel-forming processes and definitions related to channel formation and effective discharge. The following sections review effective discharge definitions and methods associated with them.

2.1 Channel-forming Processes

The process in which river channels are formed is a simple concept based on equilibrium between the hydrologic characteristics of the river basin and the hydraulic parameters of the channel. Although the concept of channel equilibrium is basic, the processes that occur within the river system to reach equilibrium are extremely complex. River systems are constantly changing their channel form in order to transport the amount of sediment and water that is being introduced into the system. Depending on the frequency of the flows and the amount of sediment being transported, the channel form may change simply by formation of bars and meanders as a result of low flows. On a larger scale, the entire channel may be affected, resulting in the complete migration and reforming of the channel as a result of more catastrophic flow events.

It was initially believed that the infrequent flow events of immense magnitude were the most effective in the progressive formation of river channels. However, Wolman and Miller (1960) observed that although this belief might be supported by numerous observations of catastrophic events such as large floods, the catastrophic events are not necessarily responsible for the formation and development of landforms. Their

COLORADO STATE UNIV. LIBRARIES

evidence showed that evaluation of the effectiveness of a specific mechanism and importance of different geomorphic processes in channel formation involves the frequency of occurrence as well as the magnitude of the events. Therefore, the effectiveness of an event, in terms of the amount of work done on the channel, is measured by the magnitude and the frequency with which it occurs (Wolman and Miller, 1960). The relative amount of work performed by events with a given magnitude and frequency is measurable in part by the comparison of the amount of total sediment transported by the individual events.

Movement of sediment is essentially dependent upon the shear forces present in the channel for a given flow. Based on the channel geometry and resulting flow characteristics within the channel, sediment is transported from the bed and banks as a result of the shear stresses between the sediment particles and forces associated with a given flow. Generally, as the magnitude of a flow event increases, the amount of sediment transported also increases as a result of the increase in shear stress present in the channel. A relationship between discharge and sediment transport can be described by the following equation:

$$Q_s = aQ^b \qquad \text{Equation 2.1}$$

where:

Q_s = sediment discharge;

a = scale factor coefficient;

Q = discharge; and

b = shape factor coefficient.

From Equation 2.1, it is evident that as discharge increases, sediment discharge increases exponentially. As a result, the infrequent high-magnitude events transport sediment at the highest rate and do the most work on the channel per event. However, these events may occur so infrequently that there is a relatively small impact on the shape and formation of the channel over a long period of time. Conversely, the frequent low-magnitude events transport sediment at a much lower rate and, although only minor work is done on the channel, over a long period of time these flows transport a large amount of sediment because of their high frequency of occurrence. Leopold (1994) suggested that there is an intermediate discharge that is both sufficiently frequent and effective to do the most work on the channel, and be most important in channel formation and maintenance.

Figure 2.1 depicts the relationship between sediment transport, frequency, and magnitude. The maximum of the product of the frequency-of-occurrence curve and the sediment-transport curve is the discharge at which the greatest amount of work is done. The peak of curve C from Figure 2.1 represents the discharge that is most effective in transporting sediment over a period of time. Wolman and Miller (1960) observed that the relative proportions of sediment carried by flows of various magnitudes differ considerably in different rivers. However, they also observed that for both humid and semiarid regions, the greatest part of the total sediment removed from the drainage basins was carried by small to moderate flows and not by catastrophic floods.

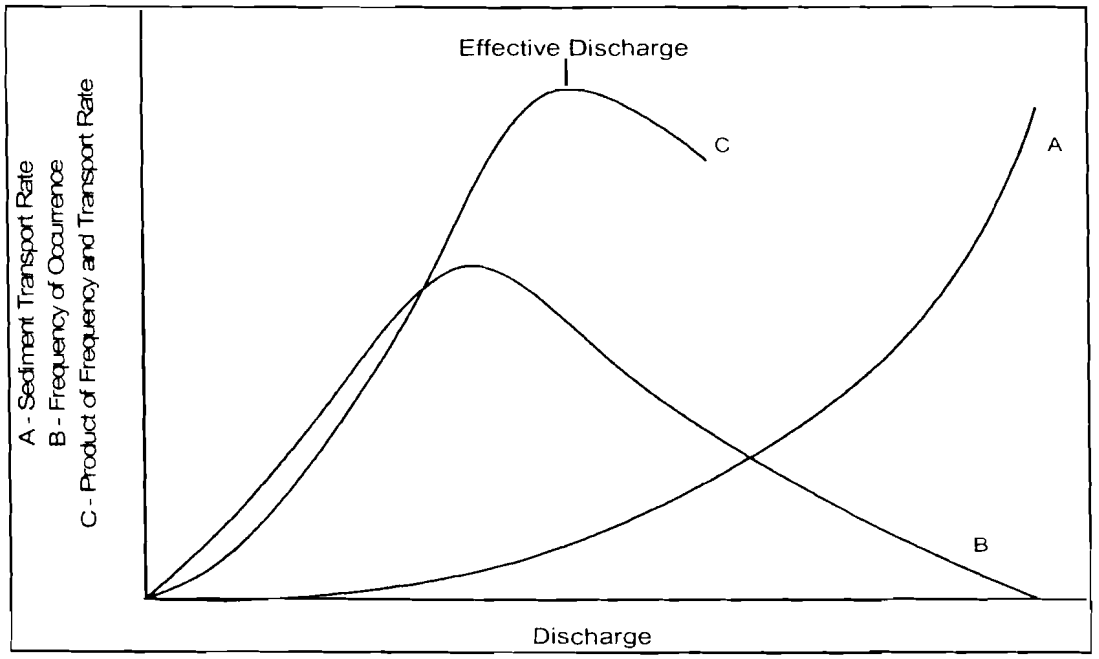

Figure 2.1 – Relationship between discharge, sediment transport, and frequency of occurrence

Mackin (1948) stated that the dimensions of a dynamically stable river must be delicately adjusted to the sediment balance so that over the medium-to-long term, sediment inputs and outputs are balanced. This was demonstrated by Wolman and Miller (1960), who showed that rivers adjust the bankfull capacity to the flow that transports the greatest quantity of sediment load over a period of years, or the flow which expends the greatest amount of geomorphic work per unit time. Wolman and Gerson (1978) stated that although high-magnitude low-frequency events can impart a marked change to the morphology in the short term, in the medium- to long-term the long duration of lesser flow events may allow the river to recover an average morphological condition. This was demonstrated by Wolman and Miller (1960), who found that approximately 90 percent of the total suspended load in alluvial rivers is transported by flows recurring more frequently than once every five years. Where sediment is mobilized at very low discharges (silt and fine sand bed streams) and/or if there is an abundant sediment supply,

the low-magnitude, high-frequency flows tend to be the most effective in doing work on the channel (Hey, 1975). Conversely, in arid and semi-arid basins where the frequencies of rainfall events are very low and base flow is often non-existent, the channels tend to adjust bankfull capacity to accommodate each storm event. As a result, because the channels tend to change shape only during these infrequent storm events, there does not appear to be a particular discharge that accounts for an average morphological condition because the channels are constantly changing.

2.2 Channel-forming Events

Wolman and Miller (1960), Hey (1975), Mackin (1948), and many other researchers have demonstrated that the dominant controls of channel form and channel maintenance are linked to discharge and sediment load. Knighton (1984) states that in a natural river, these independent variables integrate the effects of local climate, vegetation, soils, geology, and overall basin physiography. Because both discharge and sediment load vary significantly over space and time, the application of an appropriate design discharge is critical for long-term channel stability. The problem that has plagued researchers for many years is the definition of the design discharge. It was first thought that the bankfull discharge should be used as the design discharge, but this posed the problem of defining bankfull. A discharge of a prescribed recurrence interval was another definition that was used to define the design discharge. Wolman and Leopold (1957) found that the bankfull discharge had a recurrence interval of one to two years. As a result, many researchers also used the two-year discharge as the design discharge. Wolman and Miller's concept of effectiveness, based on magnitude and frequency of flows, and total sediment transported, was also used in determining the design discharge.

The concept of effectiveness based on magnitude, frequency, and sediment transport was later termed the effective discharge by Andrews (1980). Doyle et al. (1999) demonstrated from three rivers in the U.S. that the effective discharge should be used in preference to other methods and concluded that the effective discharge is the most critical geomorphic and hydraulic parameter in channel design. As Tilleard (1999) noted, the effective discharge concept provides a relationship between the hydrologic characteristics of the basin, the hydraulic characteristics of the channel, and the geomorphic characteristics of the project reach.

With the increasing availability of flow records and computational capabilities, effective discharge can be readily calculated following field reconnaissance during the early stages of project design. There are three possible approaches to determining the channel-forming discharge: bankfull discharge, flow of a given recurrence interval, and effective discharge. Soar (2000) stated that the method used should have general applicability, the capability to be applied consistently, and integrate the physical processes responsible for determining the channel dimensions. Of the three possible approaches listed above, only the effective discharge has the potential to meet these requirements.

The various methods used in determining a design discharge for a river vary concerning definition, magnitude, and frequency. The following sections discuss the definitions concerning and relating to effective discharge.

2.2.1 Bankfull

Bankfull discharge is the basis of estimating meander parameters, unfortunately there are a wide variety of definitions for bankfull discharge that provide a range of values and result in the actual selection of bankfull discharge being very subjective. The

bankfull discharge, corresponding to the bankfull depth, is often considered to be the channel-forming discharge and has been shown to occur with the frequency of about one to two years (Leopold et al., 1964). In addition to the obvious hydraulic significance, downstream hydraulic geometry and stream restoration designs are generally based on bankfull depth, width, and discharge (Rosgen, 1994). Although the determination of bankfull elevation may initially seem trivial and straightforward, the estimation of the bankfull flow condition in the field is often a difficult and subjective measurement.

To quantify the uncertainties in estimating bankfull discharge, an acceptable definition or set of definitions of the bankfull condition must first be established. The bankfull depth from which bankfull discharge is determined is very sensitive to the selection of bankfull elevation and the subjective nature of choosing bankfull elevations can yield a range of results, depending on the observer. As a result of the subjectivity and vagueness in the determination of bankfull elevation, various studies have resulted in the formulation of different methods to define bankfull discharge. These methods vary by using different exceedence frequencies for bankfull and by recognizing different features present in natural stream channels. Williams (1978) presented a stream channel cross section depicting the characteristic active channel, active floodplain, terrace areas, and the inter-relation of the bankfull conditions to these features, as shown in Figure 2.2. Although this figure is simplistic in nature, the variability of each feature in a field condition is quite dynamic and can account for a large degree of uncertainty in the estimation of bankfull discharge.

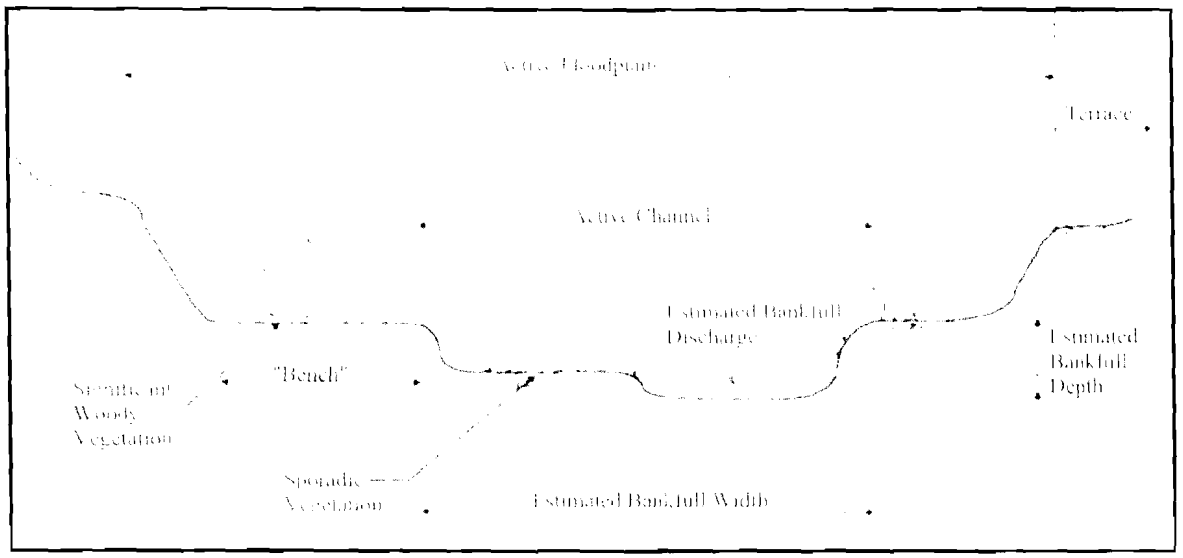

Figure 2.2 – Stream channel cross section (Williams 1978)

Various concepts of the term bankfull and bankfull discharge appear in scientific literature and are closely intertwined with the definitions of river floodplains and benches. In 1978, Williams investigated eleven different definitions of bankfull elevation determined by numerous scientists and engineers. The various definitions of bankfull elevation required recognition of sedimentary surfaces, observations or measurements of boundary features, and measured cross sections. Eleven definitions of bankfull elevation presented by Williams (1978) are listed in Table 2.1.

Williams states that the eleven different ways of defining bankfull elevation could give as many as eleven different bankfull levels at the same stream cross section. It is therefore very important that investigators continue to specify which definition of bankfull elevation or floodplain they are using.

Table 2.1 – Bankfull definitions presented by Williams (1978)

1	The height of the valley flat – Nixon (1959a)
2	The elevation of the active flood plain - Wolman and Leopold (1957)
3	The elevation of the lowest bench – Schumm (1960)
4	The elevation of the "middle bench" for rivers having three or four overflow surfaces – Woodyer (1968)
5	The elevation of the most prominent bench - Kilpatrick and Barnes (1964)
6	The average elevation of the highest surfaces of the channel bars - Wolman and Leopold (1957)
7	The height of the lower limit of perennial vegetation – Schumm (1960)
8	The elevation of the upper limit of sand sized particles in the boundary sediment – Nunnally (1967)
9	The elevation at which the width/depth ratio of the cross section becomes a minimum – Wolman (1955)
10	The stage corresponding to the first maximum of the Riley bench index – Riley (1972)
11	The stage corresponding to a change in the relation of cross sectional area to top width – Williams (1978)

Based on data that were obtained from twenty-eight gauged sites in the United States, Williams concluded that the active floodplain, minimum width-to-depth ratio, Riley bench index, and area vs. width relations were the best definitions for determining the bankfull elevation. Williams also concluded that the rating curve approach involving a survey of the entire reach is the recommended method to estimate bankfull discharge at a gauged site.

2.2.2 Frequency

Discharges of a selected frequency or recurrence interval are often used to describe channel-forming events such as bankfull, dominant, and effective discharge. Numerous studies (Biedenharn et al., 1987; Wolman and Leopold, 1957; Andrews, 1980; Hey, 1975; Orndorff and Whiting, 1999) have shown that the bankfull, dominant, and effective discharge may have recurrence intervals ranging from one to five years, but the

recurrence interval can vary among the three discharges quite dramatically depending on the drainage basin characteristics. Wolman and Leopold (1957) suggested that the bankfull discharge has a recurrence interval of one to two years. Leopold (1994) found that most investigators determined that the recurrence interval for bankfull discharge ranges anywhere from one to two-and-a-half years. However, Pickup and Warner (1976) found that the recurrence interval could range anywhere from four to ten years. Recurrence interval for the bankfull discharge varies dramatically because of different basin characteristics as well as the numerous definitions used in determining the bankfull discharge, as stated previously. Bankfull, dominant, and effective discharge have often been used interchangeably by numerous researchers in their determinations of a channel-forming discharge. Although these terms are used interchangeably, this does not mean that each term has the same recurrence interval. Andrews (1980) reported that the effective discharge for the Yampa River Basin had a recurrence interval from 1.18 to 3.26 years. In addition, Pickup and Warner (1976) found the return period of the effective discharge for a study in the Cumberland Basin was between 1.15 and 1.45 years. Furthermore, Biedenharn et al. (1987) demonstrated close agreement between the two-year discharge (Q_2) and the effective discharge for the Mississippi River, Red River, and Pearl River; and Watson et al. (1997) confirmed this similarity for ten streams in northern Mississippi. More recently, as stated in Soar (2000), Orndorff and Whiting (1999) calculated the recurrence interval of the Red River in Idaho as 1.46 years, which is very close to the average bankfull frequency suggested by Hey (1975). Although the recurrence intervals for bankfull and effective discharge are similar in range, it appears that the bankfull recurrence interval tends to be higher than that of the effective

discharge. Although the recurrence interval is not usually used in determining the effective discharge, it is widely used in comparing the results of the effective discharge calculation with that of other methods used in determining the channel-forming flow.

2.2.3 Effective Discharge

Andrews (1980) defined the effective discharge to be the discharge that transports the largest increment of annual sediment load over a given period of time. His definition follows the concepts presented by Wolman and Miller (1960) and incorporates sediment discharge, water discharge, and frequency of occurrence in determining the effective discharge. Figure 2.1 illustrates Andrews' concept of effective discharge using sediment transport and frequency of occurrence curves to determine the maximum product, which defines the effective discharge. The general procedure for determining the effective discharge is computed using the concepts and definitions presented by Wolman and Miller (1960) and Andrews (1980). Ideally, continuous measurements of sediment discharge and water discharge are needed in order to develop the frequency of occurrence and sediment transport curves. From these curves, taking the product of the two curves develops a third relationship, a product curve. The discharge relating to the maximum or peak of the product curve represents the effective discharge (Figure 2.1).

For example, Andrews (1980) calculated the effective discharge for fifteen gauging stations in the Yampa River Basin in Colorado and Wyoming. Mean daily discharge records were used in the development of the frequency of occurrence curves, and the sediment transport curves were developed using measured instantaneous suspended sediment and adding the bed load discharge, which was computed using Meyer-Peter and Müller's equation for bed load transport. Andrews found that on the

average, the effective discharge was equaled or exceeded 5.8 days per year or 1.6% of the time.

Although Andrews added the calculated bed load transport to the measured suspended sediment load in the development of the sediment transport curves, Biedenharn and Thorne (1994) used only the suspended sediment load in the development of the sediment transport curves for three Mississippi River gauging stations. Biedenharn and Thorne assumed that the total suspended sediment load approximated the total sand load based on the conclusions of Toffaleti's work in 1968. Biedenharn and Thorne determined that the bed load comprised less than five percent of the total sand load based on Toffaleti's calculations and therefore the total suspended sediment load could be assumed to represent the total load in a sand bed stream. As a result, a sediment-discharge relationship was created and a frequency of occurrence curve was developed using recorded mean daily discharge data at each site. From the two curves, the total product curve was developed and the effective discharge was determined using the maximum/peak of the product curve. The results showed that the effective discharge for the three stations along the Mississippi River was equaled or exceeded about thirteen percent of the time or 47.4 days per year.

Nash (1994) also used Andrews' (1980) method of effective discharge determination, but instead of using the MFA to determine the effective discharge, he used a mathematical equation that described the MFA method. Nash (1994) used Equation 2.1 as the sediment transport curve and then used a lognormal distribution curve to determine the frequency of occurrence. Based on average daily discharges, the following relationship was used to describe a lognormal distribution (Salas et al., 2000):

$$f(Q) = \frac{1}{Q\beta\sqrt{2\pi}} e^{\frac{-(\ln Q-\alpha)^2}{2\beta^2}} \qquad \text{Equation 2.2}$$

where:

$f(Q)$ = frequency of occurrence of a given discharge, Q;

$ln\ Q$ = natural logarithm of discharge;

α = mean of the natural logarithm of discharge; and

β = standard deviation of the natural logarithm of discharge.

Nash (1994) refers to a transport effectiveness function, which is determined by the product of Equations 2.1 and 2.2. Transport effectiveness, E, is determined as follows:

$$E = \frac{aQ^b}{Q\beta\sqrt{2\pi}} e^{\frac{(\ln Q-\alpha)^2}{2\beta^2}} \qquad \text{Equation 2.3}$$

where (aQ^b) simply describes the transport rate of Equation 2.1.

The peak of the product curve or transport effectiveness curve represents the effective discharge. Effective discharge is determined mathematically by setting the derivative of Equation 2.3 to zero with respect to Q and solving for Q (Nash, 1994). Therefore, the following equation was used by Nash to determine effective discharge, Q_e:

$$Q_e = e^{\beta^2(b-1)+\alpha} \qquad \text{Equation 2.4}$$

By using Equation 2.4, Nash was able to determine the effective discharge without having to divide the discharges into classes, and calculate the corresponding frequencies. This would appear to solve the problem of determining the number of bins to use in calculating the discharge frequency curves and would greatly simplify the process required in determining the effective discharge. By using Equation 2.4, the

effective discharge is determined simply by determining the mean and standard deviation of the natural logarithms of the flow data and the exponent b from Equation 2.1. However, Equation 2.4 assumes that the data are log-normally distributed. Although this is usually the case with hydrologic data, one must first test the data to determine whether they are truly log-normally distributed. For flow distributions that are highly skewed, the log-Pearson Type III distribution may represent the data better than the general lognormal distribution because the log-Pearson Type III distribution accounts for skew. Based on average daily discharges, the following relationship can be used to describe the log-Pearson Type III distribution (Salas et al., 2000):

$$f(Q) = \frac{1}{|\alpha|\Gamma(\beta)Q}\left(\frac{\ln Q - y_o}{\alpha}\right)^{\beta-1} e^{-\frac{\ln Q - y_o}{\alpha}} \qquad \text{Equation 2.5}$$

where:

$f(Q)$ = frequency of occurrence of a given discharge, Q;

$ln\ Q$ = natural logarithm of discharge;

$\Gamma(\beta)$ = Gamma distribution of β;

α = scale parameter;

β = shape parameter; and

y_o = location parameter.

Scale, shape, location parameters, and Gamma distribution can be determined from the following equations:

$$\alpha = \frac{\sigma\gamma}{2} \qquad \text{Equation 2.6}$$

$$\beta = \left(\frac{2}{\gamma}\right)^2 \qquad \text{Equation 2.7}$$

$$y_o = \mu - \alpha\beta \qquad \text{Equation 2.8}$$

$$\Gamma(\beta) = (\beta + 4.5)^{\beta - 0.5} e^{-(\beta + 4.5)} \sqrt{2\pi}\left[1 + \sum_{i=0}^{5} \frac{c_i}{\beta + i}\right] \qquad \text{Equation 2.9}$$

where:

μ = mean of the natural logarithm of discharge;

σ = standard deviation of the natural logarithm of discharge;

γ = skewness coefficient of the natural logarithm of discharge data; and

c_i = constants (c_0= 76.18, c_1= -86.51, c_2= 24.01, c_3= -1.23, c_4= 0.0012, and c_5= -0.536×10^{-5}).

2.3 Effective Discharge Determination using Magnitude-Frequency Analysis

Magnitude-Frequency Analysis (MFA) is the most common method used in the determination of effective discharge. Although the concepts used in MFA are fairly simple, the actual process of determining the effective discharge can be somewhat problematic. The range of flows experienced by the river during the period of record are divided into a number of classes and then the total amount of sediment transported by each class is calculated. This is achieved by multiplying the frequency of occurrence of each flow class by the sediment load for that flow class. Primary input data used in the analysis consist of: i) flow data, and ii) a sediment transport rating relationship. The calculated value of the effective discharge depends to some extent on the steps used to manipulate the input data to define the flow regime and sediment transport function. The first step is to group the discharge data into flow classes and determine the number of events occurring in each class during the period of record.

2.3.1 Frequency and Bin Size Determination

Previous investigations that have used MFA to calculate effective discharge have used arithmetic and logarithmic discharge scales to develop the histograms needed for the analysis. Class intervals are needed because instantaneous flow measurements over time are unavailable. Instead, gauge records contain a sample of the real flow distribution relative to a specific time interval, such as 15-minute data. Subsequently, the frequency of any discharge cannot directly be determined from a sample distribution but must be inferred from the frequency of a specific range of measured discharges.

Table 2.2 summarizes the type of discharge scales and number of class intervals used in previous investigations and demonstrates that the majority of calculations have used an arithmetic discharge scale.

Table 2.2 – Type of class interval and number of classes used to calculate effective discharge in a selection of studies (after Soar, 2000)

Reference	Class Interval	Number of Classes
Andrews (1980)	arithmetic	20
Webb and Walling (1982)	arithmetic	23
Ashmore and Day (1988)	arithmetic	15-24
Carling (1988)	arithmetic	8-12
Lyons et al. (1992)	arithmetic	35
Biedenharn and Thorne (1994)	arithmetic	50-54
Nash (1994)	logarithmic*	n/a
Hey (1997)	arithmetic	25
Watson et al. (1997)	logarithmic	35
Goodwin et al. (1998)	arithmetic*	n/a
Soar et al. (1999)	logarithmic	23
Thorne et al. (1998)	arithmetic or logarithmic**	25
Sichingabula (1999)	arithmetic	20
Biedenharn et al. (2000)	arithmetic	25

*used theoretical probability distribution;
**recommended using logarithmic intervals if there are zero frequencies in the flow frequency histogram or if the effective discharge falls within first class.

The type of class interval (arithmetic or logarithmic) and number of discharge classes used can influence the effective discharge calculation dramatically. The following section examines the different types of class intervals that have been used in previous investigations.

2.3.1.1 Arithmetic Class Intervals

Andrews (1980) used arithmetic class intervals in his investigation of effective discharge for the Yampa River Basin in Colorado and Wyoming. He divided the range of discharges into twenty equal increments. The sediment-load-duration curve was then integrated between the limits of each increment, and multiplied by 365 days. A smooth curve was fitted to the computed points, and the discharge that transported the most sediment during the period of record was recorded as the effective discharge. Andrews found that the stream flow duration of the effective discharge varies between gauging stations and ranged from 1.5 to 11 days per year.

Biedenharn and Thorne (1994) also used arithmetic class intervals in their investigation of three gauging sites along the Lower Mississippi River. Discharges varied from a low of about 4,250 m^3/s to a high just over 56,600 m^3/s. They tested ranges of flow increments from 140 m^3/s up to 6,000 m^3/s to determine the class interval that would accurately describe the effective discharge by producing a relatively smooth curve. Based on their tests, a flow increment of 1,000 m^3/s was selected for the analysis. Effective discharge was found to be about 30,000 m^3/s, was exceeded on average about 13% of the time, and had a return period of about one year.

Finally, Hey (1997) found that twenty-five class intervals produced a relatively continuous flow frequency distribution and a smooth sediment-load histogram with a

well-defined peak for determining the effective discharge. Hey (1997) also found that increasing the number of class intervals produced anomalous results. However, this appears to depend on the drainage basin characteristics and type of sediment transported within the basin.

These are just a few of the numerous investigations that have used arithmetic class intervals in the determination of effective discharge. It appears from the literature that the majority of effective discharge investigations have used the arithmetic class interval to develop the flow frequency histogram. Although the majority has used the arithmetic method, there have also been investigations that have used a logarithmic class interval in the determination of the effective discharge.

2.3.1.2 Logarithmic

Nash (1994) was the first to use logarithmic class intervals in the determination of the effective discharge. However, instead of actually using a set number of classes, Nash used an analytical method for determining the frequency of occurrence of a given discharge. As stated previously, Nash determined effective discharge mathematically by setting the derivative of Equation 2.3 to zero with respect to Q and solving for Q. Nash compared the discharge frequency histograms of fifty-five streams with the lognormal distribution and found that seventeen of the histograms fit closely, whereas the rest varied as a result of kertosis, skew, bi-modal, and multi-modal peaks. From the results, it is evident that the analytical method proposed by Nash has a number of limitations and should only be used if the lognormal distribution represents the actual flow frequency histogram.

Watson et al. (1997) also used logarithmic class intervals in an investigation of ten streams in the Yazoo River Basin, Mississippi. Based on the USGS flow-duration procedure, the flow data were divided into thirty-five classes, used in the development of the flow duration curves, and then used in determining the total sediment load for each stream. Watson found that the recurrence intervals for the ten Mississippi streams varied between one and two years and the effective discharge ranged from 1,592 ft^3/s to 21,392 ft^3/s between the ten streams.

Finally, Thorne et al. (1998) used logarithmic class intervals in their determination of effective discharge. Although the preferred method was to use arithmetic classes, they found that for streams in which the effective discharge occurred within the first arithmetic bin, the flow distribution would be better represented if logarithmic class divisions were used. This allowed the lower end of the flow-frequency distribution to be better defined and the corresponding sediment-transport curve to become smoother and better defined, as well. Determining which method to use to develop the flow-frequency curve employed in the effective discharge calculation has plagued investigators for many years.

2.3.1.3 Summary of Frequency and Bin Size Determination

Soar (2000) states that for an unbiased estimation of the actual effective discharge, discharge class intervals cannot vary in size. If the discharge interval systematically increases, as in a logarithmic scale, then the resultant sample frequency distribution is incorrectly skewed in the negative direction. As a direct result, the product of the sediment load and flow frequency will tend to follow a similar trend. This is because in MFA, the sediment load transported by the mean discharge of a class is

multiplied by a frequency corresponding to the probability of falling within that class. This probability increases with class size. As a result, with logarithmic class intervals, the systematic increase in the size of class interval with increasing discharge will overestimate the effective discharge. However, depending on the type of flow, logarithmic class intervals may be needed in order to define the low-magnitude high-frequency discharges that occur in the majority of sand bed streams.

Intuitively, it might be expected that the smaller the class interval and, therefore, the greater the number of classes, the more accurate would be the outcome. However, if too small an interval is used, discontinuities appear in the discharge frequency distribution. These, in turn, produce an irregular sediment load histogram, with multiple peaks. Therefore, the selected class interval should be small enough to accurately represent the frequency distribution of flows, but large enough to produce a continuous distribution, with no classes having a frequency of zero (Biedenharn and Thorne, 1994). This may result in several attempts at calculating the effective discharge, until a relatively continuous flow-frequency distribution and smooth sediment load histogram with a well-defined peak is produced.

Although there are no definite rules for selecting the most appropriate interval and number of classes, Yevjevich (1972) stated that the class interval should not be larger than $s/4$, where 's' is an estimate of the standard deviation of the sample. For hydrological applications he suggested that the number of classes should be between ten and twenty-five, depending on the sample size. Hey (1997) found that twenty-five classes with equal, arithmetic intervals produced a relatively continuous flow-frequency distribution and a smooth sediment load histogram with a well-defined peak. However,

Watson et al. (1997) and Biedenharn and Thorne (1994) showed that the use of logarithmic classes may be required if the flow distribution is skewed towards the low-magnitude, high-frequency events, especially in sand bed streams. As a result, the researcher must choose a method that best represents the type of flow distribution and sediment characteristics that are present in the basin of interest. Because sediment transport is such an important part of the MFA in determining the effective discharge, the following section examines the methods that previous investigators have developed for sediment transport relationships used in MFA.

2.3.2 Sediment-rating Curves

The total sediment that is transported by a given discharge within a stream can be broken down in three ways (Julien 1995): measurement method, transport mechanism, or sediment source (Tables 2.3 and 2.4). From these tables it is evident that where the sediment comes from, how it is transported, and the process by which it is measured are not all-inclusive. Whether the sediment is boulders, gravel, or sand largely determines how the sediment is transported.

Table 2.3 – Classification of the total sediment load for a sand bed stream

Measurement Method	Transport Mechanism	Sediment Source
Unmeasured Load	Bed Load	Bed Material Load
Measured Load	Suspended Load	Wash Load

Table 2.4 – Classification of the total sediment load for a gravel bed stream

Measurement Method	Transport Mechanism	Sediment Source
Unmeasured Load	Bed Load	Bed Material Load
Measured Load	Suspended Load	Wash Load

Nash (1994) and Hey (1997) found that effective discharge calculations for sand bed streams usually use suspended sediment load for the total load after demonstrating that the bed load does not affect the calculation or that the bed load is less than 10 percent of the total load being transported. Conversely, Andrews (1980) used the suspended sediment load as well as the calculated bed load in his investigation of some gravel bed streams in Colorado and Wyoming. When bed load and suspended load are both significant fractions of the total load, then both should be included in the determination of the effective discharge. Andrews showed that when measured load is available, the bed load can be calculated using an appropriate bed load function and then added to the suspended load fraction to determine the total sediment load in the river.

Biedenharn et al. (2000) stated that in most alluvial rivers the channel morphology is usually formed from the sediments that are derived from the bed material load. As a result, the bed material should be used in the determination of the effective discharge. At gauged sites where the total load primarily consists of suspended load, the bed material load portion of the measured load should be used in developing the sediment transport-rating curve used in the effective discharge calculation (Biedenharn et al., 2000). If a significant portion of the bed material load is transported as bed load, then the bed load and suspended load should be added together and used in the effective discharge calculation. If sediment data are not available, it may be necessary to estimate the sediment transport by selecting a suitable sediment transport equation based on the type of sediment present in the channel. Once the measured sediment data have been analyzed or estimated using an appropriate sediment equation, a sediment transport relationship must be developed.

Measured load is usually expressed as a single-power function of discharge (Equation 2.1). Previous investigations have shown that a single sediment-rating curve overestimated the sediment load at low discharges and underestimated the sediment load at high discharges (Kuhnle et al., 1999). Similarly, Hey (1997) used two different rating curves in his investigations: one for in-bank flow and another for over-bank flow. However, Dubler (1997) used a single sediment transport-rating curve in his investigation of ten Mississippi streams and found the rating curve to represent the sediment data fairly well. Nash's (1994) analytical solution of effective discharge also showed that a single sediment rating relationship fit the observed data for all fifty-five streams in his investigation fairly well (r average 0.88), but tended to be inaccurate at high discharges. As a result, investigators again must use good judgment in the selection of a sediment transport relationship in order to accurately calculate the effective discharge.

2.3.3 Product – Effective Discharge

The final step in the calculation of effective discharge is to determine the discharge that corresponds to the maximum of the product curve, curve C in Figure 2.1. Although this maximum is very evident in a curve with a single peak, it can be quite difficult to determine the true effective discharge for a multi-modal product curve. Nash (1994) found that there were a total of six different types of product curves as a result of his investigation of fifty-five U.S. streams. Although the true maximum of the product curve can easily be determined, it may not represent the true effective discharge. Some of the bias that is introduced into the selection of the sediment-rating curve is carried into the development of the product curve. As a result, if the sediment-rating curve over- or under-predicts the true sediment transport, then the product curve also tends to over- or under-predict the true effective discharge.

Previous investigations have shown that depending on the method used to develop the flow frequency and sediment-transport curves, the resulting effective discharge can vary dramatically. Thorne et al. (1999) showed that although arithmetic class intervals are the preferred method for developing the flow-frequency curve, logarithmic class intervals might be preferred if the arithmetic effective discharge falls within the first bin size. This occurs most often in sand bed streams when the low-magnitude flows have an extremely high frequency of occurrence. Because these low flows have such a high frequency of occurrence, the effective discharge usually falls within the first bin size for an arithmetic class interval because the first bin size is so large. Recently, several methodological developments have attempted to improve the effective discharge calculation in an attempt to alleviate the error caused by assigning the effective discharge to a specified discharge class. The following section examines a few of the new developments in effective discharge calculation.

2.4 Recent Developments

As stated in Soar (2000), Orndorff and Whiting (1999) acknowledged that the effective discharge is highly dependent on the number of classes used and that fitting a statistical distribution, such as the lognormal probability density function assumed by Nash (1994), may misrepresent the empirical distribution of flows, particularly with multi-modal distributions. They suggested using statistical software to develop an empirically-based probability density function (PDF) from the actual flow record. The effective discharge could then be determined by multiplying the empirically-based PDF by the sediment transport relationship and setting the derivative equal to zero (Nash, 1994).

Sichingabula (1999) recommended calculating an event-based, rather than the conventional class-based, effective discharge. Sichingabula found that a different effective discharge is obtained for every different class size used in the effective discharge calculation and concluded that "...the problem with the conventional method of determining the effective discharge is the need to discretise the time series and pull out an isolated range rather than recognize the overall variability and episodic nature of sediment transport events".

Similarly, Soar (2000) states:

> *... this technique may involve developing a cumulative distribution from thousands of discharge measurements (depending on the sampling time base) and interpolation of the resultant flow duration curve for hundreds or thousands of classes (appropriate to the size of the database and capacity of the channel). Therefore, handling this quantity of data requires a computer program, which probably explains why the method has not been developed previously.*

An example of this technique was shown by Soar (2000) in Figure 2.3 for the Delaware River at Trenton, New Jersey. From the case study, an event-based frequency distribution was approximated by using 1,000 discharge classes, giving a class size of only 3.68 m^3/s, compared to 147.18 m^3/s when the conventional 25 classes were used.

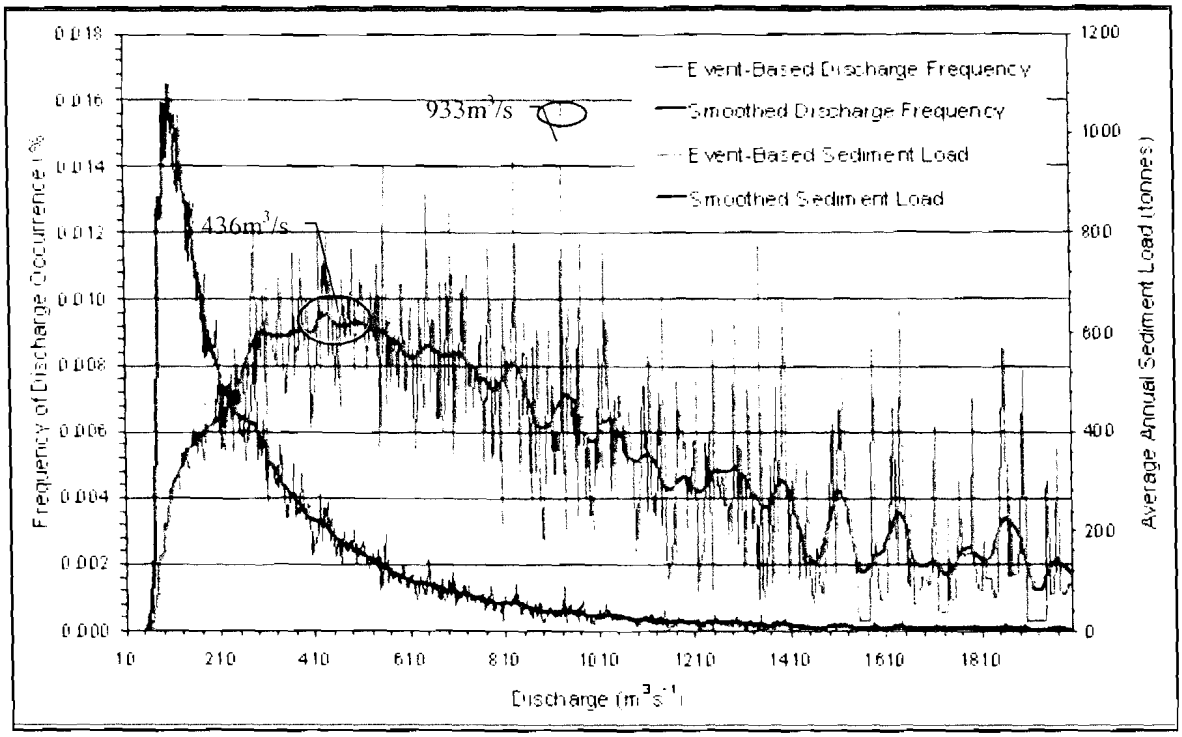

Figure 2.3 – Flow and sediment frequency distributions for Delaware River at Trenton, New Jersey.

Soar (2000) found that the effective discharge of the event-based distributions was 933.4 m^3/s, compared to an effective discharge of 436 m^3/s computed by extracting the trend of the event-based distribution. Soar concluded that

> *...the effective discharge of the smoothed distribution is more realistic of the general form of the distribution and, if used to restore stable channel dimensions, has the highest probability of being the most effective discharge in the restored channel.*

In the case of the Delaware River site, Soar found that the conventional 25-class frequency distribution produced an effective discharge of 416 m^3/s. As seen in Figure 2.3, there is a range of discharges between about 300 m^3/s and 550 m^3/s that transport similar magnitudes of sediment load. As a result, it would appear that the smoothed event-based and class-based effective discharges are similar in their results.

2.5 Previous Effective Discharge Determination for DEC Sites

Previous investigations of the effective discharge for DEC streams include Dubler (1997) and Hendon (1995). Dubler (1997) used a logarithmically based flow distribution with thirty-five class intervals and calculated the effective discharge using both 15-minute and average daily flow records. Dubler found that 15-minute flow records should be used over daily averages because daily averages tend to under-predict the total annual sediment yield by about fifty percent. As a result, this will also affect the results of the effective discharge calculation. Additionally, because of the flashiness of the hydrograph or rapidity with which the stage increases at a cross section within the DEC basins, 15-minute flow data are needed in order to accurately develop the flow-duration curve used in the effective discharge calculation. Dubler also used Nash's (1994) analytical solution to determine the effective discharge, but found that the resultant effective discharges were much smaller than those calculated using the logarithmic division of bins, and chose not to use Nash's method in his investigation of the DEC streams.

Hendon (1995) also investigated whether 15-minute or mean daily data should be used in the determination of the total sediment load. Although Hendon was not specifically determining the effective discharge, she was determining the total sediment yield based on two different discharge time intervals. Becuase the effective discharge is ultimately determined by finding the discharge that transports the largest amount of sediment, Hendon was in part determining the type of data that are needed in order to calculate the effective discharge. Results from Hendon's and Dubler's investigations are similar in that they both determined that 15-minute discharge data should be used over

mean daily discharge in the calculation of sediment yield for the Yazoo River Basin in Mississippi.

2.6 Summary of Literature Review

Wolman and Miller (1960), Hey (1997), Mackin (1948), Andrews (1980), and many other researchers have demonstrated that the dominant controls of channel form and channel maintenance are linked to discharge and sediment load. Dominant, effective, and bankfull discharge are commonly used terms when describing channel maintenance or form. Effective and dominant discharge are often considered interchangeable terms and bankfull discharge is frequently equivalent to the effective discharge. Additionally, a one- to two-year recurrence interval has been found to be common among channel-forming events. Wolman and Miller (1957) showed that the bankfull discharge had a recurrence interval of one to two years and as a result, the two-year discharge was also used by many researchers as the design discharge.

Wolman and Miller's concept of effectiveness, based on magnitude and frequency of flows and total sediment transported, was also used in determining the design discharge. The concept of effectiveness based on magnitude, frequency, and sediment transport was later termed the effective discharge by Andrews (1980). Andrews (1980) defined the effective discharge as that increment of discharge that transports the largest fraction of annual sediment load over an extended period of time. Andrews' (1980) definition is practical to planning and design of sediment control structures because the definition accounts for both magnitude and frequency.

From the literature it is evident that the effective discharge is often determined using frequency of occurrence and sediment-transport curves. However, simplified

relationships, recurrence intervals, and bankfull determinations are also used to estimate channel-forming events. There are three general approaches to determining the channel-forming discharge: bankfull discharge, flow of a given recurrence interval, and effective discharge. Although there are numerous methods that investigators have used in the determination of the channel-forming discharge, Doyle et al. (1999) demonstrated from three rivers in the U.S. that the effective discharge should be used in preference to other methods and concluded that the effective discharge is the most critical geomorphic and hydraulic parameter in channel design. Therefore, the importance of the effective discharge determination in the DEC Project is to identify the discharge that transports the largest portion of the sediment and to use this knowledge to aid in the design of erosion control measures.

3 METHODS FOR DETERMINATION OF EFFECTIVE DISCHARGE

Several methods of analysis will be described in the following sections concerning the determination of effective discharge in the Yazoo River Basin. Determining effective discharge using Andrews' (1980) definition requires the following basic relationships: a flow-duration or frequency curve and a sediment-transport curve as a function of discharge. Ideally, a long-term gauging site is necessary to calculate the effective discharge most accurately. However, many of the DEC sites are not gauged and therefore additional methods for determining discharge and sediment transport data needed to calculate the effective discharge at ungauged sites will be discussed.

3.1 Yazoo River Basin (DEC)

The Yazoo River Basin is located in the north central part of the State of Mississippi. A total of thirty-three sites are currently being surveyed and analyzed by the U.S. Army Corps of Engineers and Colorado State University. Currently, thirteen DEC streams have USGS gauges installed. Stream flow and sediment data from these gauging stations were used to investigate and determine the effective discharge for each of the DEC sites in this study. 15-minute water discharge values were available from the USGS in Jackson, Mississippi and stage-activated pumped sampler sediment concentration data were also available for this study. Data provided by the USGS were the basis for the effective discharge calculations.

3.1.1 Site Locations

Data from thirteen USGS gauges in the Yazoo River Basin were used to determine the effective discharge for a total of twenty-three sites investigated in this study. Table 3.1 lists the creeks that were analyzed in this study and the corresponding latitude and longitude, period of flow record, and general site characteristics for each study site. Figure 3.1 shows the location of each site within the basin and is marked using the reference numbers provided in Table 3.1.

3.1.2 Site Characteristics

Stream characteristics in the Yazoo River Basin can vary dramatically depending on the location of the study sites within the basins. Of the twenty-three sites used in this study, the drainage areas range from 10.24 square miles at Long Creek to 220 square miles at the lower end of Hickahala 22. General characteristics for each stream site are presented in Table 3.1. The first sixteen streams are sites that Colorado State University is currently monitoring, and for which cross-sectional survey data are available. The remaining streams are sites that only the USGS monitors using stream gauges. USGS and DEC sites were used in determining the effective discharge.

Table 3.1 – USGS and DEC study site locations and site characteristics

Ref #	Year	Station Name (*USGS gauge #*)	Latitude	Longitude	Period of Record	Drainage Area	Channel Slope	Channel Length	d_{50}
	(most current survey)	[illegible]			15 minute discharge data	(sq. miles)	(ft/mile)	(mile)	(mm)
1	1997	Abiqua 3	33° 19' 13.43"	90° 00' 38.55"	N/A	25.16	6.3	10.5	0.26
2	1997	Abiqua 4	33° 21' 41.97"	90° 05' 31.63"	N/A	42.41	10.0	20.2	0.48
3	1996	Abiqua 6 - *#07287150*	33° 20' 24.60"	90° 09' 05.55"	1991-current	93.89	3.7	26.9	0.5
4	1996	Abiqua 23 - *#07287160*	33° 20' 28.80"	90° 14' 14.30"	1991-current	94.43	1.6	31.9	0.35
5	2000	Fannegusha	33° 16' 43.23"	89° 56' 06.85"	N/A	17.65	6.7	5.4	0.31
6	1999	Harland 3	33° 02' 21.23"	90° 10' 54.45"	N/A	26.89	7.1	9.9	0.5
7	1999	Harland 23	33° 04' 32.63"	90° 10' 04.44"	N/A	40.3	5.4	12	0.5
8	2000	Hickahala 11	34° 40' 43.41"	89° 41' 20.64"	N/A	10.41	8.8	5.2	0.51
9	2000	Hickahala 22	34° 39' 16.32"	89° 58' 25.00"	N/A	220.2	4.7	21.4	0.41
10	1998	Hotopha	34° 19' 29.55"	89° 47' 33.64"	N/A	19.19	4.1	6.2	0.31
11	2000	Otoucalofa	34° 09' 31.12"	89° 31' 57.29"	N/A	47.11	9.4	12.1	0.39
12	1998	Long	34° 14' 21.70"	89° 50' 34.72"	N/A	10.24	5.6	5.7	0.38
13	2000	Senetobia - *#07277730*	34° 37' 02.32"	89° 56' 30.00"	1986-current	82	7.6	15.1	0.41
14	1999	Tapashaw Creek near Derma - *#07282090*	33° 46' 75.06"	89° 14' 80.05"	1998-current	95	2.9	11.57	0.17
15	2000	Yalobusha River at Derma - *#07281977*	33° 50' 28.02"	89° 16' 56.07"	1998-current	158	6.2	15.8	0.18
16	2000	Yalobusha River at Vardaman - *#07281960*	33° 51' 58.02"	89° 10' 23.07"	1998-current	86.3	7.3	12.67	0.18
17	none	Batupan Bogue at Grenada - *#07285400*	33° 46' 26.02"	89° 47' 15.07"	1993-current	240	6.5	23.6	0.3448
18	none	Fannegusha Creek near Howard - *#07287355*	33° 08' 13.02"	90° 11' 40.07"	1987-current	107	8.5	25.1	0.408
19	none	Harland Creek near Howard - *#07287404*	33° 06' 05.02"	90° 10' 23.07"	1987-current	62.1	13.2	14.1	0.398
20	none	Hickahala near Senetobia - *#07277700*	34° 37' 54.02"	89° 55' 30.07"	1986-current	121	9.2	18.1	0.423
21	none	Hotopha Creek near Batesville - #07273100	34° 21' 50.02"	89° 52' 42.07"	1996-current	35.1	12	13.3	0.377
22	none	Otoucalofa near Water Valley - *#07274252*	34° 08' 36.02"	89° 38' 59.07"	1985-current	97.1	8.8	18.9	0.389
23	none	Long Creek near Pope - #07275530	34° 12' 50.02"	89° 58' 54.07"	1987-current	79.2	12.2	13.7	0.446

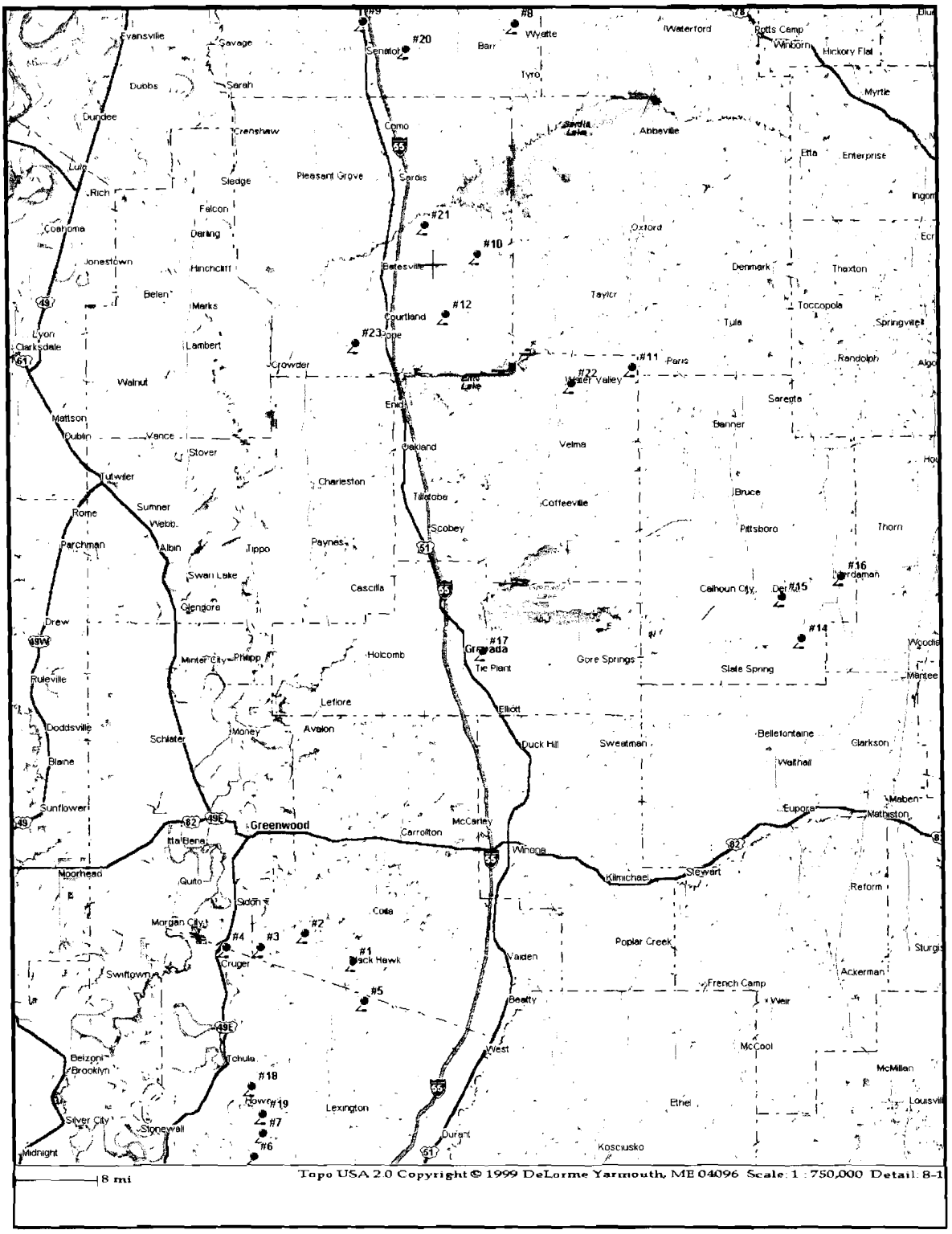

Figure 3.1 – Site locations for analysis indicated by numbered pin markers

3.2 Analytical Effective Discharge Calculation

Nash (1994) presented the idea of using an analytical method for calculating the effective discharge based on the use of the lognormal frequency equation and a sediment transport relationship. In order to use Nash's procedure, the discharge frequency must be log-normally distributed. In this study the observed flow distribution for each creek was calculated and then compared to the analytical flow distribution calculated using Equation 2.2 in the literature review.

A Chi-Square test (Equation 3.1) was used to determine whether the observed distribution was log-normally distributed and whether an analytical solution to the effective discharge could be developed using Nash's method.

$$\chi^2_{calc} = \sum_{i=1}^{k} \frac{(f_i - f_c)^2}{f_c} \qquad \text{Equation 3.1}$$

where:

f_i = observed frequency; and

f_c = calculated frequency.

Nash (1994) showed that the effective discharge could be determined mathematically by setting the derivative of Equation 2.3 in the literature review to zero with respect to Q and solving for Q (Nash, 1994). Therefore, the following equation was used to determine effective discharge analytically, Q_e:

$$Q_e = e^{\beta^2(b-1)+\alpha} \qquad \text{Equation 3.2}$$

where:

b = shape factor coefficient;

α = mean of the natural logarithm of discharge; and

β = standard deviation of the natural logarithm of discharge.

Mean and standard deviation for the two-parameter log-normal distribution were estimated using the method of moments. Parameters were estimated using the following equations:

$$\mu_y = \frac{1}{2} \ln \left(\frac{\mu_x^2}{1 + \frac{\sigma_x^2}{\mu_x^2}} \right) \qquad \text{Equation 3.3}$$

$$\sigma_y = \left(\ln \left(1 + \frac{\sigma_x^2}{\mu_x^2} \right) \right)^{\frac{1}{2}} \qquad \text{Equation 3.4}$$

where μ_y and σ_y are the estimators for α and β, respectively (Salas et al., 1995).

The analytical solution for effective discharge was used only in comparing the results of the MFA, Q_2, and bankfull determinations of effective discharge.

3.3 Discharge Computations using Regionalized Equations

The ability to determine discharges at ungauged sites is a very important concept when investigating flow characteristics within a stream reach. One method for determining discharges at an ungauged site is to determine a dimensionless discharge relationship that could be used to transfer discharge records from a gauged site to an ungauged site. In 1976, Colson and Hudson developed a regional regression equation to determine recurrence intervals for discharges at ungauged sites. Discharge determination for various recurrence intervals is necessary for two reasons. First, several authors have suggested a recurrence interval of approximately two years for the effective discharge.

Second, comparisons and dimensional discharge indices can be made between USGS gauged sites and ungauged DEC sites.

The following are the relationships proposed by Colson and Hudson (1976):

$$
\begin{aligned}
Q_2 &= 189\ A^{0.91} S^{0.31} (L+2)^{-0.50} \\
Q_5 &= 326\ A^{0.96} S^{0.34} (L+3)^{-0.59} \\
Q_{10} &= 459\ A^{0.98} S^{0.36} (L+4)^{-0.65} \\
Q_{25} &= 883\ A^{0.99} S^{0.32} (L+5)^{-0.74} \\
Q_{50} &= 1120\ A\ S^{0.34} (L+6)^{-0.77} \\
Q_{100} &= 2260\ A\ S^{0.25} (L+6)^{-0.88}
\end{aligned}
\qquad \text{Equation 3.5}
$$

Where:

Q_x = discharge at recurrence interval x years, (cfs);

A = drainage area (square miles);

S = channel slope, (feet per mile) which is the difference of elevation at points 10% and 85% along the channel from the point of discharge to the drainage divide; and

L = main channel length (miles).

The 2-year recurrence interval discharge was used to make watershed comparisons. USGS gauged sites were used to determine discharge records for the ungauged DEC sites by using the dimensionless discharge ratio of Q/Q_2 and then multiplying the ratio by the 2-year recurrence discharge for the ungauged DEC site. Colson and Hudson's (1976) method of discharge determination is useful for ungauged sites because the parameters are easily obtained. Because of the short period of record (<12 years) of the USGS gauges used in this study, the 2-year discharge for each site was calculated using the regionalized regression equations developed by Colson and Hudson (1976).

3.4 Effective Discharge Computation using Magnitude Frequency Analysis

The procedure for determining effective discharge using a MFA consists of three major steps; (1) construction of a flow-frequency distribution, (2) determination of sediment transport as a function of discharge, and (3) construction of a sediment load histogram as a function of discharge for the period of record. It is through the analysis of these three steps that the effective discharge can be determined. However, the process that is used to construct and evaluate each of these steps can greatly change the results of the effective discharge calculation. Because the results of the effective discharge calculations are highly dependent on the class size used as well as the type of sediment transported, a computer program was written to determine the effective discharge for each site using various types of inputs. A description of the effective discharge program used for this study is presented in Section 3.5. The following sections provide the general procedures that were followed in determining effective discharge for this study. Specific inputs into the effective discharge program are discussed in Section 3.5.1.

3.4.1 Flow-frequency Distributions

General steps that were used to generate the flow-frequency distributions for each site are schematically presented in Figure 3.2 and are as follows;

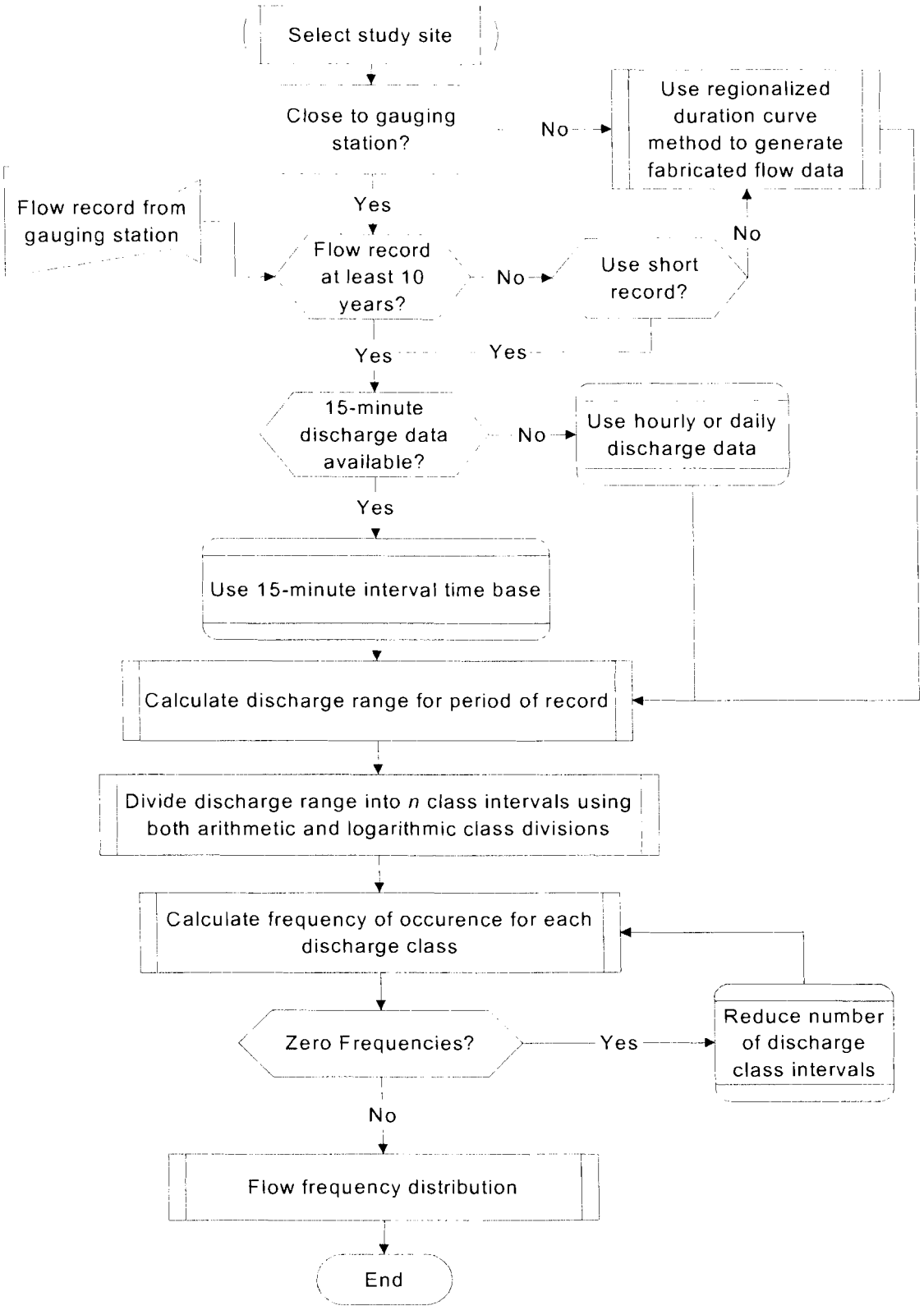

Figure 3.2 – Flow chart for generating flow-frequency distributions (after Soar 2000)

3.4.1.1 Evaluate the flow record

Flow records from thirteen USGS gauging stations in Mississippi were used to develop the flow-frequency distributions for each of the twenty-three sites used in this study. If a gauging record was either unavailable or unrepresentative, the flow-frequency distribution was derived using a dimensionless discharge index proposed by Watson et al. (1997) using the 2-year recurrence discharge to normalize the discharge data (Q/Q_2). For ungauged sites, the 2-year discharge was estimated from a regionalized discharge frequency relationship (Colson and Hudson, 1976), which is based on the drainage area, channel slope, and channel slope length. Dimensionless discharge index (Q/Q_2) was then used to transfer flow duration relationships from USGS gauged sites to nearby DEC sites that did not have gauging stations present.

3.4.1.2 Determine the discharge-averaging time base

In constructing the flow-frequency distribution for each site, the time base needed to be sufficiently short to ensure that short-duration, high-magnitude events were properly represented. Watson et al. (1997) showed that mean daily flows underestimated the total sediment load by as much as 58% compared to 15-minute flow data. As a result, 15-minute discharge data were used in constructing the flow-frequency distributions for each of the twenty-three sites in this study.

3.4.1.3 Calculate the discharge range for the period of record

The range of discharges for each site was calculated by subtracting the minimum discharge in the flow record from the maximum discharge. This difference was recorded as the discharge range and was used in determining the class intervals for each site.

3.4.1.4 Calculate discharge class intervals (arithmetic and logarithmic)

Discharge class intervals for each of the sites in this study were calculated based on both arithmetic and logarithmic class divisions for a number of different class sizes. For arithmetic class divisions, the class intervals were determined by dividing the discharge range by the total number of class intervals, n, that were of interest. For rivers in which the bed material load moves predominantly as suspended load, the first discharge class goes from zero to the class interval, the second class is the class interval to twice the class interval, and so on until the upper limit of the discharge range is reached.

For logarithmic class divisions, the class intervals were determined using the USGS method for logarithmic class divisions. Based on the number of class intervals of interest (n), the first class is zero. Second class has an upper limit equal to the minimum discharge and the upper limit of the nth class is equal to the maximum discharge. Remaining classes were found by taking the natural-log of the maximum discharge and subtracting the natural-log of the minimum discharge; the resulting value was then divided by n-2 and became the step size for each class interval. The step size was added to the preceding value and the upper discharge class values were calculated by taking the anti-$\log_e$. Appendix A provides sample calculations for determining the arithmetic and logarithmic class sizes used in this study. Because all of these calculations were carried out by the effective discharge computer program, a large number of variations could be carried out at one time and analyzed to determine the most appropriate class size for determining the effective discharge at each site.

3.4.1.5 Calculate flow-frequency distributions

Frequency of occurrence of each discharge class was determined from the record of observed flows and used to construct the frequency of occurrence curves for each site. Soar (2000) recommended that all discharge classes display flow frequencies greater than zero and that there are no isolated peaks at the high end of the discharge classes. If this is not the case, it is likely that either the class interval is too small for the discharge range, or the period of record is too short. Soar (2000) showed that both zero frequencies and extreme flow-events (outliers), could be eliminated by incrementally reducing the number of classes. Frequency of occurrence computations were made for each of the twenty-three sites within the Yazoo River Basin using 15-minute discharge records and both arithmetic and logarithmic class divisions.

3.4.2 Sediment Rating Curves and Yang's equation

A water and sediment discharge relationship is an integral part of the effective discharge determination. Suspended sediment samples were collected by the USGS at each of the USGS gauging stations used in this study. Two types of sediment data were available from the USGS; observed depth-integrated samples and automatic pump samples. Observers collected single, vertically-integrated suspended sediment samples at various times throughout the month. Data were also supplemented by sampling during selected storms. Each site is equipped with a PS-69 automatic point sampler which is stage activated; this was the basis for the pump sample data. PS-69 sampling procedures are described by Guy and Norman (1970).

From the data obtained from the USGS, sediment-rating curves were developed, which are used to compute total suspended sediment discharge as a function of water discharge. A relationship was developed for all the gauged sites. For ungauged sites,

Yang's (1973) total sediment load equation was used to determine the sediment concentration for each bin size. Comparison of Yang's results with that of the USGS showed that Yang's equation predicted the sediment transport quite well and therefore could be used for determining the sediment transport at ungauged sites. General steps that were used to generate the sediment-rating curves for each site are schematically presented in Figure 3.3 and are as follows.

3.4.2.1 Define composition of bed material load

Sediment composition for the majority of the sites within this study consists of sands, silts, and clays. As a result, a large portion of the sediment within these systems is transported as suspended sediment. Julien (1995) divided the dominant mode of sediment transport into the following three zones: bedload, mixed load, and suspended load. Each sediment zone is based on a ratio of the shear velocity to the fall velocity, and the ratio of depth to the particle size. Julien showed that suspended load is the dominant mode of transport for values greater than 2.5 for the ratio of shear velocity to fall velocity. For a range of conditions occurring in the DEC streams: d_{50} particle sizes vary from 0.5 mm to 0.063 mm; average slope of 0.001; depth ranging from 0.15 m to 1.5 m; and the shear velocity to fall velocity ratio varies from 1.37 to 32.4. Therefore, for conditions occurring in the DEC monitoring streams, suspended load is the dominant transport mode. This implies that the suspended sand discharge closely approximates total bed material load, and that the suspended sediment discharge can be used as the total sediment load for each site.

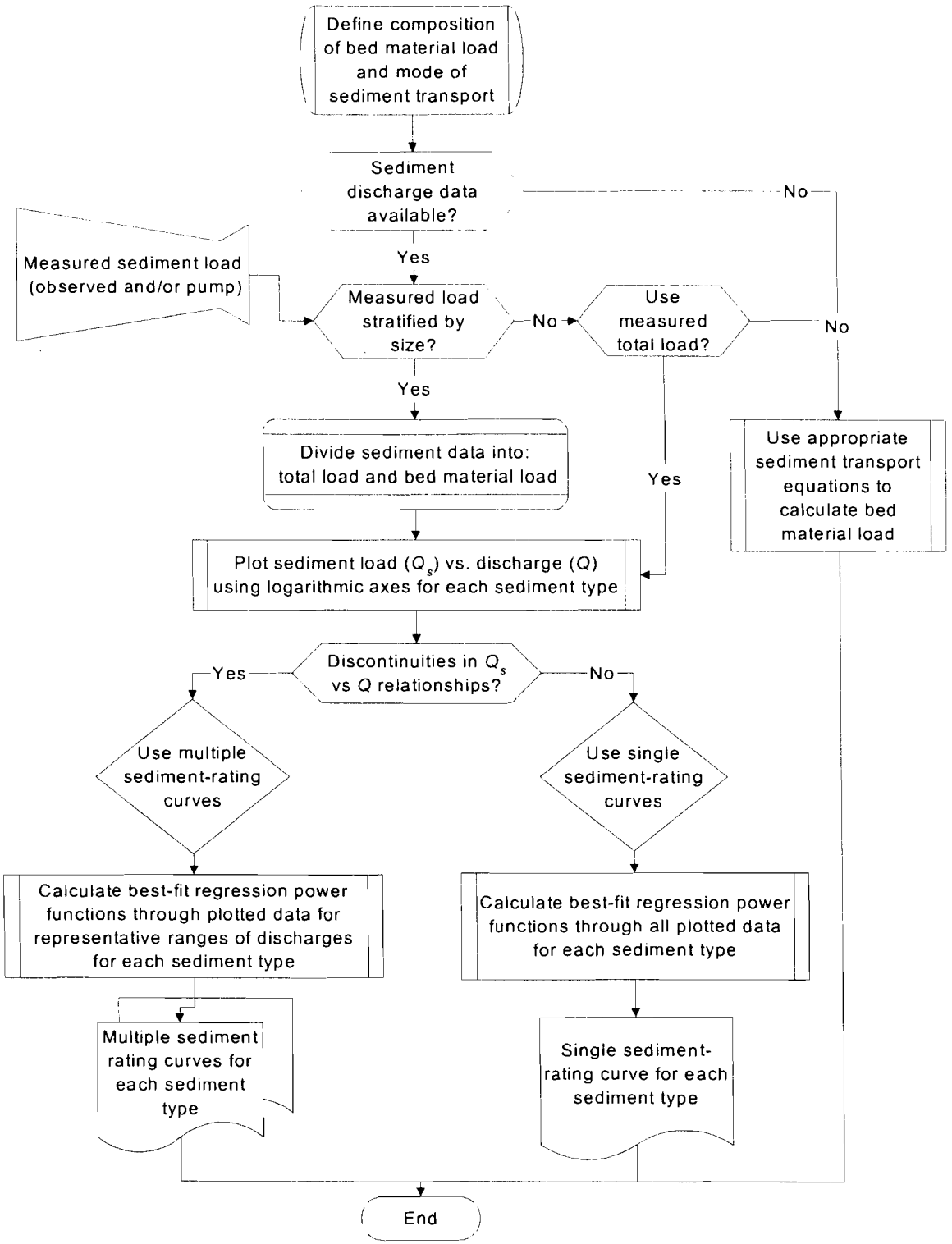

Figure 3.3 – Flow chart for generating sediment rating curves (after Soar 2000)

3.4.2.2 Determine sediment data availability

Sediment transport data are required to generate the bed material load rating curves for each site. Sediment data for each site were obtained in two ways; either from recorded suspended sediment measurements from USGS gauging stations or by using Yang's (1973) total sediment transport equation to determine the sediment transport for the ungauged DEC sites. Table 3.2 shows the period of record of sediment data for each of the USGS gauged sites and which DEC sites required the use of Yang's equation in order to determine the sediment transport. Sediment transport data using Yang's equation were calculated within the effective discharge program and therefore were not generated prior to executing the program.

Table 3.2 – Period of record for USGS and DEC sediment data

Station #	Station Name	Period of Record
Yazoo River Basin (DEC Streams)		Auto/Observed Sediment data
N/A	Abiaca 3 (DEC)	Yang's Equation
N/A	Abiaca 4 (DEC)	Yang's Equation
N/A	Fannegusha (DEC)	Yang's Equation
N/A	Harland 1 (DEC)	Yang's Equation
N/A	Harland 23 (DEC)	Yang's Equation
N/A	Hickahala 11(DEC)	Yang's Equation
N/A	Hickahala 22 (DEC)	Yang's Equation
N/A	Hotopha (DEC)	Yang's Equation
N/A	Otoucalofa(DEC)	Yang's Equation
N/A	Long (DEC)	Yang's Equation
7287160	Abiaca 21 near Cruger (DEC)	91-current
7287150	Abiaca 6 near Seven Pines (DEC)	91-current
7285400	Batupan Bogue near Grenada	86-current
7287355	Fannegusha near Howard	87,88,89,99
7287404	Harland near Howard	87-current
7277700	Hickahala near Senatobia	86-current
7273100	Hotopha near Batesville	86-current
7274252	Otoucalofa near Water Valley	85-current
7275530	Peters (Long) Creek near Pope	86-current
7277730	Senatobia (DEC)	86-90
7282090	Topashaw near Derma (DEC)	98-current
7281977	Yalobusha River @ Derma (DEC)	98-current
7281960	Yalobusha River @ Vardaman (DEC)	98-current

3.4.2.3 Plot sediment load data

Bed material load for each of the USGS sites was determined by removing the wash load from the suspended sediment samples. Four different types of sediment load data were investigated to determine the effects that sediment transport has on the effective discharge determination. The following are the four types of sediment data that were investigated: USGS automatic pump samples, observed sediment data obtained by USGS personnel, bed load data based on bed material gradations, and Yang's total sediment load equation. Sediment loads (y-axis) were plotted as a function of discharge (x-axis) on a scatter plot, with both axes on logarithmic scales. Figure 3.4 depicts a log-log form of total suspended sediment as a function of water discharge for Abiaca 21 near Cruger.

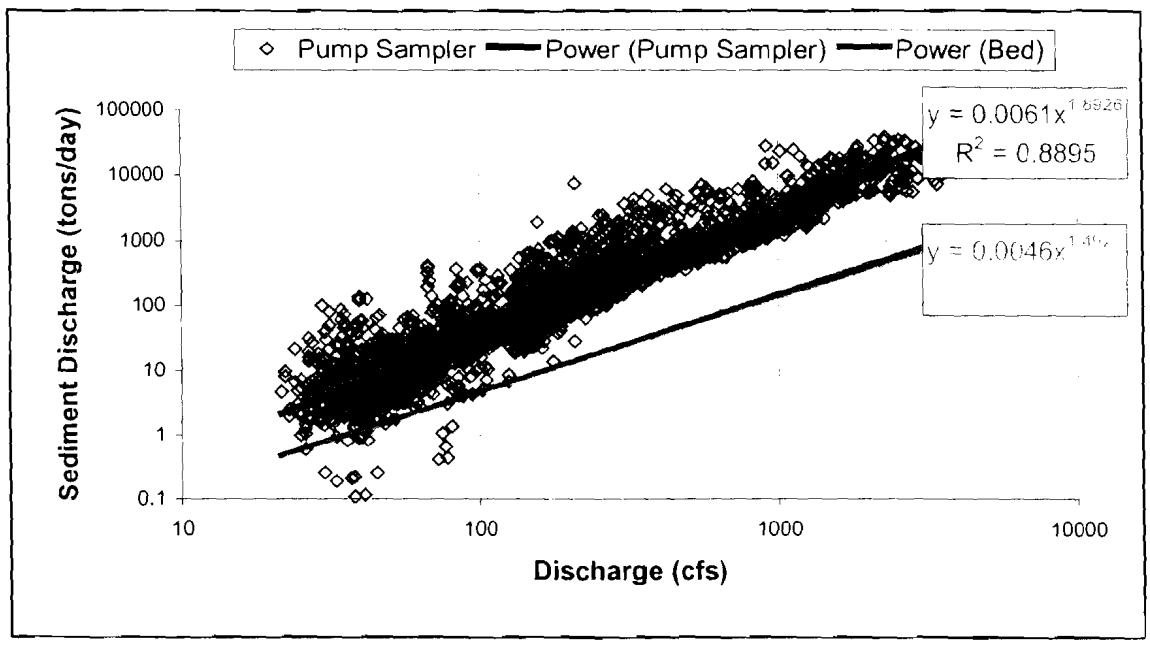

Figure 3.4 – Sediment-discharge data for Abiaca 21 near Cruger

3.4.2.4 Determine sediment-rating curves

A power function best-fit regression line was used to produce a sediment load function of the form given below:

$$Q_s = aQ^b \qquad \text{Equation 3.6}$$

Where:

Q_s = sediment discharge;

a = scale factor coefficient;

Q = discharge; and

b = shape factor coefficient.

Sediment rating regression constants for each USGS gauge are presented in Appendix B. The following define each of the sediment data types used in this study:

- Observed - sediment data were obtained from USGS personnel using depth-integrated suspended sediment samplers at various times throughout the year;
- Pump - sediment data were obtained from automatic stage-activated pump suspended sediment samplers;
- Bed - bed material sediment data were obtained by removing the wash load portion of the observed sediment data; and
- Yang - sediment regression data were obtained from the results of the effective discharge program given the required channel characteristics needed to use Yang's total sediment load equation.

Using hydraulic characteristics computed from HEC-RAS for the ungauged sites, total sand load was calculated for a range of discharges using Yang's total sediment load function. Figure 3.5 is a comparison of the four sediment types for Abiaca 21 near Cruger. From Figure 3.5, it is evident that the bed material load and Yang's total load rating curves are similar as well as the pump and observed rating curves. In determining the effective discharge, the bed load sediment-transport curve was used for gauged sites and Yang's sediment-transport curve was used for ungauged sites.

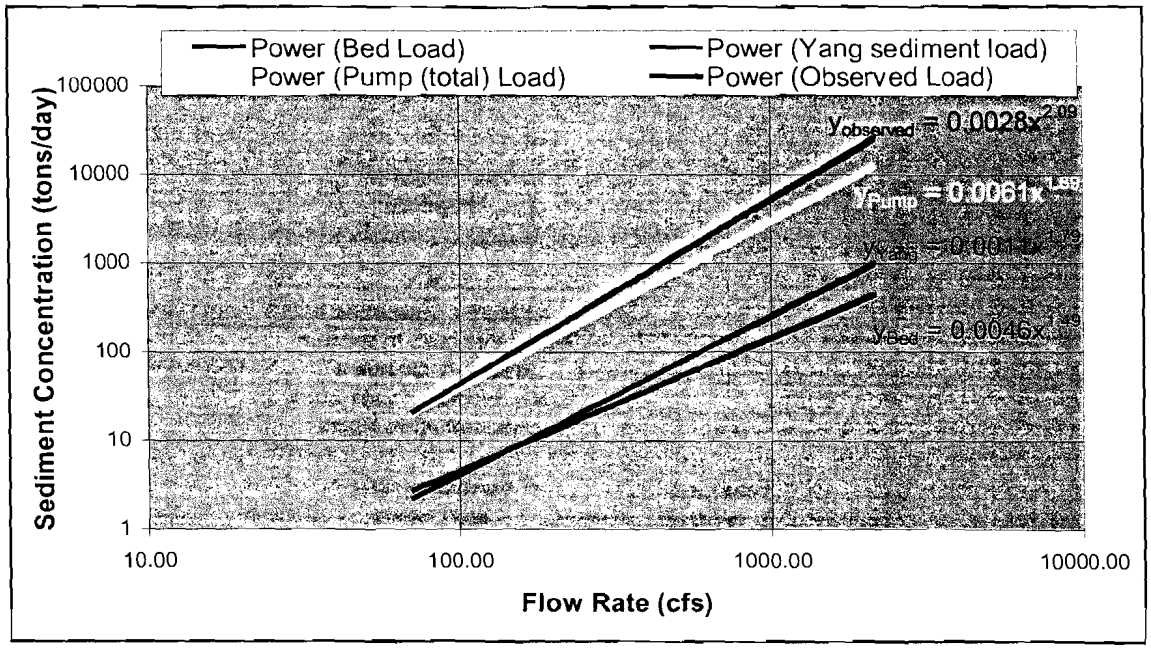

Figure 3.5 – Comparison of sediment-discharge rating curves for Abiaca 21 near Cruger

3.4.3 Sediment Load Histogram – Effective Discharge

The sediment load histogram was generated using the flow-frequency distributions and the calculated sediment transport functions presented above. General steps that were used to generate the sediment load histograms for each site are presented schematically in Figure 3.6 and are as follows:

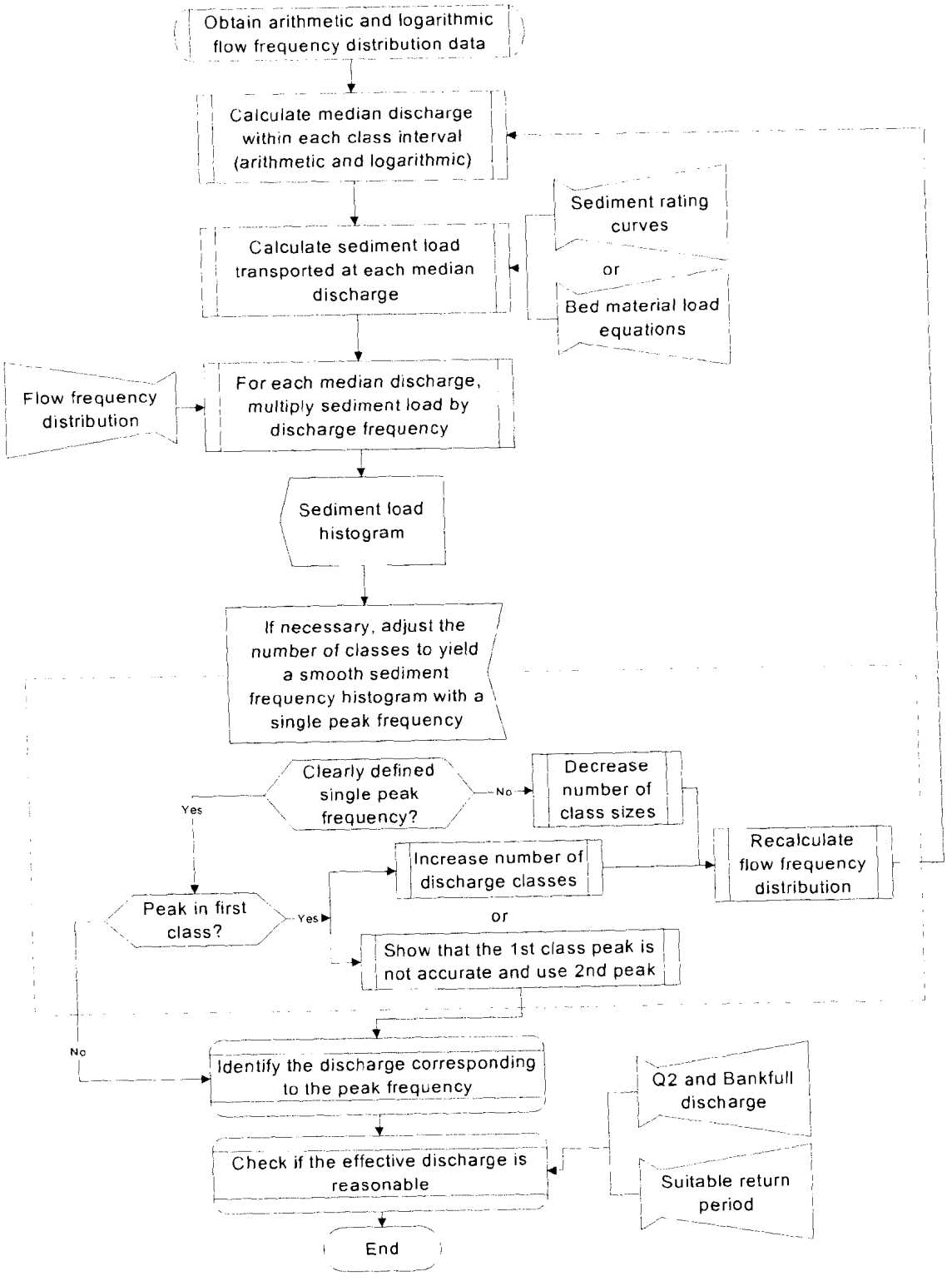

Figure 3.6 – Flow chart for generating sediment load histograms (after Soar 2000)

3.4.3.1 Calculate representative discharges

Discharges used to generate the bed material load histogram were the arithmetic mean discharges in each class of the flow-frequency distribution for arithmetic class divisions, and the geometric mean discharges in each class of the flow distribution for the logarithmic class divisions. These discharges were then used to construct the sediment load histograms.

3.4.3.2 Construct the sediment load histogram

Sediment transport rate for each discharge class was calculated from the sediment transport rating curves generated in Section 3.4.2. This load was then multiplied by the frequency of occurrence of that discharge class to find the average annual sediment load transported by that discharge class during the period of record. Results of the calculations were then plotted as a histogram. This facilitates the calculation of average annual sediment yield, which is the sum of the sediment loads in each discharge class. Tables 3.3 and 3.4 are examples of the arithmetic and logarithmic sediment load histogram results for Abaica 21 near Cruger using fifty bins, respectively. Due to the large amount of data in the result tables (50 rows), only part of the tables are presented.

Table 3.3 – Arithmetic sediment load histogram for Abiaca 21 near Cruger

Reference #	Bin Size	Bin Probability	Sediment Concentration (x1000 tons/day)	Product (tons/day)	Total Sediment Yield (tons/day)
1	71.13	0.68895	0.0019	1.3323	**16.54**
2	142.26	0.20312	0.0074	1.4931	
3	213.38	0.04357	0.0157	0.6850	
4	284.51	0.01559	0.0267	0.4166	
5	355.64	0.00895	0.0401	0.3594	
6	426.77	0.00625	0.0558	0.3485	
7	497.90	0.00447	0.0735	0.3287	
8	569.02	0.00308	0.0933	0.2876	
9	640.15	0.00238	0.1149	0.2735	
10	711.28	0.00238	0.1384	0.3293	
11	782.41	0.00192	0.1636	0.3148	
12	853.53	0.00173	0.1905	0.3294	
13	924.66	0.00144	0.2189	0.3146	
14	995.79	0.00151	0.2490	0.3758	
15	1066.92	0.00140	0.2806	0.3921	
16	1138.05	0.00120	0.3136	0.3760	
17	1209.17	0.00115	0.3481	0.4010	
18	1280.30	0.00142	0.3840	0.5449	
19	1351.43	0.00081	0.4213	0.3423	
20	1422.56	0.00075	0.4599	0.3437	
21	1493.69	0.00086	0.4998	0.4313	
22	1564.81	0.00070	0.5410	0.3809	
23	1635.94	0.00068	0.5834	0.3939	
24	1707.07	0.00048	0.6270	0.3034	
25	1778.20	0.00066	0.6719	0.4415	
26	1849.32	0.00050	0.7179	0.3603	
27	1920.45	0.00035	0.7651	0.2707	
28	1991.58	0.00026	0.8135	0.2085	
29	2062.71	0.00028	0.8629	0.2399	
30	2133.84	0.00042	0.9135	0.3793	
31	2204.96	0.00032	0.9651	0.3136	
32	2276.09	0.00033	1.0178	0.3344	
33	2347.22	0.00022	1.0715	0.2321	
.	.	.	.	.	
.	.	.	.	.	
.	.	.	.	.	
45	3200.75	0.00002	1.7934	0.0324	
46	3271.88	0.00001	1.8596	0.0134	
47	3343.01	0.00006	1.9267	0.1183	
48	3414.14	0.00003	1.9946	0.0648	
49	3485.27	0.00000	2.0634	0.0075	
50	3556.39	0.00002	2.1331	0.0385	

Table 3.4 – Logarithmic sediment load histogram for Abiaca 21 Creek near Cruger

Reference #	Bin Size	Bin Probability	Sediment Concentration (x1000 tons/day)	Product (tons/day)	Total Sediment Yield (tons/day)
1	0.00	0.00000	0.0000	0.0000	**15.54**
2	13.61	0.00001	0.0001	0.0000	
3	15.28	0.00006	0.0001	0.0000	
4	17.16	0.00088	0.0001	0.0001	
5	19.27	0.00249	0.0001	0.0003	
6	21.64	0.00813	0.0002	0.0014	
7	24.31	0.01912	0.0002	0.0042	
8	27.30	0.03404	0.0003	0.0096	
9	30.65	0.05351	0.0004	0.0191	
10	34.43	0.07125	0.0005	0.0323	
11	38.66	0.07508	0.0006	0.0430	
12	43.42	0.08839	0.0007	0.0641	
13	48.76	0.08708	0.0009	0.0797	
14	54.76	0.08880	0.0012	0.1024	
15	61.50	0.08033	0.0015	0.1167	
16	69.06	0.06672	0.0018	0.1218	
17	77.56	0.04923	0.0023	0.1128	
18	87.10	0.05087	0.0029	0.1461	
19	97.82	0.03521	0.0036	0.1266	
20	109.86	0.03088	0.0045	0.1387	
21	123.37	0.02622	0.0056	0.1470	
22	138.55	0.01944	0.0070	0.1359	
23	155.60	0.01850	0.0087	0.1611	
24	174.75	0.01366	0.0108	0.1479	
25	196.25	0.00994	0.0135	0.1337	
26	220.39	0.00786	0.0167	0.1311	
27	247.51	0.00669	0.0207	0.1384	
28	277.96	0.00555	0.0256	0.1421	
29	312.16	0.00526	0.0317	0.1666	
30	350.57	0.00455	0.0391	0.1780	
31	393.71	0.00410	0.0482	0.1979	
32	442.15	0.00370	0.0595	0.2198	
33	496.55	0.00326	0.0732	0.2386	
.	.	.	.	.	
.	.	.	.	.	
.	.	.	.	.	
45	1998.46	0.00112	0.8182	0.9128	
46	2244.35	0.00118	0.9941	1.1773	
47	2520.49	0.00076	1.2068	0.9194	
48	2830.60	0.00084	1.4635	1.2365	
49	3178.88	0.00049	1.7732	0.8643	
50	3570.00	0.00014	2.1465	0.2945	

3.4.3.3 Find the effective discharge

Soar (2000) suggested that the sediment load histogram should display a continuous distribution with a single mode (peak). When this is the case, the effective discharge corresponds to the mean discharge of the modal class (that is, the discharge class that corresponded to the peak of the sediment load histogram). However, when the peak of the sediment load histogram occurs in the first bin or is multi-modal, additional analysis is required in order to determine the effective discharge. This was the case for all of the arithmetic effective discharge calculations and seven of the logarithmic calculations performed in this study (Figures 3.7 and 3.8, respectively).

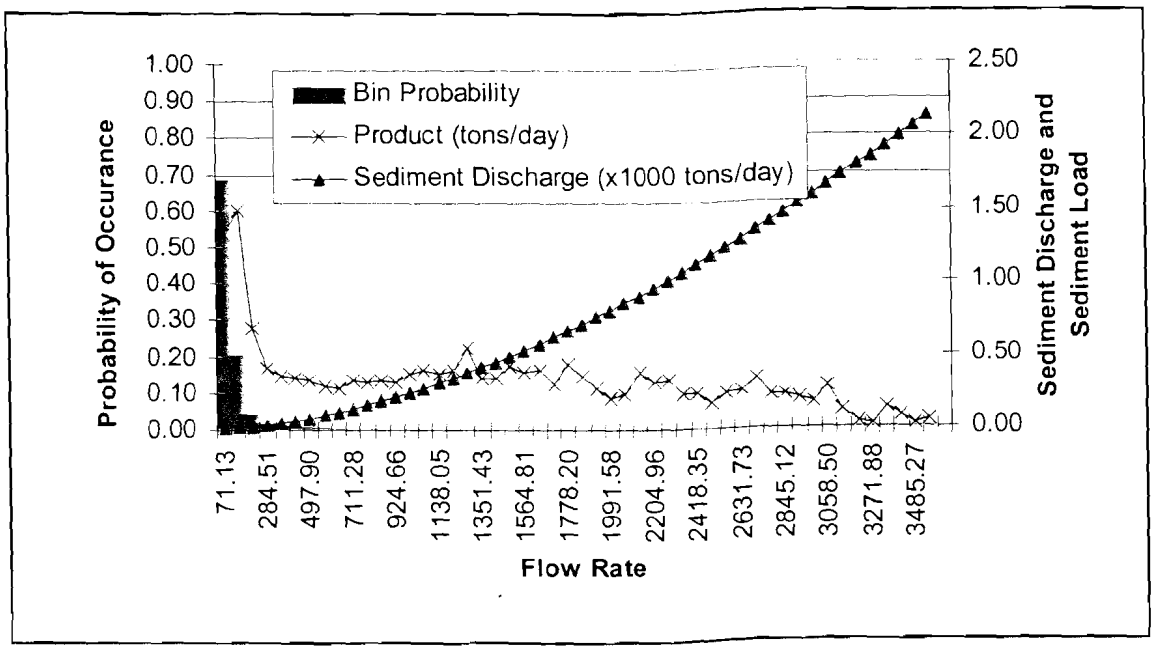

Figure 3.7 – Arithmetic effective discharge plot for Abaica 21 near Cruger (50 bins)

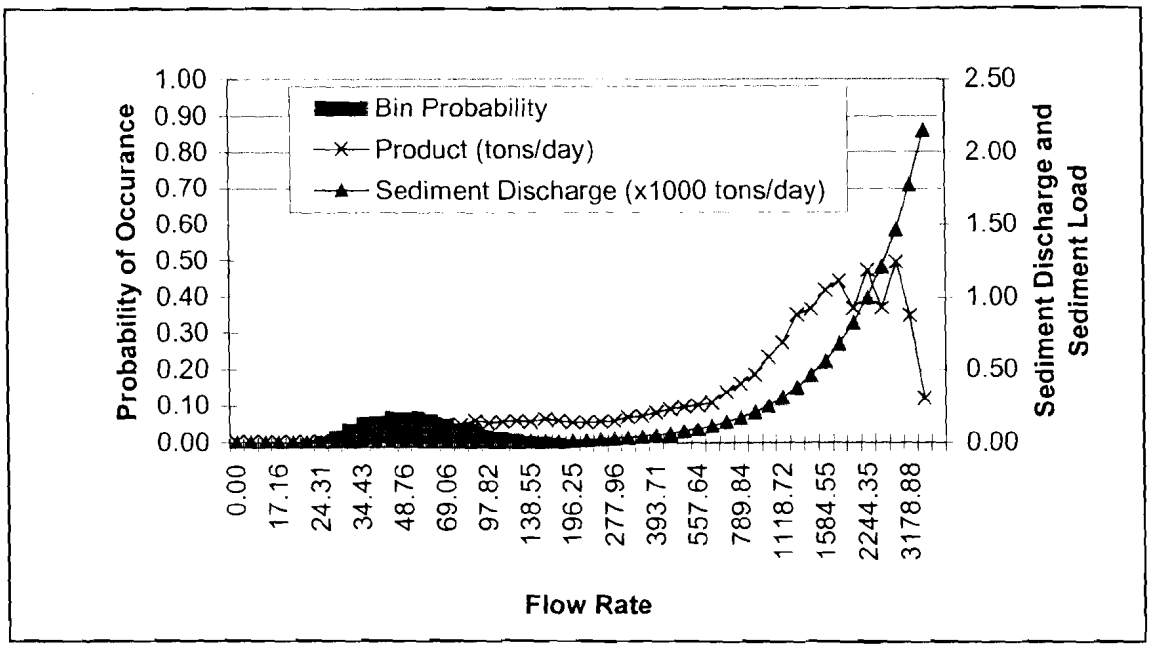

Figure 3.8 – Logarithmic effective discharge for Abiaca 21 near Cruger (50 bins).

Biedenharn and Thorne (1994) determined that the effective discharge for the Mississippi River occurred over a range of flows that transported approximately 55% of the total sediment yield. As a result, the cumulative distribution function (CDF) plots of sediment transport for DEC streams versus discharge were used to graphically interpret the range of flows that appeared to transport the largest amount of sediment (Figure 3.9). The percent of sediment transported by the initial effective discharge calculation was added to this graph to determine whether the amount of sediment being transported was within the range presented by Biedenharn and Thorne (1994).

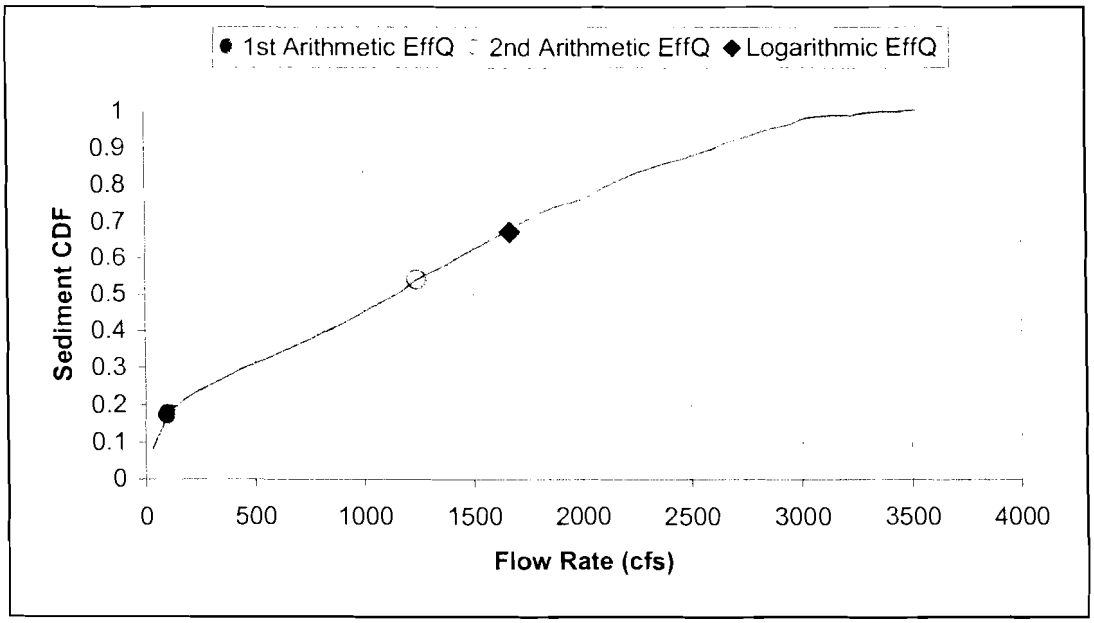

Figure 3.9 – Arithmetic sediment CDF plot for Abaica 21 near Cruger (50 bins)

Figure 3.9 shows that the effective discharge associated with the first arithmetic bin for Abiaca 21 transports approximately seventeen percent of the total sediment yield while the second arithmetic peak transports approximately fifty-four percent of the total sediment yield. Based on the findings of Biedenharn and Thorne (1994), it was determined that the effective discharge most likely does not occur in the first bin, and the second peak was used as the effective discharge (Figure 3.9). In order to use the second arithmetic peak in determining the effective discharge, a systematic method for eliminating the first arithmetic peak had to be established. As a result, if the discharge associated with the first arithmetic bin was less than the mean discharge and accounted for less than twenty percent of the flow area, then the first bin was ignored and the second peak of the sediment load histogram was used to determine the effective discharge. However, if the discharge associated with the first bin was greater than the mean discharge or accounted for more than twenty percent of the flow area, then the first bin

was used in determining the effective discharge. The above procedure was used to determine the effective discharge for each site.

3.4.3.4 Check if the effective discharge is reasonable

Once the effective discharge was determined, it was important to check that the effective discharge for each site was within a reasonable range. Return period for the effective discharge varies between sites because the value reflects the flow and sediment transport regime for each site. For each site, the return period of the calculated effective discharge was checked to ensure that it was within acceptable bounds. Regionalized frequency curves were used to determine the 2-year return flow and compared to the calculated effective discharge. Predicted effective discharge return periods outside the range of 1 to 3 years were queried (Thorne et. al, 1998).

An additional check compared the percent of total sediment yield transported by the calculated effective discharge. From the findings of Biedenharn and Thorne (1994), the percent of sediment transported by the effective discharge was expected to be around fifty-five percent. This value was used as a check to determine whether the sediment transported by the calculated effective discharge is reasonable.

Finally, a morphological check was conducted; a comparison of the effective discharge to observed minimum discharges required for substantial sediment transport. Observed minimum discharges were determined during field reconnaissance by measuring the bed material load transported at low discharges using bed load sediment traps in conjunction with depth-integrated suspended sediment samples.

Bed load sediment traps were designed and constructed to better define the proportion of bed material load that is transported at various low flows. Figure 3.10 is a photo of one of the sediment traps used in this study.

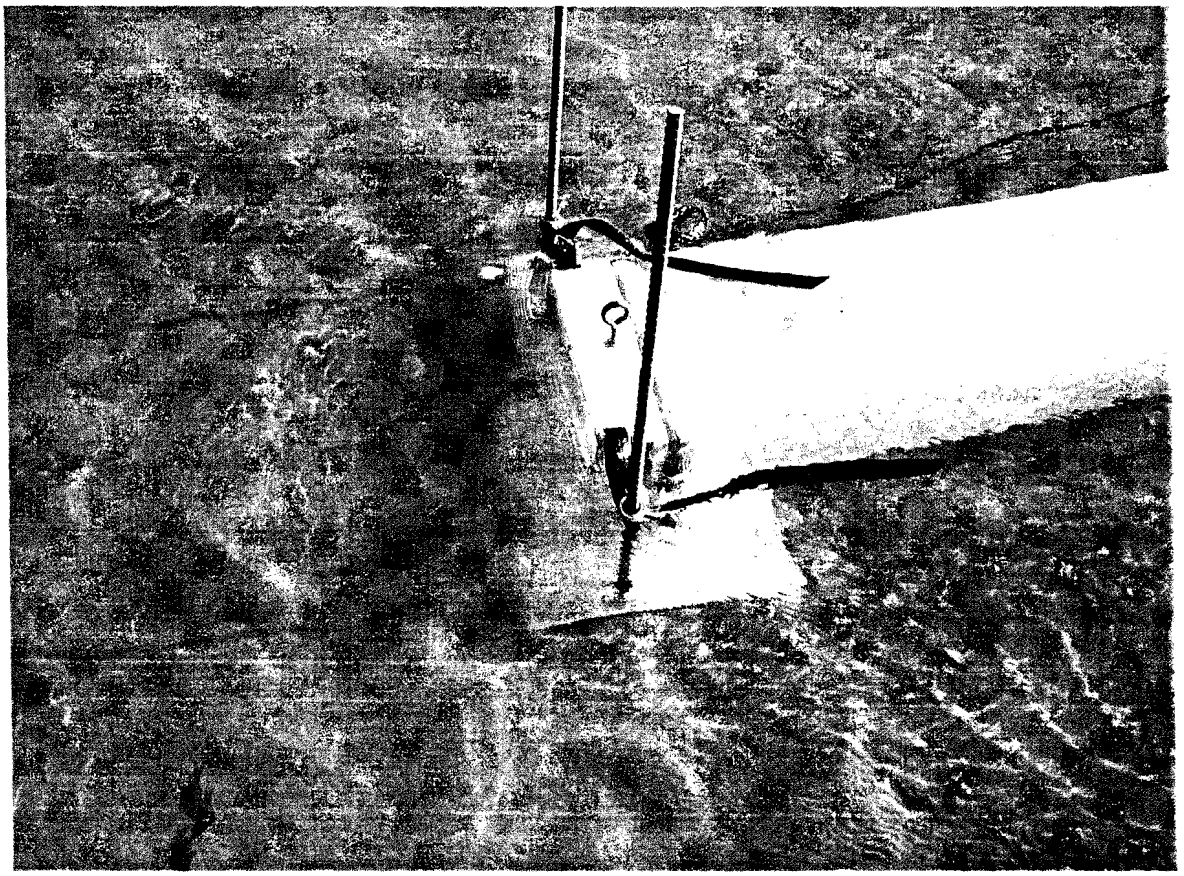

Figure 3.10 – Bed material load sediment trap

Sediment traps consist of three major parts: base plate, trap opening, and a six-foot 0.0625 mm mesh sampling bag. The base plate was placed along the bed of the channel and rebar was used to hold the base plate and sediment trap in place. Sediment trap and sampling bag were then placed on top of the base plate and secured in place using rebar and eye hooks (Figure 3.10). Sediment traps were dispersed across the width of the stream and were left in the stream for an average of three hours while suspended sediment samples and discharge measurements were made, representing a single low-

flow discharge at each site. Sediment traps were then removed from the stream and the sediment from each trap was collected. Sediment samples were then analyzed to determine the grain size distribution and amount of bed material load collected for each site. In addition to the bed material load, suspended sediment load was also collected using depth-integrated samples to determine the total sediment load for each stream.

Suspended sediment samples were analyzed for total suspended solids (TSS) according to the procedures described in the Standard Methods for Examination of Water and Wastewater (1998). A 47-mm, 1 μm pore-size filter disc was weighed to the nearest 0.1 mg using a Mettler AE 100 balance. The filter was then placed in a filter holder and adjusted in a filtering flask. A representative, well-mixed sediment sample (150 to 600 mL) was then filtered by applying a vacuum to the flask. After filtering, the filter was removed and placed in a drying oven at 103°C. After twenty-four hours, the filter was removed and weighed. Total suspended solids were then calculated as follows:

$$TSS(mg/L) = (A - B)/C \qquad \text{Equation 3.7}$$

where:

TSS = total suspended solids

A = weight of the filter disk with dried residue (mg);

B = weight of the filter disk (mg); and

C = sample volume (L).

Based on the results of the observed sediment transport at these low flows, a minimum discharge required to morphologically alter the channel was estimated by determining the amount of bed load that was transported at the corresponding low flows. Results showed that the amount of sediment that was being transported within the stream

at these low flows was negligible and therefore was not changing the morphology of the channel.

3.4.4 Summary

Using the procedures stated above, sediment load histograms were determined for each of the twenty-three sites within the Yazoo River Basin using 15-minute discharge records and both arithmetic and logarithmic class divisions for numerous class sizes. After analyzing the results of the effective discharge calculations and performing the checks stated above, the most representative effective discharge for each site was determined. Appendix C shows graphical results of the effective discharge computations using fifty arithmetic and logarithmic class divisions.

3.5 Effective Discharge Program

The following sections provide general information about how to run the effective discharge program that was written for this study. The effective discharge program used in this study was written by: Brian McCaig, Lejo Flores, and Chris Holmquist-Johnson. All of the calculations performed within the effective discharge program follow the procedures presented in the previous sections. General inputs that are required by the program to calculate effective discharge consist of the following three items: (1) discharge data, (2) sediment transport data, and (3) bin size information. Discharge data, sediment data, and bin information used to evaluate the effective discharge for each of the twenty-three sites are presented in Appendix D.

3.5.1 Inputs and Execution of the Program

The general process for executing the effective discharge program consisted of six steps: (1) creating a discharge input file, (2) selecting the range of years to analyze, (3)

selecting method of sediment transport calculations, (4) if available, selecting a minimum flow required to transport sediment, (5) selecting bin size information, and (6) selecting the type of output options that are of interest.

3.5.1.1 Step 1 – Creating the discharge input file

The format of the discharge data required by the effective discharge program consists of three general columns: date and time, stage, and discharge. Each water year is represented by a new set of columns and the program allows a total of seventy-eight years of flow data to be analyzed at one time. The time interval of the discharge data is not limited, but 15-minute discharge data were used in this study. Table 3.5 is an example of the discharge input sheet used for Senatobia Creek. Because of the length of the discharge files (approximately 35,000 data points per year for 15-minute flow data) only a portion of the input file is presented.

Table 3.5 – Discharge input file for Senatobia Creek

1995			1996			1997		
Time	Stage	Q	Time	Stage	Q	Time	Stage	Q
10/1/94 0:15	10.07	12	10/1/95 0:15	9.37	11	10/1/96 0:15	4.44	15
10/1/94 0:30	10.07	12	10/1/95 0:30	9.37	11	10/1/96 0:30	4.43	15
10/1/94 0:45	10.07	12	10/1/95 0:45	9.37	11	10/1/96 0:45	4.43	15
10/1/94 1:00	10.07	12	10/1/95 1:00	9.37	11	10/1/96 1:00	4.44	15
10/1/94 1:15	10.07	12	10/1/95 1:15	9.38	12	10/1/96 1:15	4.44	15
10/1/94 1:30	10.07	12	10/1/95 1:30	9.38	12	10/1/96 1:30	4.44	15
10/1/94 1:45	10.07	12	10/1/95 1:45	9.38	12	10/1/96 1:45	4.43	15
10/1/94 2:00	10	10	10/1/95 2:00	9.38	12	10/1/96 2:00	4.43	15
10/1/94 2:15	10.01	11	10/1/95 2:15	9.38	12	10/1/96 2:15	4.44	15
10/1/94 2:30	10.01	11	10/1/95 2:30	9.38	12	10/1/96 2:30	4.44	15
10/1/94 2:45	10.01	11	10/1/95 2:45	9.39	12	10/1/96 2:45	4.43	15
10/1/94 3:00	10.01	11	10/1/95 3:00	9.39	12	10/1/96 3:00	4.43	15
10/1/94 3:15	10	10	10/1/95 3:15	9.39	12	10/1/96 3:15	4.43	15
10/1/94 3:30	10.01	11	10/1/95 3:30	9.39	12	10/1/96 3:30	4.43	15
10/1/94 3:45	10	10	10/1/95 3:45	9.39	12	10/1/96 3:45	4.43	15

Once the discharge input sheet was created, the effective discharge program was executed. Figure 3.11 is an example of the input screen that appears once the program is started.

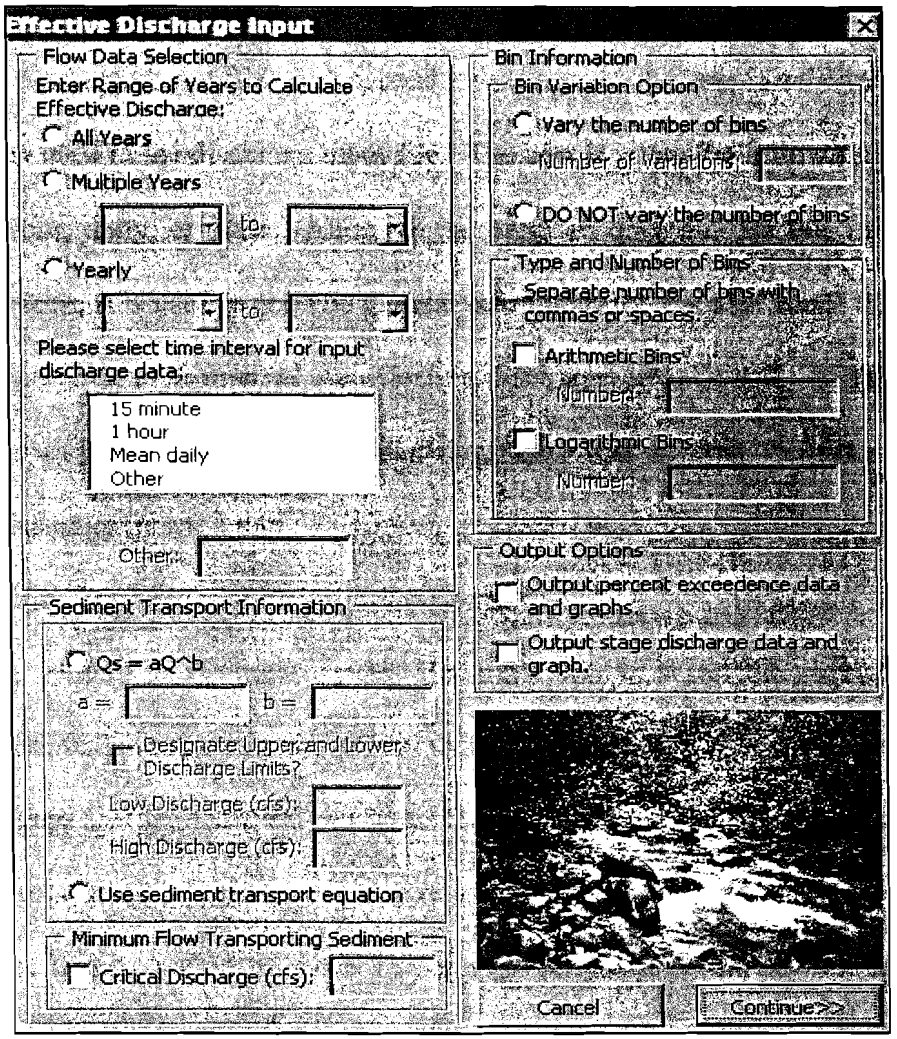

Figure 3.11 – Example input screen for effective discharge program

3.5.1.2 Step 2 – Selecting the range of years to analyze

The first section of the input screen has two general sections that require inputs (Figure 3.11). First of these consists of selecting the range of years for which the effective discharge should be calculated. Second consists of selecting the time interval used for the discharge data.

The first input allows the user to determine the effective discharge in three different ways: using the entire period of record, a specified range of years, or each year within the period of record individually. By allowing the user to select a range of years, the effective discharge for a period of record of interest can be determined without having to alter the discharge input file. The second input requires the user to select the discharge time interval used in the discharge input file. The user is given the following options: 15-minute, 1-hour, daily, or other. Although the program does not use this information in any calculations, it is used to provide general information to the user about the validity of using the specified time interval for effective discharge calculations. In this study, the entire range of flows and 15-minute discharge data was used in the determination of effective discharge for each site.

3.5.1.3 Step 3 – Sediment transport functions

This section of the input screen allows the user to select the sediment transport function that will be used in the effective discharge calculations. The user has two options (Figure 3.11): a sediment-rating curve, or a sediment transport equation.

The sediment-rating curve option requires the user to enter values for the a and b coefficients. Determination of these values was discussed previously in Section 3.4.2. Additionally, the user had the option to enter an upper- and lower-bound discharge for which the sediment-rating curves are valid. If sediment data are not available in order to determine these coefficients, then the user must use a sediment transport equation. Selecting the sediment transport equation option results in the program calling a sediment transport module, and the following information is required in order to use the sediment equation option: energy slope, median grain size (d_{50}), hydraulic radius as a function of

discharge, and the channel roughness. The current program allows the user to select the following sediment transport equations: Yang's sand d_{50}, Brownlie, Meyer-Peter and Muller, Parker, and Bagnold total load. Based on the channel characteristics of the sites in this study, Yang's d_{50} equation was used for sites where sediment data were not available. Appendix D contains a list of the inputs used for Yang's equation for each site in this study.

Figures 3.12 and 3.13 are examples of the sediment transport equation input screens for Yang's sand d_{50}.

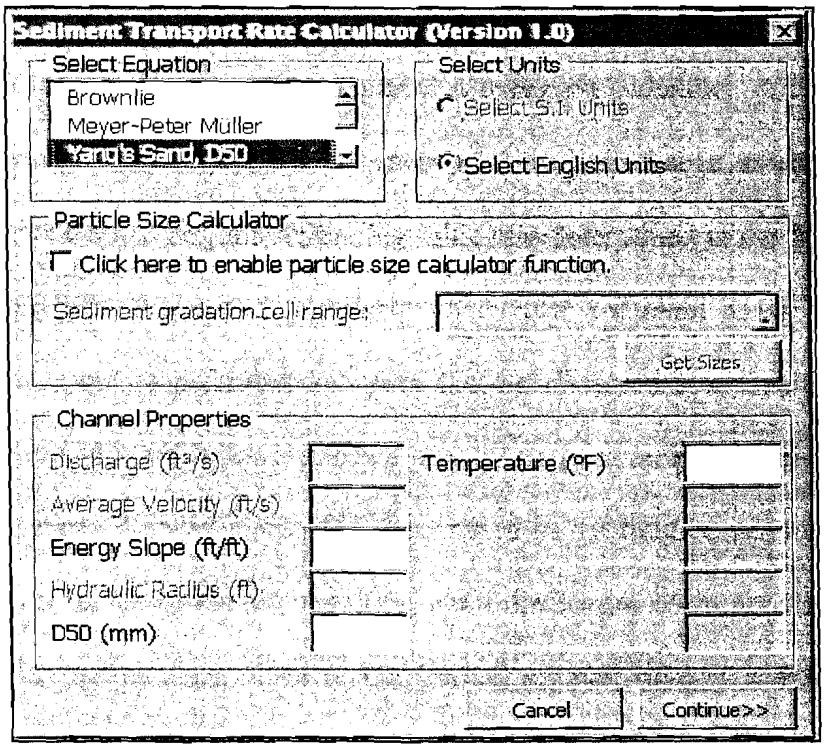

Figure 3.12 – Input screen for sediment transport equation option

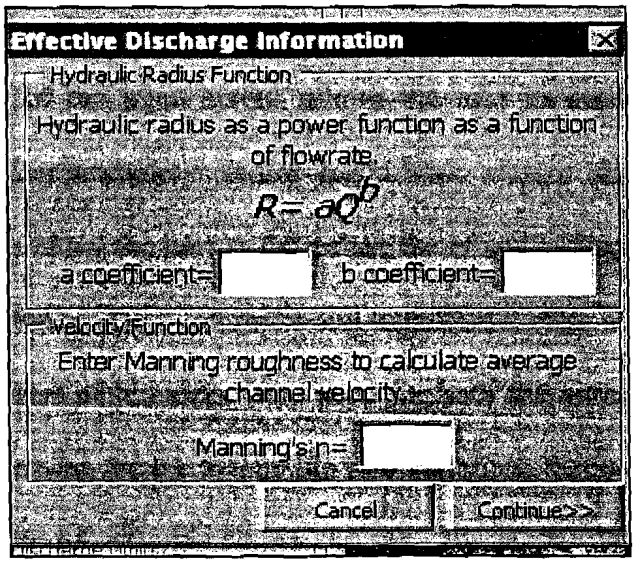

Figure 3.13 – Input screen for Yang's sand d_{50} sediment transport equation

3.5.1.4 Step 4 – Minimum flow required to transport sediment

This option allows the user to enter a critical discharge at which sediment transport does not occur. For this study, this value was determined in the field for a given low-flow discharge. As stated previously, bed load sediment traps were used to determine the amount of sediment transported at an observed low-flow discharge. In gravel bed streams, this value corresponds to the discharge at incipient motion. However, for sand bed streams, this value must be determined in the field because of the extreme instability of sand particles and the resulting small discharges corresponding to incipient motion for sand bed streams. Due to the limited amount of data obtained using the sediment traps, presented in section 3.4.3.4, this value was left blank. If data are not available to determine this value, then it may be left blank and the program will ignore this input.

3.5.1.5 Step 5 – Bin size information

This section of the input screen allows the user to select the number of bin variations and whether arithmetic and/or logarithmic classes should be used (Figure 3.11). These options allow the user to determine the effective discharge for a number of bin sizes as well as for both the arithmetic and logarithmic class size divisions. For this study, twenty variations of bin sizes were used for both the arithmetic and logarithmic class sizes. The following are the twenty bin size variations that were used in this study: 5, 10, 15, 20, 25, 30, 35, 40, 45, 50, 55, 60, 65, 70, 75, 80, 90, 100, 125, and 150. Arithmetic and logarithmic class sizes were selected in order to compare the resulting effective discharge for each method.

3.5.1.6 Step 6 – Output options

This section of the input screen allows the user to select two additional outputs of the program (Figure 3.11): a stage-discharge plot, and a CDF plot of time, discharge, and sediment load. The stage-discharge plot uses the stage and discharge information on the input sheet to construct a stage-discharge plot for the period of record. As a result, if the input sheet does not have stage data, this option cannot be selected. For this study, both the stage discharge and the percent exceedence plots were selected. As stated previously, the percent exceedence plot of sediment load was used to analyze and validate the results of the effective discharge computations.

3.5.2 Outputs of the Program

Once the program has been executed, a number of sheets are generated containing the outputs of the program. The following section provides a general description of each output sheet that was generated in this study. Given the input requirements presented above, the following are the output sheets that are generated for each bin size variation

and class size method. If both arithmetic and logarithmic class sizes are selected, a total of seven sheets of output are generated for each bin size variation: arithmetic effective discharge plot, arithmetic output data, arithmetic percent exceedence, logarithmic effective discharge plot, logarithmic output data, logarithmic percent exceedence, and a summary sheet that shows the results of all the calculations for each bin variation. The summary sheet also generates a discharge frequency as well as a summary of standard statistics (mean, median, skew, and standard deviation) for the period of record. The following sections take a closer look at each of these output sheets.

3.5.2.1 Effective discharge plot

Effective discharge plots consists of three series; the flow frequency histogram, sediment-transport curve, and the sediment load histogram for both the arithmetic and logarithmic class divisions. Figures 3.14 and 3.15 are examples of the arithmetic and logarithmic effective discharge plots for Long Creek, respectively.

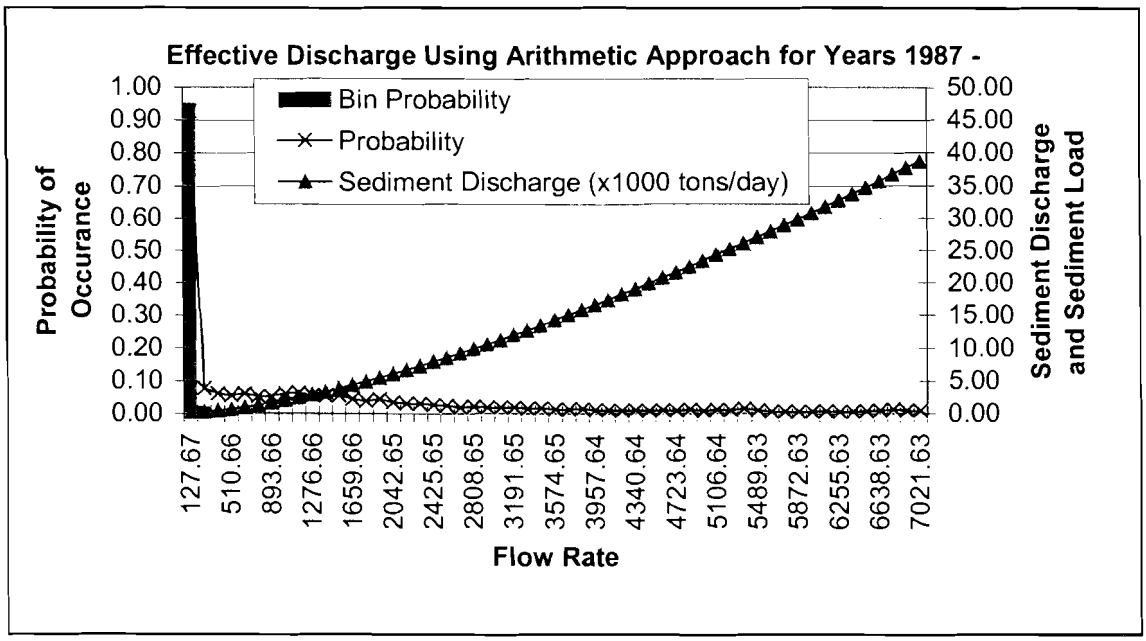

Figure 3.14 – Long Creek arithmetic effective discharge plot for 55 bins

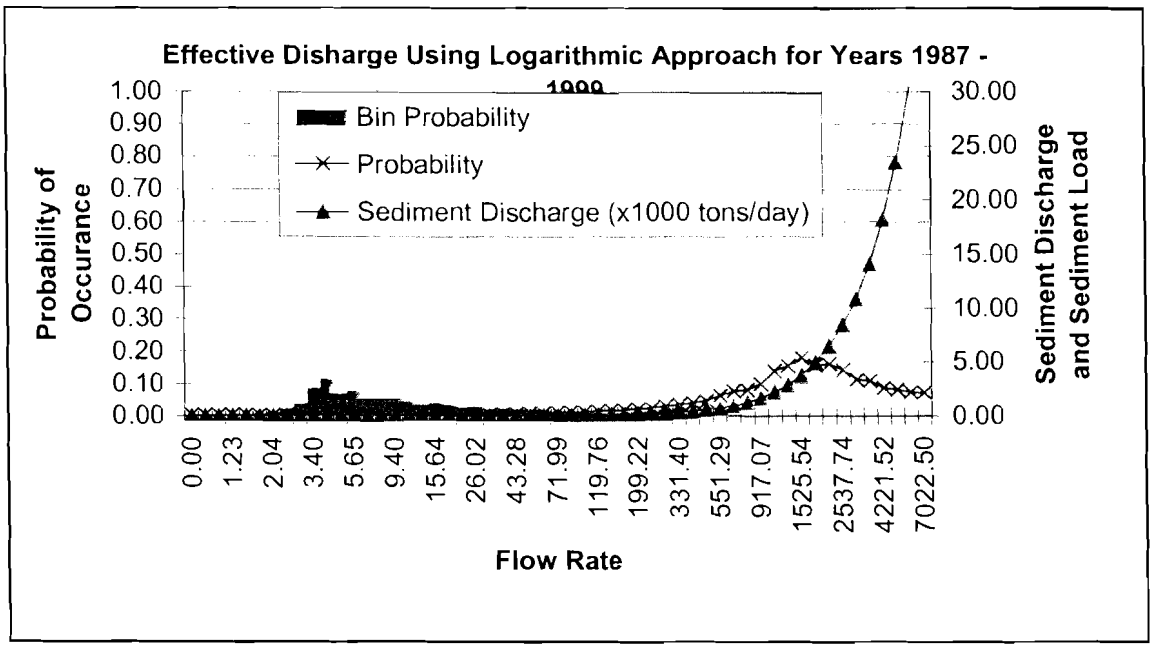

Figure 3.15 – Long Creek logarithmic effective discharge plot for 55 bins

Effective discharge plots are used as a graphical interpretation of each part of the effective discharge computation. The three series provide a graphical interpretation of the flow frequency, sediment transport, and total sediment load for the period of record for each site of interest. Effective discharge plots are generated from data that are obtained from the effective discharge data sheets.

3.5.2.2 Effective discharge data

Effective discharge data sheets are generated using the procedures presented previously and summarize the results of the effective discharge computations for each bin size variation. Table 3.6 is an example of an effective discharge data sheet for Long Creek for fifty-five arithmetic bins. Data sheets contain flow frequency, sediment transport, total sediment load for each bin size, and total sediment yield for the period of record. Highlighted rows are the effective discharges that the program calculated using

the first and second peaks of the sediment load histogram. The first peak is highlighted in yellow, whereas the second peak is highlighted in light blue.

Table 3.6 – Effective discharge data sheet for Long Creek (55 arithmetic bins)

Effective Discharge Output (55 Arithmetic Bins) 1987-1999									
		Min Q	0.8745						
		Max Q	7022.5						
Number of Intervals			55						
Interval Index			127.67						
Ref #	Bin Size	Mean Q	Freq	Bin Prob	PDF	CDF	Sed Q (x1000 tons/day)	Product (tons/day)	Total Sediment Yield (tons/day)
1	127.67	63.83	468635	0.95127	0.00E+0	0.95127	0.0486	46.2221	**103.53**
2	255.33	191.50	10297	0.02090	1.64E-04	0.97217	0.1757	3.6720	
3	383.00	319.16	3983	0.00808	6.33E-05	0.98025	0.3625	2.9311	
4	510.66	446.83	2180	0.00443	3.47E-05	0.98468	0.5991	2.6513	
5	638.33	574.50	1618	0.00328	2.57E-05	0.98796	0.8789	2.8866	
6	766.00	702.16	1060	0.00215	1.69E-05	0.99011	1.1971	2.5758	
7	893.66	829.83	784	0.00159	1.25E-05	0.99170	1.5500	2.4668	
8	1021.3	957.49	753	0.00153	1.20E-05	0.99323	1.9348	2.9573	
10	1276.6	1212.8	462	0.00094	7.35E-06	0.99544	2.7906	2.6170	
11	1404.3	1340.4	390	0.00079	6.20E-06	0.99623	3.2579	2.5791	
12	1531.9	1468.1	349	0.00071	5.55E-06	0.99694	3.7493	2.6561	
13	1659.6	1595.8	232	0.00047	3.69E-06	0.99741	4.2636	2.0078	
14	1787.3	1723.4	184	0.00037	2.93E-06	0.99779	4.7996	1.7926	
15	1914.9	1851.1	193	0.00039	3.07E-06	0.99818	5.3562	2.0983	
16	2042.6	1978.8	127	0.00026	2.02E-06	0.99844	5.9324	1.5293	
17	2170.3	2106.4	102	0.00021	1.62E-06	0.99864	6.5276	1.3515	
18	2297.9	2234.1	95	0.00019	1.51E-06	0.99884	7.1407	1.3770	
19	2425.6	2361.8	77	0.00016	1.22E-06	0.99899	7.7713	1.2146	
20	2553.3	2489.4	61	0.00012	9.70E-07	0.99912	8.4185	1.0424	
21	2680.9	2617.1	43	0.00009	6.84E-07	0.99920	9.0818	0.7927	
22	2808.6	2744.8	47	0.00010	7.47E-07	0.99930	9.7607	0.9312	
23	2936.3	2872.4	35	0.00007	5.56E-07	0.99937	10.4545	0.7427	
24	3063.9	3000.1	36	0.00007	5.72E-07	0.99944	11.1629	0.8157	
50	6383.3	6319.4	2	0.00000	3.18E-08	0.99996	33.5967	0.1364	
51	6510.9	6447.1	3	0.00001	4.77E-08	0.99996	34.5846	0.2106	
52	6638.6	6574.7	4	0.00001	6.36E-08	0.99997	35.5801	0.2889	
53	6766.2	6702.4	6	0.00001	9.54E-08	0.99998	36.5831	0.4456	
54	6893.9	6830.1	4	0.00001	6.36E-08	0.99999	37.5936	0.3052	
55	7021.6	6957.7	4	0.00001	6.36E-08	1.00000	38.6114	0.3135	

3.5.2.3 Percent exceedence data

Percent exceedence data sheets and plots are used to determine what percentage of the total sediment yield is transported by a specified discharge. This allows the user to determine a range of discharges that transport an amount of sediment over a specified period of record. Table 3.7 and Figure 3.16 are examples of the arithmetic percent exceedence data sheet for Long Creek.

Table 3.7 – Arithmetic percent exceedence data sheet for Long Creek

Percent Exceedence Output (55 Arithmetic Bins)						
Bin Size	**Bin Prob**	**CDF**	**Sediment Product (tons/day)**	**Sediment PDF**	**Sediment CDF**	**Total Sediment Yield (tons/day)**
127.67	0.95127	0.9513	46.222	0.446	0.446	103.53
255.33	0.0209	0.9722	3.672	0.035	0.481	
383	0.00808	0.9803	2.931	0.028	0.509	
510.66	0.00443	0.9847	2.651	0.026	0.535	
638.33	0.00328	0.988	2.887	0.028	0.563	
766	0.00215	0.9901	2.576	0.025	0.588	
893.66	0.00159	0.9917	2.467	0.024	0.612	
1021.33	0.00153	0.9932	2.957	0.029	0.641	
1148.99	0.00127	0.9945	2.99	0.029	0.67	
1276.66	0.00094	0.9954	2.617	0.025	0.695	
1404.33	0.00079	0.99623	2.579	0.025	0.72	
1531.99	0.00071	0.99694	2.656	0.026	0.746	
1659.66	0.00047	0.99741	2.008	0.019	0.765	
1787.32	0.00037	0.99779	1.793	0.017	0.782	
1914.99	0.00039	0.99818	2.098	0.02	0.802	
2042.65	0.00026	0.99844	1.529	0.015	0.817	
2170.32	0.00021	0.99864	1.352	0.013	0.83	
.	.	.	.	.	.	
.	.	.	.	.	.	
.	.	.	.	.	.	
6510.96	0.00001	0.99996	0.211	0.002	0.987	
6638.63	0.00001	0.99997	0.289	0.003	0.99	
6766.29	0.00001	0.99998	0.446	0.004	0.994	
6893.96	0.00001	0.99999	0.305	0.003	0.997	
7021.63	0.00001	1	0.314	0.003	1	

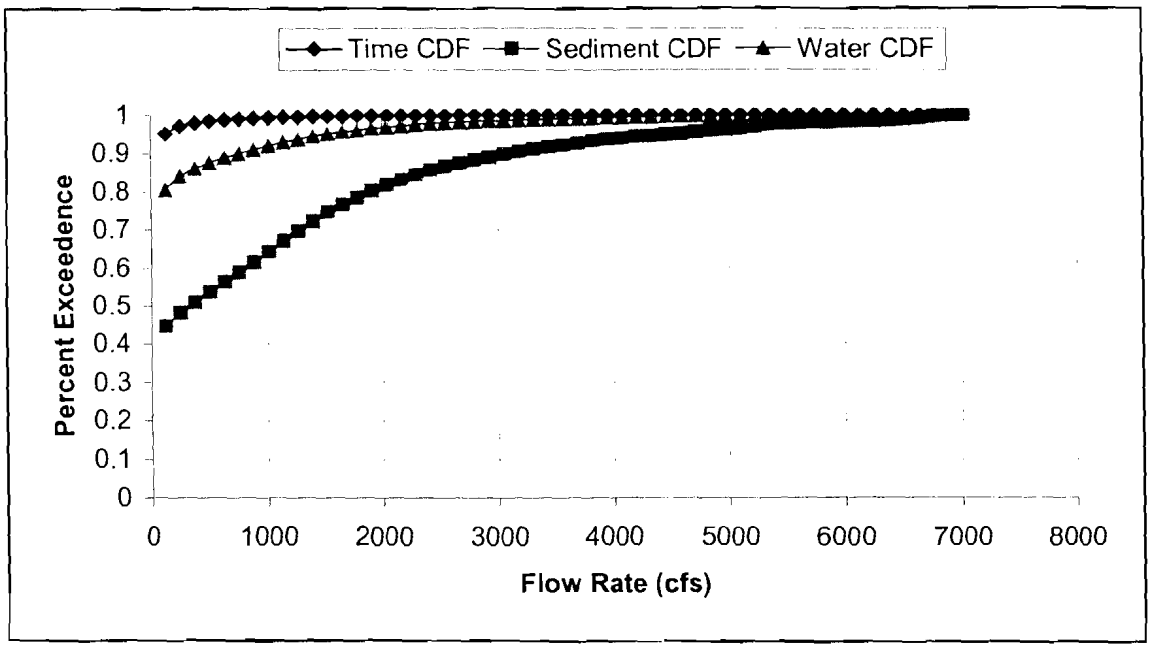

Figure 3.16 – Arithmetic percent exceedence plot for Long Creek (55 bins)

3.5.2.4 Summary sheet

Summary sheet provides a summary of the effective discharge results for each bin size variation, computation method, range of years analyzed, general statistics for discharge data, and a recurrence interval plot. The recurrence interval plot is used in determining whether the calculated effective discharge is within a reasonable range of flows. In addition to the summary table, two summary plots are also generated: sediment yield versus number of bins, and effective discharge versus number of bins. Table 3.8 and Figures 3.17 and 3.18 are examples of the summary output sheet for Long Creek.

Table 3.8 – Summary data sheet for Long Creek

EffQ (DEC Long Yang).xls Summary Sheet

Effective Discharge Type	Range of Years	Number of Bins	Effective Discharge, 1st Peak (cfs)	Effective Discharge, 2nd Peak (cfs)	Type of Sediment Discharge Relationship	Total Sediment Yield (tons/day)
Arithmetic	1987-1999	5	702.16255	2106.48765	SedTrans	3291.1105
Arithmetic	1987-1999	10	351.081275	1053.24383	SedTrans	1080.775
Arithmetic	1987-1999	15	234.054183	702.16255	SedTrans	567.12904
Arithmetic	1987-1999	20	175.540638	526.621913	SedTrans	364.11093
Arithmetic	1987-1999	25	140.43251	421.29753	SedTrans	262.76993
Arithmetic	1987-1999	30	117.027092	351.081275	SedTrans	204.55204
Arithmetic	1987-1999	35	100.308936	300.926807	SedTrans	167.87287
Arithmetic	1987-1999	40	87.7703188	263.310956	SedTrans	143.3218
Arithmetic	1987-1999	45	78.0180611	234.054183	SedTrans	125.92056
Arithmetic	1987-1999	55	63.8329591	191.498877	SedTrans	103.53023
Arithmetic	1987-1999	60	58.5135458	175.540638	SedTrans	96.186612
Arithmetic	1987-1999	65	54.0125038	162.037512	SedTrans	90.356699
Arithmetic	1987-1999	70	N/A	N/A	N/A	N/A
Arithmetic	1987-1999	75	N/A	N/A	N/A	N/A
Arithmetic	1987-1999	80	N/A	N/A	N/A	N/A
Arithmetic	1987-1999	90	N/A	N/A	N/A	N/A
Arithmetic	1987-1999	100	N/A	N/A	N/A	N/A
Arithmetic	1987-1999	125	N/A	N/A	N/A	N/A
Arithmetic	1987-1999	150	N/A	N/A	N/A	N/A
Logarithmic	1987-1999	5	1569.28958	78.3656573	SedTrans	900.29145
Logarithmic	1987-1999	10	1301.23133	4003.55687	SedTrans	141.73234
Logarithmic	1987-1999	15	1246.18282	2488.54647	SedTrans	96.408593
Logarithmic	1987-1999	20	1222.4703	2014.50277	SedTrans	80.408354
Logarithmic	1987-1999	25	1787.69494	1209.26771	SedTrans	73.282204
Logarithmic	1987-1999	30	1655.56236	1200.85572	SedTrans	68.8404
Logarithmic	1987-1999	35	1569.28958	2060.76421	SedTrans	66.137879
Logarithmic	1987-1999	40	1508.61032	1911.31901	SedTrans	64.346024
Logarithmic	1987-1999	45	1463.63859	1804.02093	SedTrans	62.614727
Logarithmic	1987-1999	50	1428.98872	1723.36545	SedTrans	61.531651
Logarithmic	1987-1999	55	1401.4802	1967.59333	SedTrans	60.594145
Logarithmic	1987-1999	60	1880.38402	1379.11544	SedTrans	59.983027
Logarithmic	1987-1999	65	1810.01829	1569.28958	SedTrans	59.348235
Logarithmic	1987-1999	70	1535.08586	1344.9624	SedTrans	58.732173
Logarithmic	1987-1999	75	1506.16748	1331.63066	SedTrans	58.34552
Logarithmic	1987-1999	80	1865.49501	1481.40143	SedTrans	58.000275
Logarithmic	1987-1999	90	1441.20734	1767.9516	SedTrans	57.30287
Logarithmic	1987-1999	100	1856.73874	1409.997	SedTrans	56.827175
Logarithmic	1987-1999	125	1816.32963	1458.67085	SedTrans	56.014937
Logarithmic	1987-1999	150	N/A	N/A	N/A	N/A

Year	Average Discharge (cfs)	Ln Average Discharge (cfs)	Max Discharge (cfs)	Rank	Freq.
1990	38.8086482	2.15589201	7022.5	1	0.0625
1991	60.3234255	2.2328739	6784	2	0.125
1989	49.0820703	2.24190284	5459	3	0.1875
1992	31.7765093	2.00541006	5353	4	0.25
1995	27.1851013	2.07142067	4107.5	5	0.3125
1997	43.5792752	2.44722104	3788.29425	6	0.375
1987	21.7320464	1.99877295	3630.5	7	0.4375
1994	28.1625853	2.05357795	3577.5	8	0.5
1999	85.1689173	3.60450791	3270.53822	9	0.5625
1998	93.3045493	3.91381278	2963.90518	10	0.625
1999	28.0543738	2.00930066	2822.356	11	0.6875
1988	33.4435129	2.05209213	2493.65	12	0.75
1998	26.563507	2.00000622	2443.2213	13	0.8125
1993	16.9610225	1.9428506	2273.7	14	0.875
1996	21.1997913	1.85025926	2096.5801	15	0.9375

	Discharge	Ln Discharge
Skew	13.64989	1.329581707
Mean	40.786251	2.315618376
Median	7.155	1.967811413
Std Deviation	182.09471	1.279544666

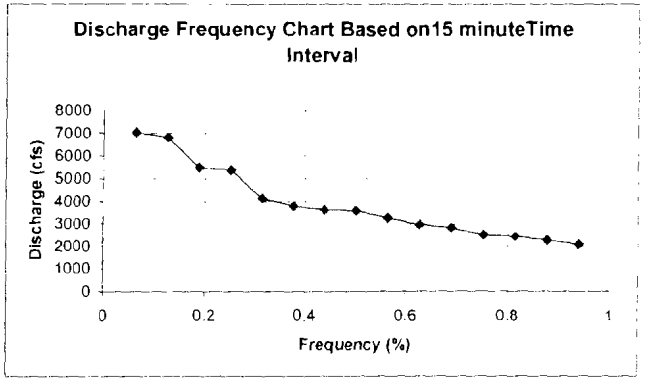

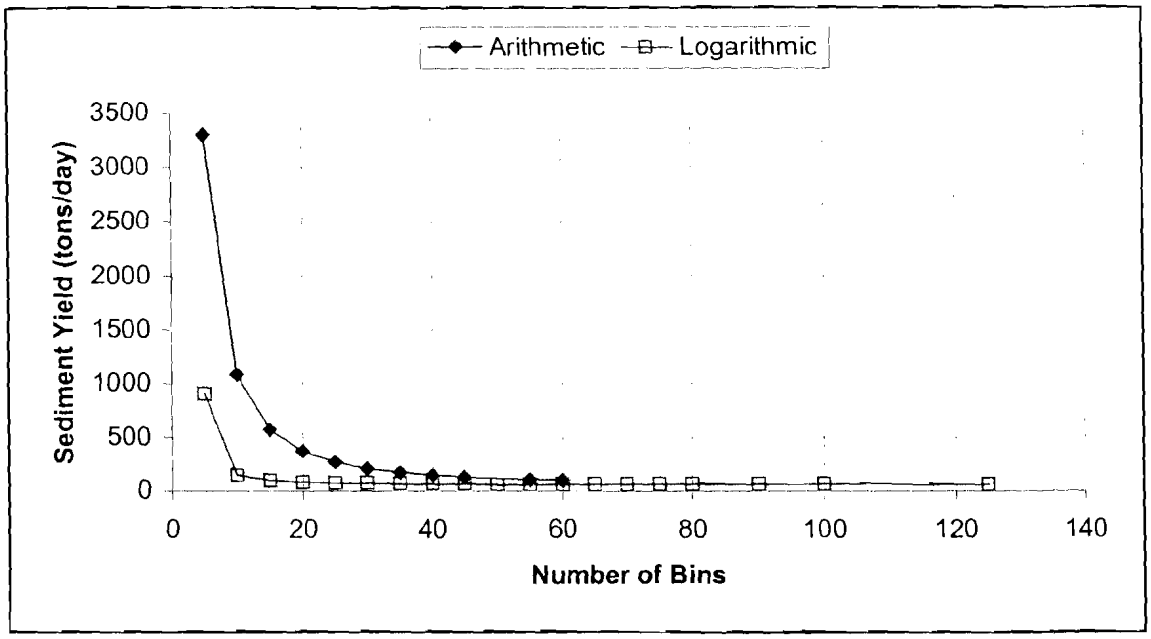

Figure 3.17 – Sediment yield versus number of bins for Long Creek.

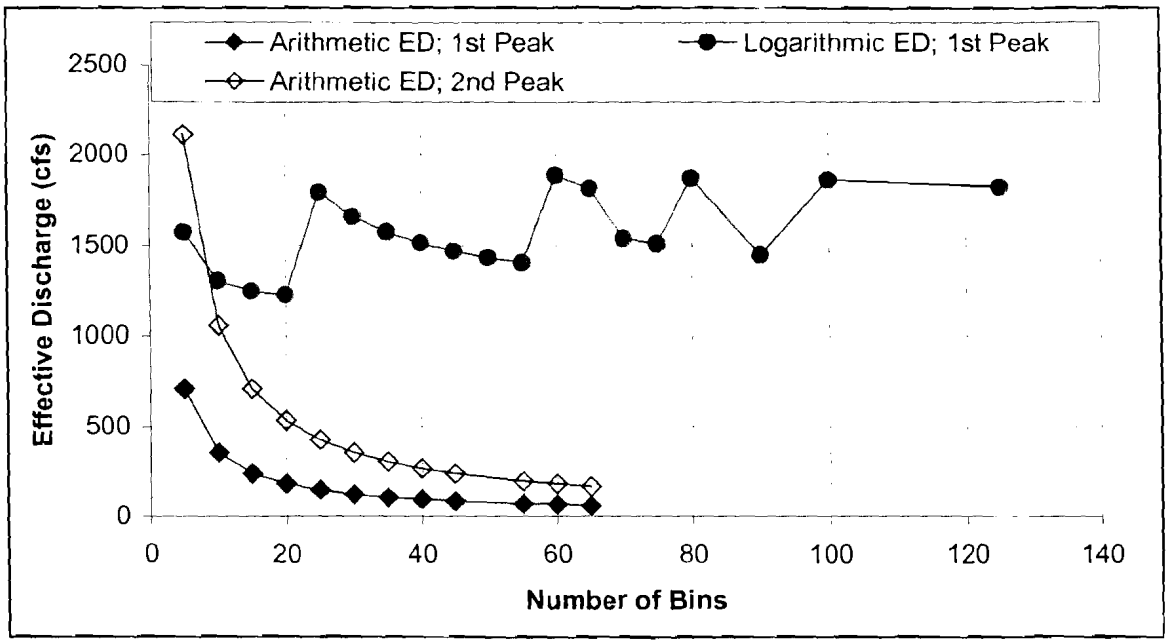

Figure 3.18 – Effective Discharge versus number of bins for Long Creek

4 ANALYSIS OF RESULTS

Results obtained from the various methods discussed are presented in the following sections. Analysis and discussion of the effective discharge results, flow duration relationships, sediment yield, and comparisons associated with each of the calculations are also presented.

4.1 Analytical Effective Discharge Calculations

Nash (1994) suggested a direct approach for determining effective discharge given that the discharge data are log-normally distributed. Using the discharge data available from the USGS, a Chi-squared test was used to determine whether the discharge data were log-normally distributed. Results of the chi-squared test with $\alpha = 0.05$ failed to reject the null hypothesis that the 15-minute discharge data were log normally distribution at each site. As a result, the analytical effective discharge computation was tested using the following equation (Nash, 1994):

$$Q_e = e^{\beta^2(b-1)+\alpha} \qquad \text{Equation 4.1}$$

where:

b = shape factor coefficient;

α = mean of the natural logarithm of discharge; and

β = standard deviation of the natural logarithm of discharge.

Table 4.1 and Figures 4.1 and 4.2 show the actual and calculated log-normal distributions for Abiaca 21 Creek near Cruger.

Table 4.1 – Discharge frequency distribution for Abiaca 21 Creek near Cruger

Effective Discharge Output (50 Arithmatic Bins)				μx=	102.55	mean of Q
	Min Q	13.60598		σx=	221.33	std deviation of Q
	Max Q	3570		ηx=	2.16	coefficient of variation
Number of Intervals		50		μy=	3.76	mean of ln(Q)
Interval Index		71.1278804		σy=	1.32	std deviation of ln(Q)
Reference #	Bin Size	Frequency	Bin Probability	CDF	Calculated Bin Probability	Calculated CDF
0	0	0	0.00000	0.000	0.00000	0.000
1	71.128	190813	0.68895	0.689	0.64557	0.646
2	142.256	56257	0.20312	0.892	0.17104	0.817
3	213.384	12068	0.04357	0.936	0.07050	0.887
4	284.512	4318	0.01559	0.951	0.03655	0.924
5	355.639	2480	0.00895	0.960	0.02151	0.945
6	426.767	1730	0.00625	0.966	0.01374	0.959
7	497.895	1238	0.00447	0.971	0.00930	0.968
8	569.023	854	0.00308	0.974	0.00666	0.975
9	640.151	659	0.00238	0.976	0.00479	0.980
.	.	.	.	.	.	.
.	.	.	.	.	.	.
.	.	.	.	.	.	.
45	3200.755	5	0.00002	1.000	0.00003	0.999
46	3271.882	2	0.00001	1.000	0.00003	0.999
47	3343.010	17	0.00006	1.000	0.00003	0.999
48	3414.138	9	0.00003	1.000	0.00003	0.999
49	3485.266	1	0.00000	1.000	0.00002	1.000
50	3556.394	5	0.00002	1.000	0.00002	1.000

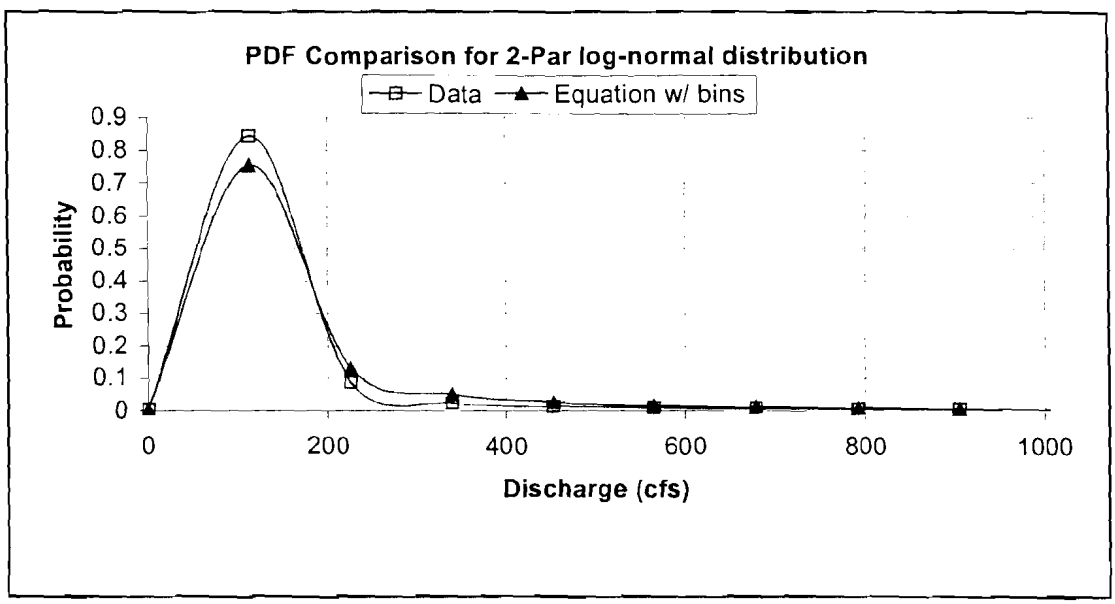

Figure 4.1 – Observed and calculated PDF for Abaica 21 Creek near Cruger

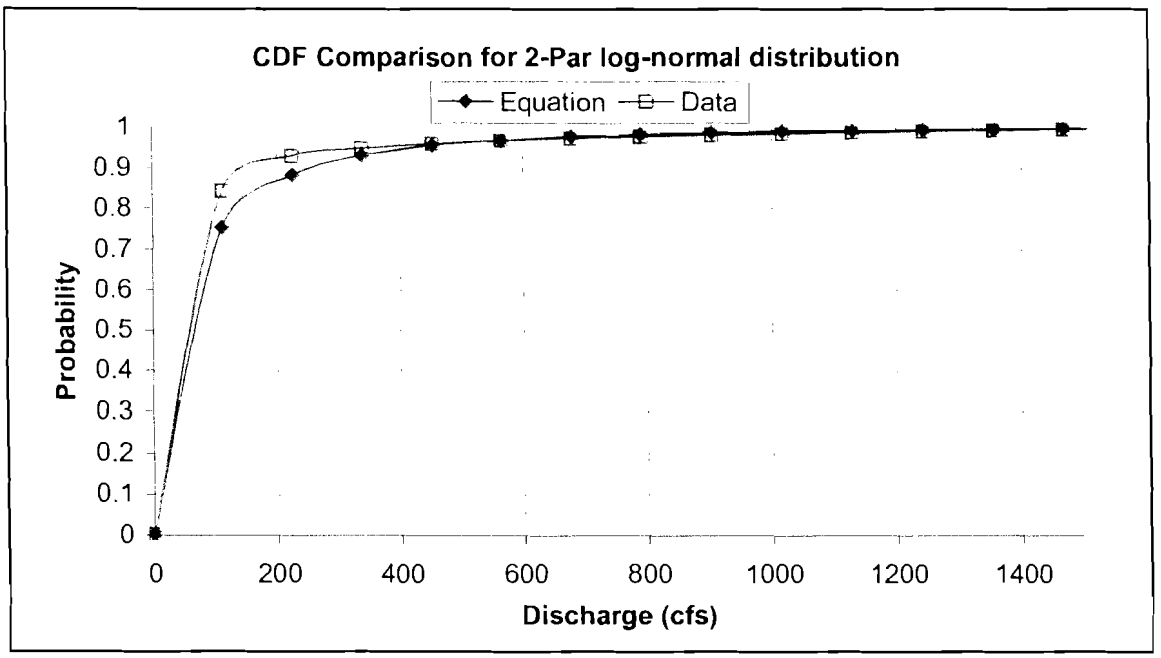

Figure 4.2 – Observed and calculated CDF for Abaica 21 Creek.

Mean and standard deviation of the discharge data for each site were obtained from the output summary sheets generated by the effective discharge program. Table 4.2 summarizes the analytical effective discharge computations using Nash's method. For each site, effective discharge was computed using observed total sediment data, pump total sediment data, bed material sediment data, and computed sand load data using Yang's sand load equation.

Analytical effective discharge values presented below were found to be much smaller compared to the calculated 2-year recurrence interval discharge for each site (Figure 4.3). The smaller effective discharge values computed from the analytical method would suggest that the lognormal distribution proposed by Nash (1994) does not account for the large amount of skew (>8) observed in the discharge data for the sites in this study. Nash's lognormal frequency distribution does not take into account skew of

the discharge data and, as a result, the analytical effective discharge does not provide the best representation of the true discharge frequency distribution.

Table 4.2 - Analytical effective discharge for each site

	Sediment Type	Station Name (USGS gauge #)	$Qs = aQ^b$		Mean of lnQ (α)	Std Dev of lnQ (β)	Analytical $Qeff$
		DLC Site	a	b			(cfs)
1	Yang	Abiaca 3 (DLC)	0.0163	1.54	3.82	0.81	65
2	Yang	Abiaca 4 (DLC)	0.1773	1.51	3.73	0.81	58
3	bed	Abiaca 6 @ Seven Pines (#07287150)	0.0081	1.61	4.16	0.81	95
4	bed	Abiaca 21 @ Ginger (#07287160)	0.0046	1.49	4.13	0.77	83
5	bed	Batupan Bogue @ Grenada (#07285400)	0.2081	1.19	5.30	1.59	325
6	pump	Fannegusha @ Howard (#07287355)	0.0032	2.01	3.86	1.19	199
7	Yang	Fannegusha (DLC)	0.0004	1.45	2.94	1.19	36
8	bed	Harland Creek @ Howard (#07287404)	1.3512	0.0073	3.00	1.13	6
9	Yang	Harland 1 (DLC)	0.0002	1.52	2.73	1.13	30
10	Yang	Harland 23 (DLC)	0.0002	1.49	3.21	1.13	46
11	bed	Hickahala @ Senatobia (#07277700)	0.0004	1.84	4.18	0.97	146
12	Yang	Hickahala 11 (DLC)	0.0011	1.35	2.63	0.97	24
13	Yang	Hickahala 22 (DLC)	0.00005	1.53	4.54	0.97	49
14	bed	Hotopha @ Batesville (#07273100)	0.8178	1.04	2.94	1.17	20
15	Yang	Hotopha (DLC)	0.00001	1.56	2.81	1.16	35
16	bed	Otoucalofa @ Water Valley (#07274252)	0.00001	2.30	4.62	1.38	1221
17	Yang	Otoucalofa (DLC)	0.0009	1.28	4.05	1.38	98
18	bed	Long @ Pope (#07275530)	0.0283	1.44	3.43	1.20	58
19	Yang	Long (DLC)	0.00002	1.62	2.31	1.28	28
20	bed	Senatobia (#07277730)	0.00004	1.73	3.17	1.13	61
	Yang		0.0003	1.41			40
21	Yang	Topashaw @ Derma (#07282090)	0.0000009	1.64	2.52	1.76	91
22	Yang	Yalobusha @ Derma (#07281977)	0.0004	1.43	2.74	2.53	237
23	Yang	Yalobusha @ Vardaman	0.0001	1.41	1.55	3.08	227

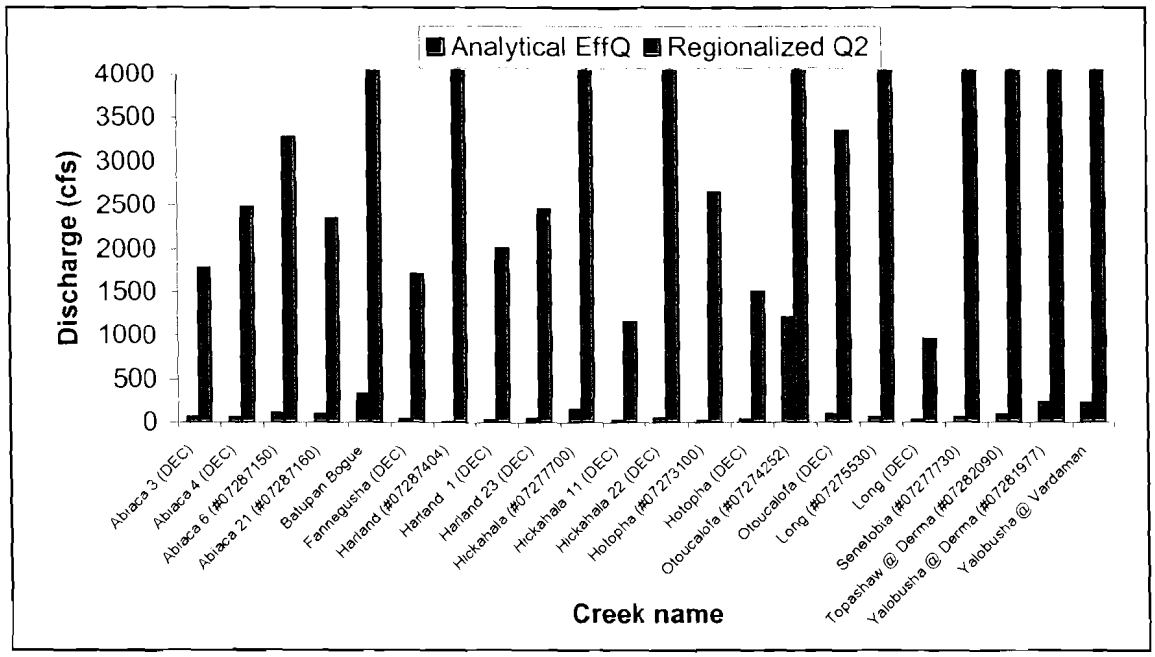

Figure 4.3 – Analytical effective discharge versus calculated 2-year recurrence discharge

4.2 Sediment Traps

Sediment transport was determined for a range of low flows for eleven sites using the procedures presented in Section 3.4.3. From the results of the sediment traps, it was determined that the amount of sediment transported at the various observed low flows was negligible in terms of the effective discharge. Table 4.3 is an example of the bed material load and suspended sediment load concentrations for Fannegusha Creek.

From the results of the sediment traps and suspended sediment samples, the average total sediment concentration for all the creeks sampled was 50 mg/L. Resulting bed material load was determined by removing the wash load portion from the total load. Average bed material load concentration was determined to be around 1 mg/L. The recorded discharges ranged from 7 to 76 cfs and depths ranged from 0.7 to 2.1 feet.

Table 4.3 – Suspended and bed load concentrations for Fannegusha Creek

Suspended sediment sample						
	A	B	C=B-A	D	E=1000*(C/D)	
Sample #	Original Wt (grams)	Final Wt (grams)	Dry Wt (mg)	Total Vol (mLiters)	Conc. (mg/L)	Avg Conc. (mg/L)
15	1.5364	1.5472	10.8	250	43.20	45.47
11	1.5396	1.5509	11.3	250	45.20	
28	1.869	1.8762	7.2	150	48.00	
Sediment trap sample						
A	B	C	D	E	F	G=(D/E)*F
# of Traps	Dry Weight (grams)	Time (hours)	Trap Area (ft2)	X-Sec Area (ft2)	X-Sec Q (cfs)	Trap Q (cfs)
2	338.9	2	0.5	31.30	40.34	0.64
			H=A*G*C	I=1000*B/H		Adjusted
			Total Vol thru Trap (liters)	Conc. (mg/L)	% >D10	Conc. (mg/L)
			262818.94	1.29	0.7	0.90

From the observed results, it was evident that at these low flows, a minimal amount of sediment transport actually occurred. These results were used to assist in the analysis of the arithmetic effective discharge determination and to provide information about the type and amount of sediment transport that occurs in the first bin size.

Figure 4.4 shows the largest observed sediment discharge from the sediment traps (Abiaca 6), along with the sediment-rating curves for each sediment type. Total sediment load calculated from the sediment traps and suspended samples produce sediment loads that match the USGS total sediment samples. However, from the graph it is evident that the amount of bed material load transported at the low flows is much less than predicted by the rating curves. As a result, it is evident that the current sediment-rating curves overestimate the amount of bed material load that is transported at these low flows. Overestimation of the sediment rating curves results from the limited amount of sediment transport data at these low flows.

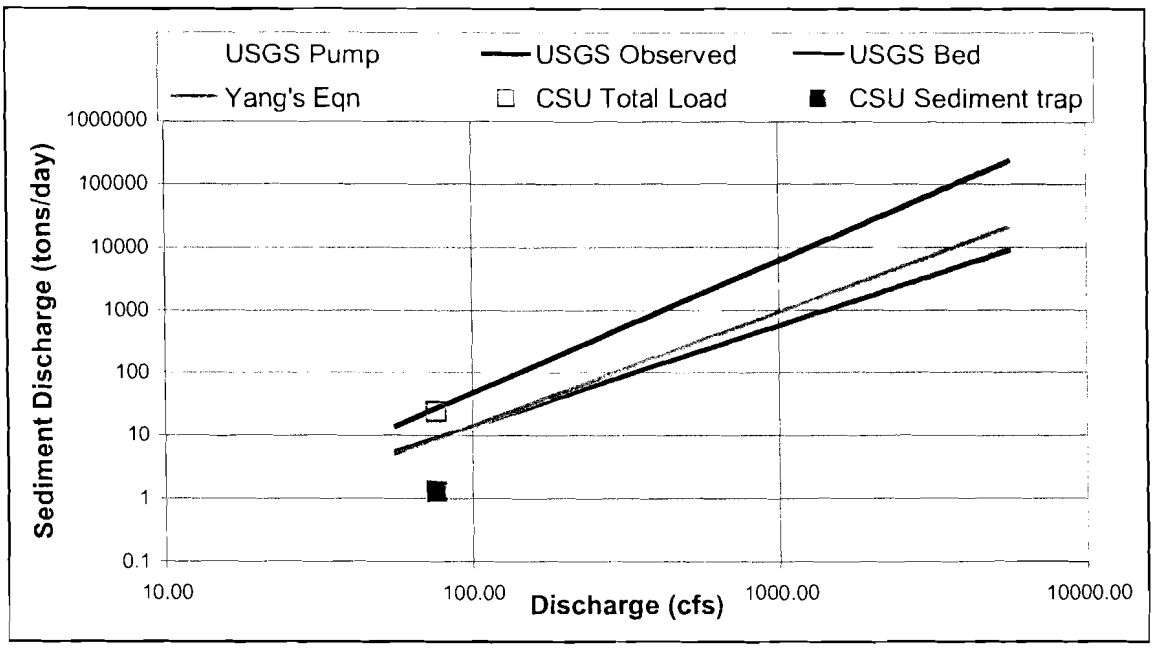

Figure 4.4 – Plot of observed sediment transport at low flow for Abiaca 6

4.3 Magnitude Frequency Analysis – Effective Discharge

Effective discharge was computed using both arithmetic and logarithmic class sizes for twenty-three sites using Andrews' (1980) method and four different types of sediment data: observed total sediment load, automatic pump sediment total load, bed material sediment load, and total sand load computed with Yang's equation. Bed material load and Yang's equation were used to determine the effective discharge corresponding to the bed material load, whereas the pump and observed sediment data were used to make comparisons of the total sediment yield for each site. Final effective discharge determinations for each site were computed using the bed material load at USGS gauges and/or Yang's sediment load data for ungauged sites using fifty bins.

A typical results summary sheet is shown as Figure 4.5. From the results of the effective discharge program it was determined that fifty bins produced the most representable sediment load histogram for each site. Similarly, it was found that in

general, bin sizes greater than fifty produced zero frequencies in the flow frequency distributions and were therefore not used in the analysis. By choosing fifty bins, the error associated with the upper logarithmic bin sizes and the size of the first arithmetic bin was minimized. From the effective discharge program summary sheet (Figure 4.5), it is evident that as the number of bins increases, the resulting effective discharge decreases.

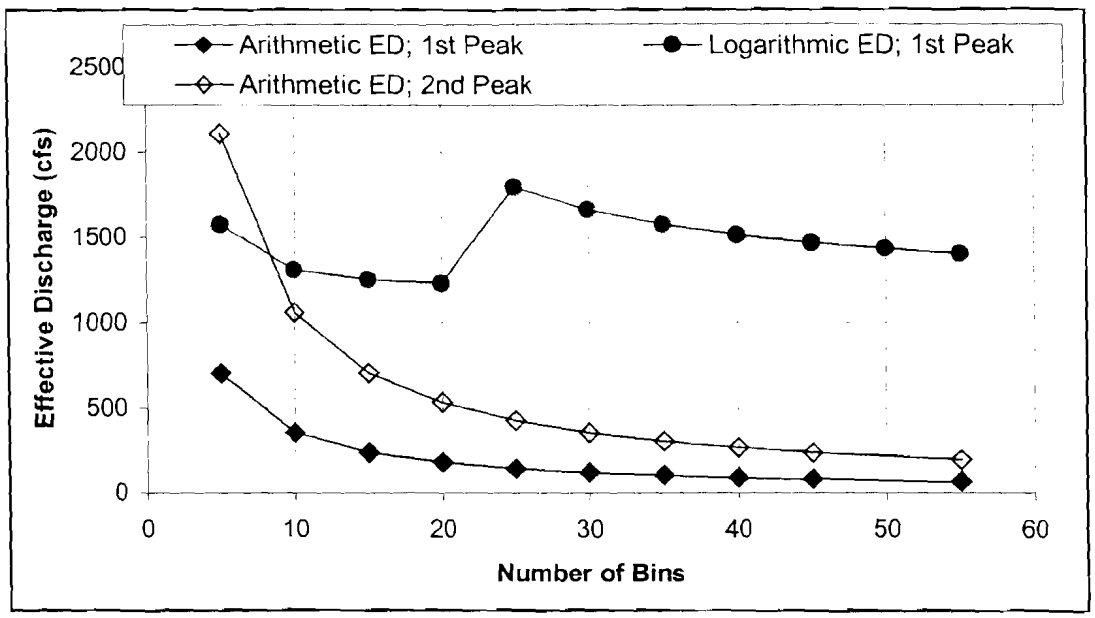

Figure 4.5 – Effective Discharge vs. number of bins for Long Creek

4.3.1 Classification of Problematic Computations

Using the methods presented in Chapter 3 to determine the arithmetic and logarithmic effective discharge, four different types of sediment load histograms (Type I, Type II, Type III, or Type IV) were observed to occur, depending on the method used in determining the effective discharge. Using arithmetic bins, the sediment load histogram either produced a Type I histogram with the peak in the first bin followed by a continuous decrease in the histogram (Figure 4.6), or a Type II histogram with the peak in the first bin followed by additional peaks (Figure 4.7). Using logarithmic bins, the sediment load histogram either produced a Type III histogram with a very distinguishable peak (Figure

4.8) or a Type IV histogram with multiple peaks (Figure 4.9). Effective discharge calculations that produced a Type I or Type IV histogram indicated that the calculation procedure was not appropriate in determining the effective discharge because a representative peak could not be determined or reproduced.

Eliminating the Type I and Type IV effective discharge histograms resulted in a total of five sites for which effective discharge could be determined arithmetically, and eleven sites for which effective discharge could be determined logarithmically. As a result, effective discharge could only be determined for twelve of the twenty-three sites investigated in this study. It should be noted that numerous researchers (Soar, 2000; Andrews, 1980; Nash, 1994; Thorne *et al.*, 1998) have suggested that a fifth type of sediment load histogram occurs. A type V histogram is associated with the arithmetic bins and is characterized by a single peak which does not occur in the first bin (Figure 4.10). However, a Type V histogram was not found to occur for any of the sites within this study.

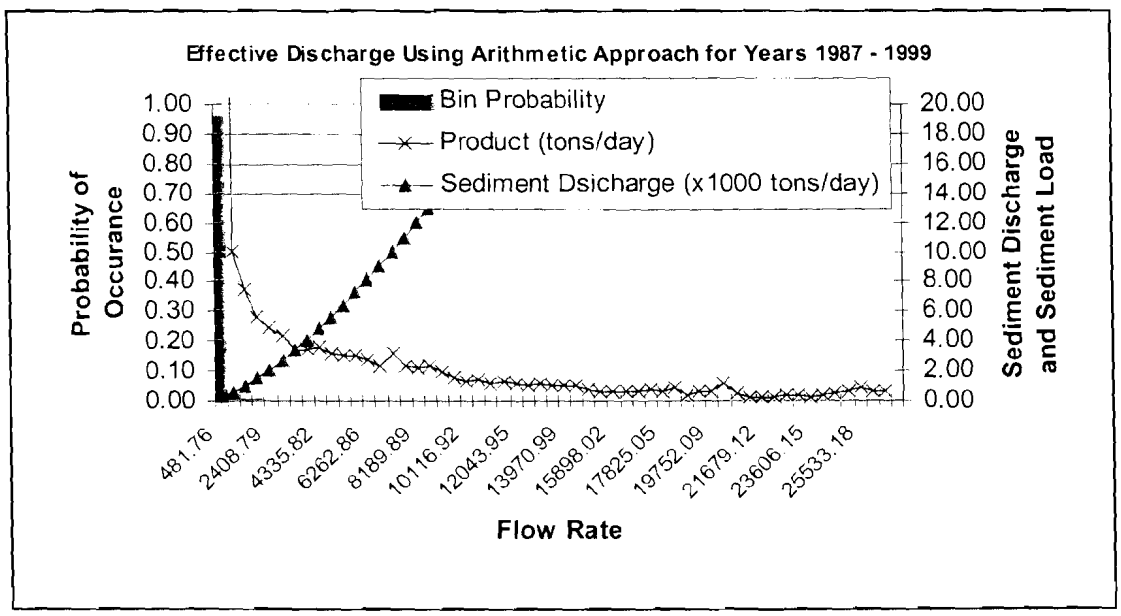

Figure 4.6 – Type I sediment load histogram (USGS Long Creek)

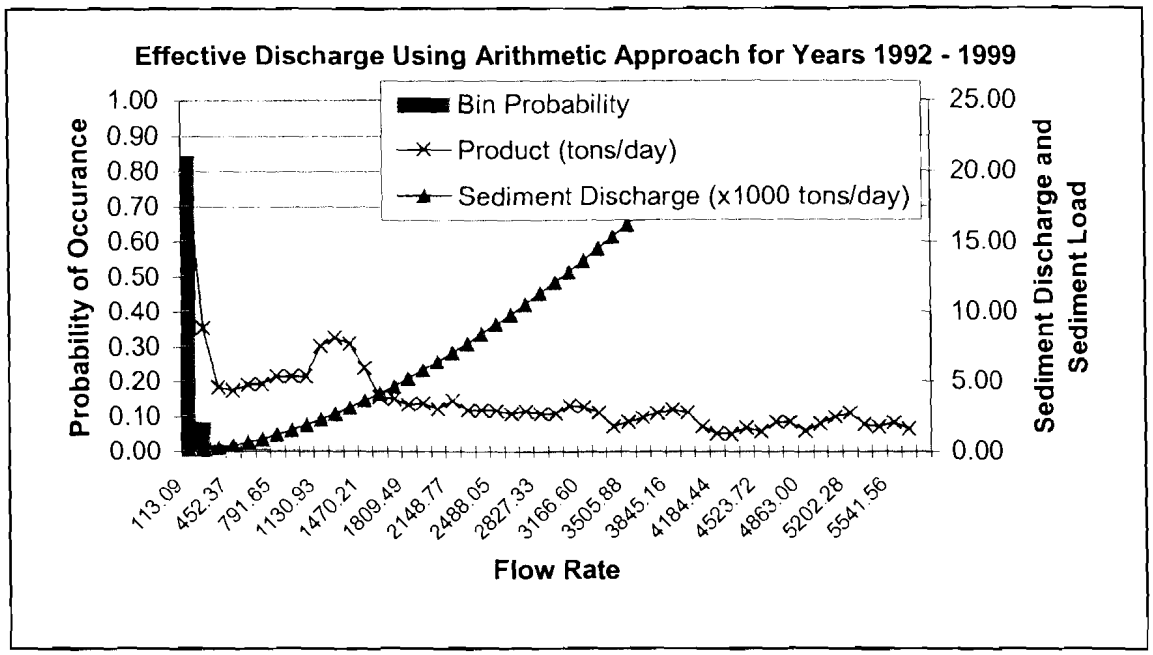

Figure 4.7 – Type II sediment load histogram (Abiaca 6 near Seven Pines)

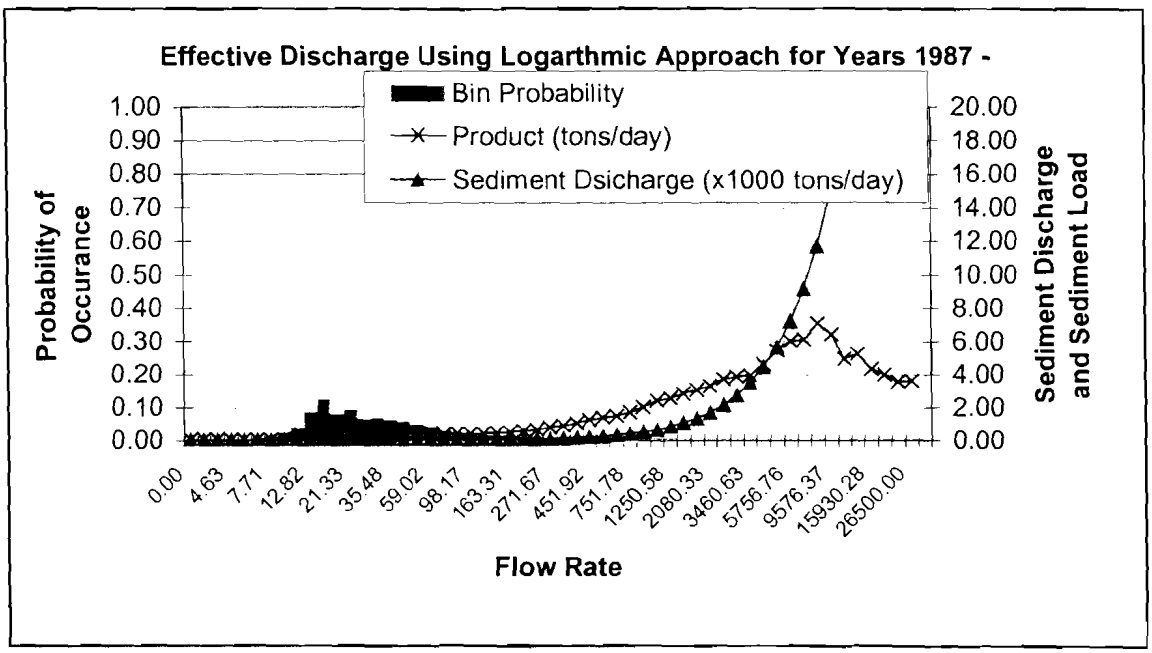

Figure 4.8 – Type III sediment load histogram (USGS Long Creek)

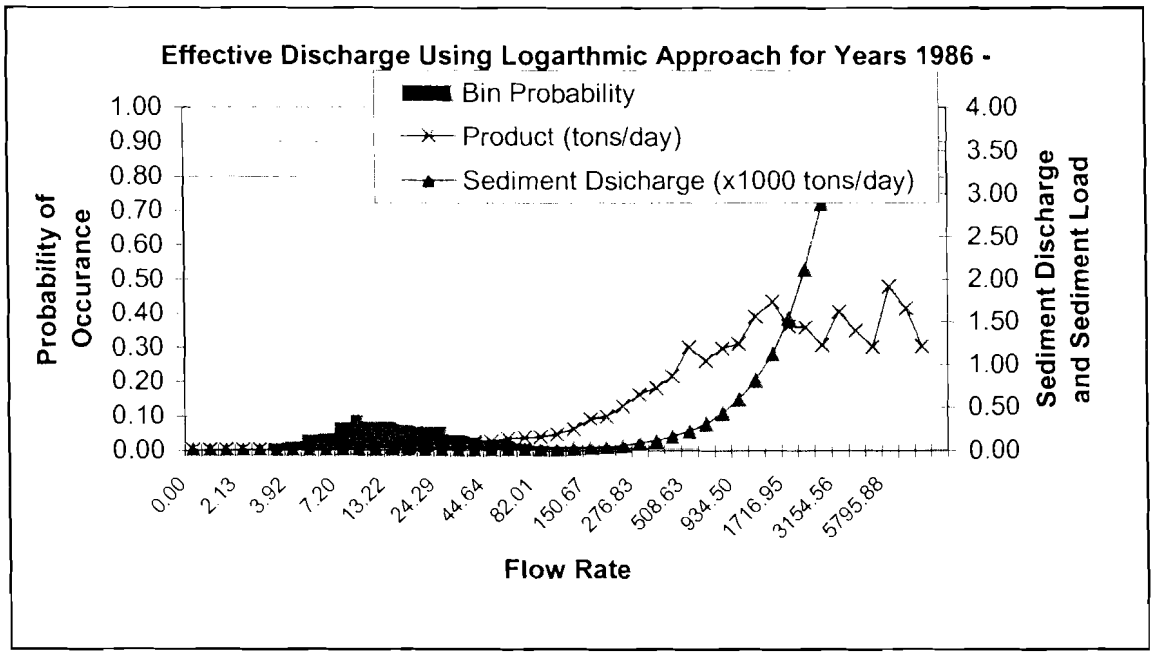

Figure 4.9 – Type IV sediment load histogram (DEC Hotopha Creek)

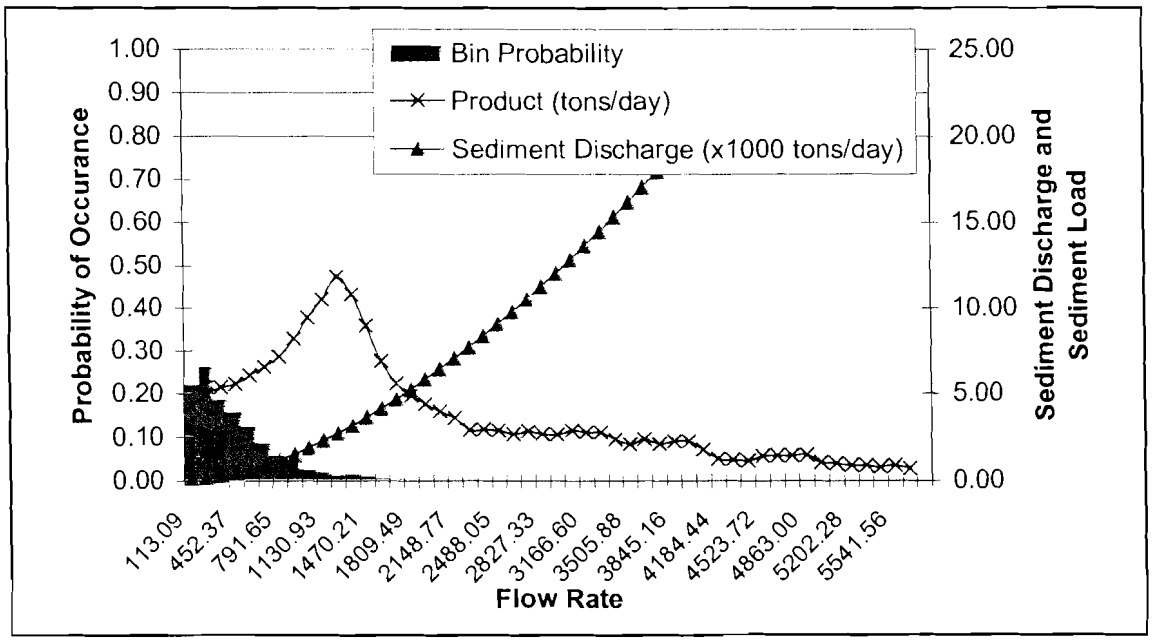

Figure 4.10 – Type V sediment load histogram

Water-surface elevations for each effective discharge were plotted on surveyed cross sections of each site in order to determine whether the calculated effective discharge was reasonable. Figure 4.11 illustrates the effective discharge stage at the gauged section of Abiaca 21 Creek.

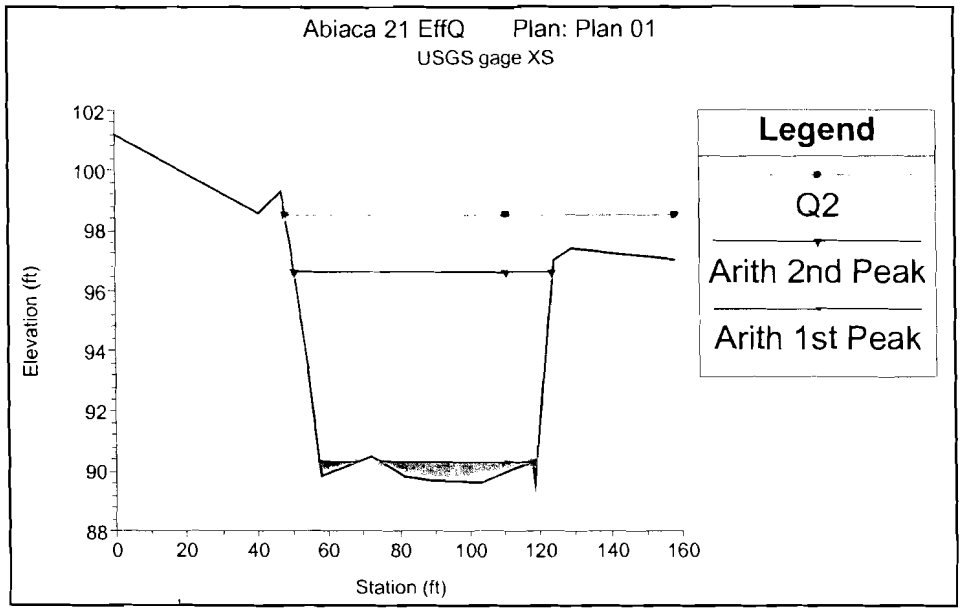

Figure 4.11 – Cross-section plot of effective discharge

Analyses of these plots were used to assist in the elimination of the first arithmetic peak in the effective discharge calculations. From Figure 4.11, it is evident that the stage associated with the first arithmetic bin is not reasonable since it only accounts for five percent of the total flow area. By identifying the effective discharge stage, cumulative percent of sediment transported by the effective discharge, and ratio of Q_{eff}/Q_2, a range of flows corresponding to the effective discharge was determined for each of the twelve sites. Cross sections of the remaining sites are shown in Appendix E. Results of the effective discharge calculations are presented in Table 4.4.

Table 4.4 – Results of effective discharge calculations using 50 bins

			Arithmetic Method		Logarithmic Method	
	Sed type	Station Name	Histogram Type	Arith *Qeff*	Histogram Type	Log *Qeff*
		DEC or USGS location		(cfs)		(cfs)
1	Yang	Abiaca 3	Type II	692	Type III	710
2	Yang	Abiaca 4	Type II	776	Type III	796
3	bed	Abiaca 6 near Seven Pines	Type II	1187	Type III	1218
4	bed	Abiaca 21 near Cruger	Type II	1244	Type IV	N/A
5	bed	Batupan Bogue at Grenada	Type II	2126	Type IV	N/A
6	N/A	Fannegusha at Howard	N/A	N/A	N/A	N/A
7	Yang	Fannegusha	Type I	N/A	Type III	2352
8	bed	Harland Creek near Howard	Type I	N/A	Type IV	N/A
9	Yang	Harland 1	Type I	N/A	Type IV	N/A
10	Yang	Harland 23	Type I	N/A	Type IV	N/A
11	bed	Hickahala near Senetobia	Type I	N/A	Type III	6064
12	Yang	Hickahala 11	Type I	N/A	Type III	1285
13	Yang	Hickahala 22	Type I	N/A	Type III	8708
14	bed	Hotopha Creek near Batesville	Type I	N/A	Type III	552
15	Yang	Hotopha	Type I	N/A	Type IV	N/A
16	bed	Long creek near Pope	Type I	N/A	Type III	7451
17	Yang	Long	Type I	N/A	Type III	1406
18	bed	Otoucalofa Canal near Water Valley	Type I	N/A	Type IV	N/A
19	Yang	Otoucalofa	Type I	N/A	Type IV	N/A
20	bed	Senetobia	Type I	N/A	Type III	5104
	Yang	Senetobia	Type I	N/A	Type III	3555
21	Yang	Topashaw at Derma	Type I	N/A	Type IV	N/A
22	Yang	Yalobusha at Derma	Type I	N/A	Type IV	N/A
23	Yang	Yalobusha at Vardaman	Type I	N/A	Type IV	N/A

4.3.2 Cumulative Sediment Discharge

In addition to determining the effective discharge from the bed material load histograms, a CDF plot of sediment versus discharge was generated to compare effective discharge with a range of sediment-transporting flows (Biedenharn and Thorne 1997). A plot was generated for each site and then combined into one common plot using the Q/Q_2 ratio to generate a bed material sediment CDF versus dimensionless discharge graph (Figure 4.12). Additionally, the effective discharge for each site was also graphed to determine the range of sediment transport that corresponded to the effective discharge in this study.

Biedenharn and Thorne (1997) showed that for the Mississippi River, the sediment load CDF produced an "S-shaped" curve, and the range of discharges transporting seventy percent of the total sediment load (from 15% to 85% of the CDF curve) corresponded to the steepest section of the CDF curve. For the DEC streams, this S-shaped trend was not present.

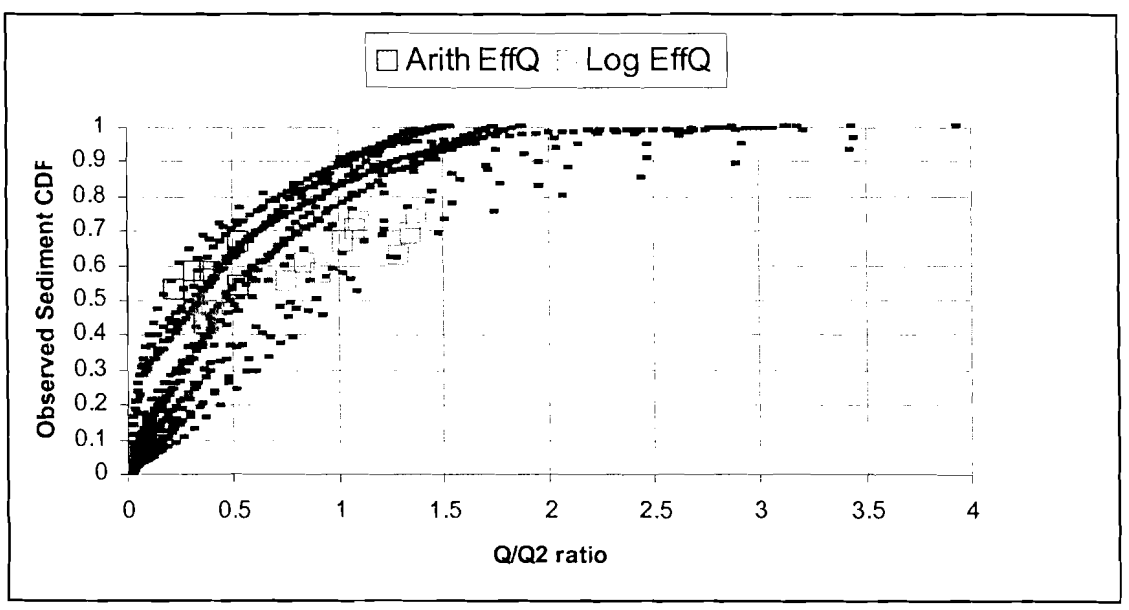

Figure 4.12 – Sediment CDF versus Q/Q_2 for bed material load

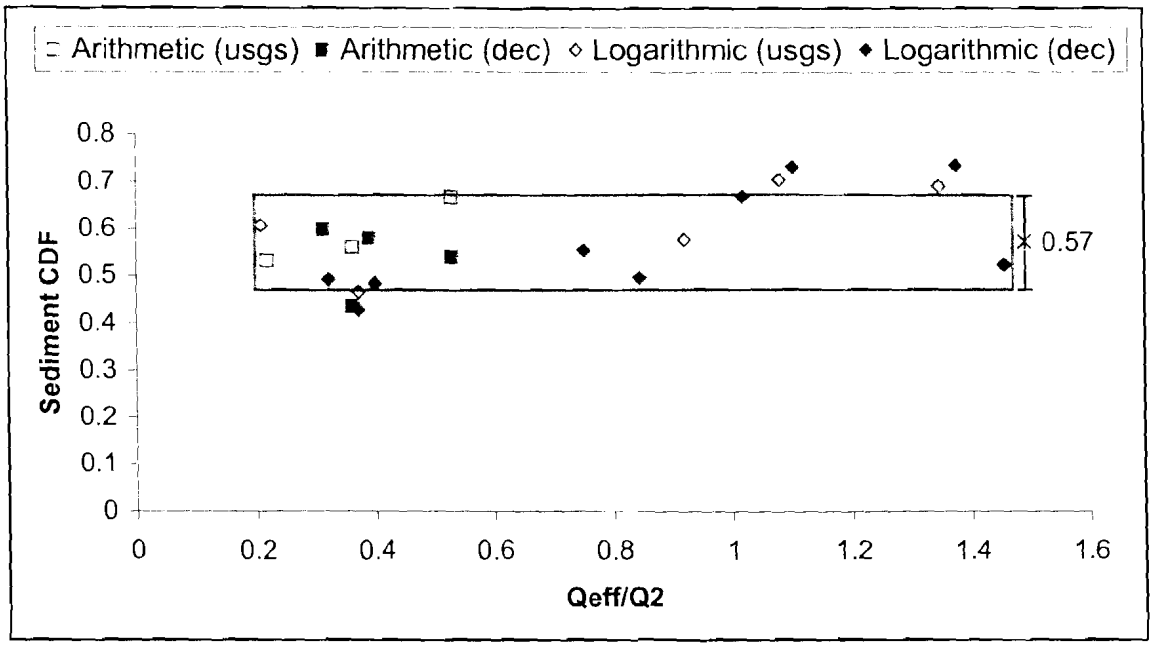

Figure 4.13 –Sediment CDF vs. EffQ/Q_2.

Figures 4.12 and 4.13 indicate that the effective discharge occurs over a range of discharges that transport from 47 to 67 percent of the total sediment load (μ=0.57 and σ=0.1). The corresponding range for the Qeff/Q2 ratio is approximately 0.2 to 1.4. Because the Q2 is a regionalized value (+/- 44%), the sediment CDF is a better estimate of the effective discharge compared to that of the Qeff/Q2 ratio.

4.4 Effective Discharge Comparison

4.4.1 MFA - Logarithmic vs. Arithmetic Distribution

Use of arithmetic versus logarithmic class sizes has been the subject of a debate in the determination of effective discharge. Although the logarithmic method clearly defines the low flow frequencies, logarithmic classes cause bin sizes to vary and result in a bias toward the larger bin sizes. The effective discharge has a greater probability of occurrence than the smaller discharge bin sizes. As a result, the logarithmic method tends to over-estimate the effective discharge (Figure 4.14). Although the arithmetic method

uses equal class sizes, the first bin size is large relative to the first logarithmic bin, and results in the effective discharge occurring in the first bin because of the high frequency of low flow events.

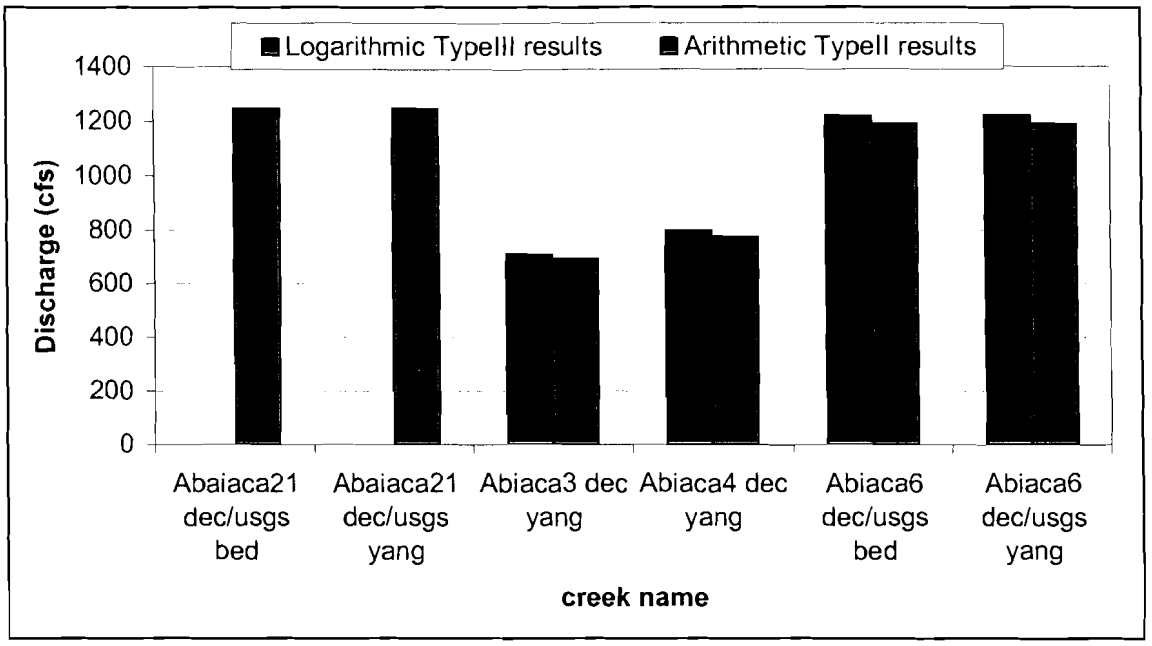

Figure 4.14 – Discharge bin size vs effective discharge method.

Although the logarithmic bins tend to overestimate the effective discharge, Figure 4.14 illustrates that for fifty arithmetic and logarithmic bins, the effective discharge is within fifty cfs for the two methods. This suggests that if a large number of bins are used in generating the logarithmic frequency curves, the error associated with the upper bin sizes may be minimized.

From the results of the effective discharge calculations in this study, the logarithmic effective discharge calculations showed that seven of the twenty-three sites resulted in multi-modal distributions (Type IV histogram) of the sediment load histogram, regardless of the number of bins used. As a result, a consistent and reproducible effective discharge could not be determined for these seven sites. Similarly,

the arithmetic calculations showed that seventeen of the twenty-three sites resulted in histograms with a single peak in the first bin (Type 1 histogram). As a result, a reasonable and reproducible effective discharge could not be determined for these seventeen sites.

Figure 4.15 is a plot of effective discharge method versus skewness of the discharge PDF. From the graph it is evident that for a skew greater than nine, arithmetic bins produce a Type I histogram and could not be used for these data. Therefore, the data suggest that for DEC sites with a skew greater than nine, logarithmic bins should be used because of the error produced by the high frequency of low flow data. Although this graph provides some insight into when each method should be used, it should be noted that effective discharge could only be determined for twelve of the twenty-three sites in this study.

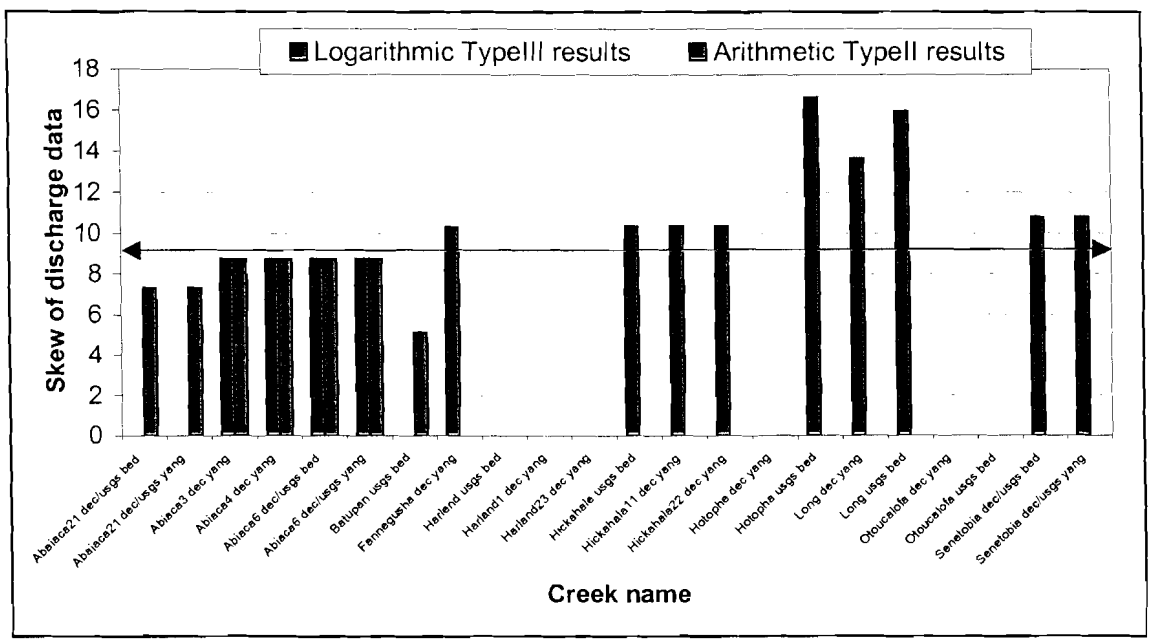

Figure 4.15 – Skew versus Effective discharge method

4.4.2 Effective Discharge versus Q2

Numerous researchers (Biedenharn et al. 1987, Wolman and Leopold 1957, Andrews 1980, Hey 1975, Orndorff and Whiting 1999) have shown that the recurrence interval for the effective discharge ranges from 1 to 5 years. As a result, the 2-year regional recurrence interval discharge was calculated for each site and compared with the recurrence interval of the effective discharge. Table 4.5 lists the Q_{eff}/Q_2 ratio for the twelve sites and suggests the average effective discharge to be equal to $0.8Q_2$.

The two-year discharge regression equation developed by Colson and Hudson (1973) has an estimated error range of $\pm$ 44%. Figure 4.16 illustrates effective discharge versus Q_2 for all twelve sites and includes the 44% error band associated with the Q_2 discharge. The Q_2 error band encompasses approximately 70% of the computed logarithmic effective discharges.

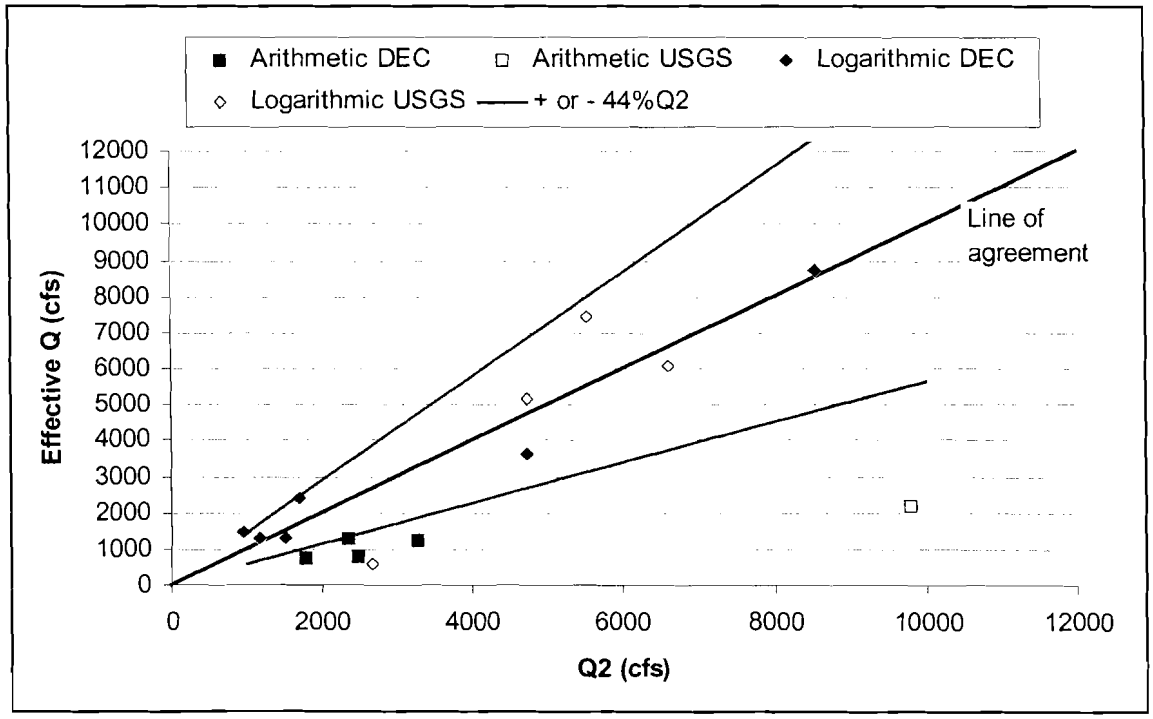

Figure 4.16 – Effective Discharge versus Q2 for all sites with 44% error band

Table 4.5 – Qeff/Q2 ratio for each site

	Station Name	Arith *Qeff*	Arith *Qeff/Q2*	Q2 regionalized	Log *Qeff*	Log *Qeff/Q2*
DEC or USGS location				(cfs)	(cfs)	
bed	Abiaca 21 near Cruger (DEC)	1244	0.52936	2350		
bed	Abiaca 6 near Seven Pines (DEC)	1187	0.36134	3285	1218	0.370776
bed	Hickahala near Senetobia			6591	6064	0.920042
bed	Hotopha Creek near Batesville			2660	552	0.207519
bed	Long creek near Pope			5535	7451	1.346161
bed	Senetobia (DEC)			4727	5104	1.079755
Yang	Abiaca 3 (DEC)	692	0.38898	1779	710	0.399101
Yang	Abiaca 4 (DEC)	776	0.31328	2477	796	0.321356
Yang	Fannegusha (DEC)			1711	2352	1.374635
Yang	Hickahala 11(DEC)			1166	1285	1.102058
Yang	Hickahala 22 (DEC)			8553	8708	1.018122
Yang	Long (DEC)			967	1406	1.453981

4.5 Annual Sediment Yield

Computation of annual sediment yield is a secondary result of calculating effective discharge. Summing the product of the sediment transport and frequency of occurrence curves, or the sum of the total load column from the effective discharge output sheet, obtains the total sediment yield. Summation of the product produces an average daily sediment transport rate; therefore, annual sediment yield is found by multiplying the summation result by 365 days. Table 4.6 presents annual sediment yield for each of the thirteen gauged sites. The data approximate bed material load as 23% of the total measured sediment discharge.

Table 4.6 – Annual sediment yield for each site.

		Logarithmic Bins		Arithmetic Bins	
Sediment Type	**Station Name**	**Avg. sediment yield**	**Annual sediment yield**	**Avg. sediment yield**	**Annual sediment yield**
	DEQ or USGS location	**(tons/day)**	**(tons)**	**(tons/day)**	**(tons)**
bed material	Abiaca 21	9	3,464	11	3,953
bed material	Abiaca 6	50	18,418	60	21,988
bed material	Batupan @ Grenada	816	297,840	1,098	400,770
bed material	Fannegusha @ Howard	N/A	N/A	N/A	N/A
bed material	Harland @ Howard	1	507	1	511
bed material	Hickahala @ Senetobia	54	19,710	70	25,550
bed material	Hotopha @ Batesville	67	24,455	264	96,360
bed material	Long creek near Pope	101	36,865	286	104,390
bed material	Otoucalofa @ Water Valley	938	342,370	854	311,710
bed material	Senetobia	1	263	2	704
bed material	Topashaw @ Derma	N/A	N/A	N/A	N/A
bed material	Yalobusha @ Derma	N/A	N/A	N/A	N/A
bed material	Yalobusha @ Vardaman	N/A	N/A	N/A	N/A
Sum		2,038	743,892	2,646	965,936
Total load	Abiaca 21 near Cruger	191	69,606	197	71,949
Total load	Abiaca 6 near Seven Pines	225	82,300	255	93,035
Total load	Batupan Bogue at Grenada	1,039	379,235	1,195	436,175
Total load	Fannegusha @ Howard	1,974	720,510	2,392	873,080
Total load	Harland Creek near Howard	805	293,825	865	315,725
Total load	Hickahala near Senetobia	521	190,165	717	261,705
Total load	Hotopha Creek near Batesville	48	17,520	137	50,005
Total load	Long creek near Pope	1,022	373,030	1,481	540,565
Total load	Otoucalofa @ Water Valley	3,609	1,317,285	3,641	1,328,965
Total load	Senetobia	332	121,180	794	289,810
Total load	Topashaw @ Derma	220	80,300	331	120,815
Total load	Yalobusha @ Derma	257	93,805	312	113,880
Total load	Yalobusha @ Vardaman	382	139,430	422	154,030
Sum		10,625	3,878,191	12,739	4,649,739

Results of Table 4.6 show that the arithmetic and logarithmic classes produce different sediment yields. This occurs as a result of the high frequency of low flows for these streams. Arithmetic bins over-predict the sediment load yield compared to logarithmic bins as a result of the high probability of occurrence of the first bin. Because the logarithmic bins vary in size and are able to better define the low-flows, the resulting sediment yield is much lower. Therefore, the sediment yield calculated for each site was determined using the logarithmic bins.

In addition to the annual sediment yield, Table 4.7 lists sediment yield characteristics for each of the twenty-three sites, including: sediment yield per acre, bed material sediment yield as percentage of the total yield, and skew of the discharge data. Average bed material sediment yield from the Yazoo River Basin is approximately 4.63 tons per acre based on observed bed material load data. Dubler (1997) showed that the skewness of the water discharge probability distribution function has an effect on the effective discharge. He showed that generally, as the skewness increased, the sediment yield also increased. Figure 4.15 depicts the relationship between skewness of the discharge frequency distributions and annual sediment yield. Otoucalofa at Water Valley and Batupan at Grenada both generated extraordinarily high sediment yields due to backwater affects and therefore were excluded from the regression of the data.

Table 4.7 – Average sediment yield characteristics for each site.

Sediment Type	Station Name	Drainage Area	Avg. Annual sediment yield	Avg. Bed material yield	Bed material % of Total yield	Skew of discharge data
	DEC or USGS location	(sq mile)	(tons)	(tons/acre)		
bed	Abiaca 21	94.43	3468	0.06	0.05	7.34
bed	Abiaca 6	93.89	18418	0.31	0.22	8.74
yang eqn	Abaica 3	25.16	15742	0.98	N/A	8.74
yang eqn	Abaica 4	42.41	156315	5.76	N/A	8.72
bed	Batupan @ Grenada	240	297840	1.94	0.79	5.12
observed	Fannegusha @ Howard	107	521950	7.62	N/A	10.89
yang eqn	Fannegusha	17.65	51100	4.52	N/A	10.30
bed	Harland @ Howard	62.1	507	0.01	0.002	9.63
yang eqn	Harland 1	26.89	118625	6.89	N/A	9.63
yang eqn	Harland 23	40.3	172280	6.68	N/A	9.63
bed	Hickahala @ Senetobia	121	19710	0.25	0.10	10.32
yang eqn	Hickahala 11	10.41	114610	17.20	N/A	10.32
yang eqn	Hickahala 22	220.2	297840	2.11	N/A	10.32
bed	Hotopha @ Batesville	35.1	24455	1.09	1.40	16.63
yang eqn	Hotopha	19.19	9490	0.77	N/A	16.78
bed	Long creek near Pope	79.2	36865	0.73	0.10	15.89
yang eqn	Long creek	10.24	21900	3.34	N/A	13.65
bed	Otoucalofa @ Water Valley	97.1	342370	5.51	0.26	6.68
yang eqn	Otoucalofa	47.11	1085875	36.02	N/A	6.70
bed	Senetobia	82	263	0.01	0.002	10.76
yang eqn	Topashaw @ Derma	95	80300	1.32	N/A	11.70
yang eqn	Yalobusha @ Derma	158	93805	0.93	N/A	6.54
yang eqn	Yalobusha @ Vardaman	86.3	139430	2.52	N/A	8.24

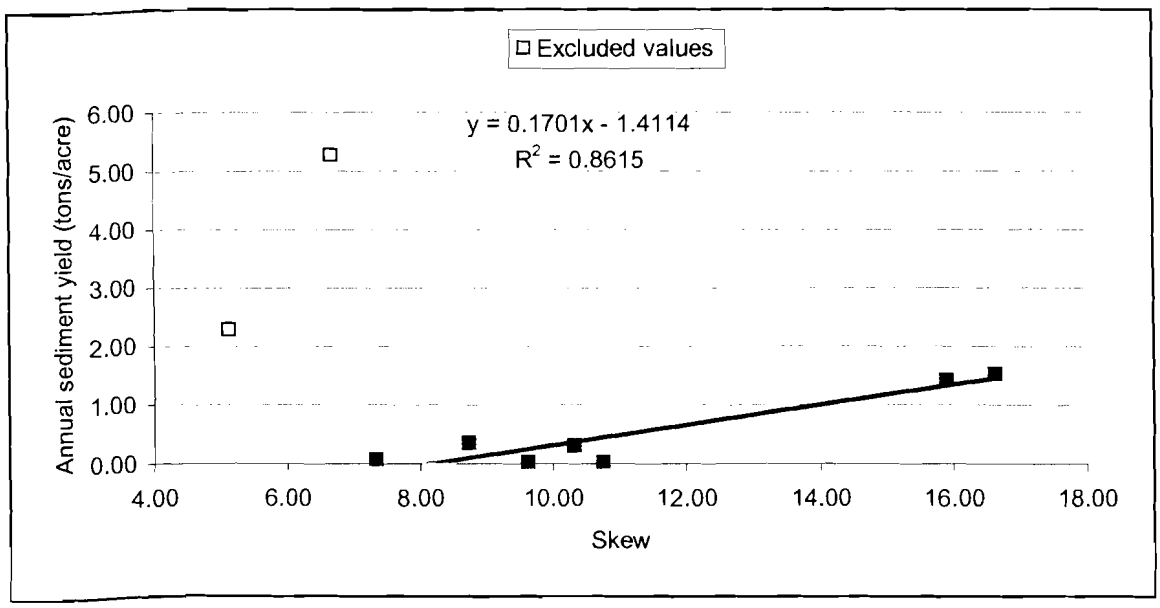

Figure 4.17 – Skewness versus annual sediment yield

5 CONCLUSIONS AND RECOMMENDATIONS

Computational methods for determining effective discharge have been presented and procedures were developed to analyze flow-duration relationships and sediment transport relationships in order to compute effective discharge for each of the twenty-three sites in the Yazoo River Basin. Analyses and comparisons were also made between arithmetic and logarithmic class size distributions and types of sediment transport concerning effective discharge, annual sediment yield, and flow duration. Conclusions of the analysis and results from the development of the effective discharge determination are presented below. In addition, recommendations for further research are also presented in this chapter.

5.1 Summary

Magnitude-Frequency Analysis (MFA) has been well documented in the engineering and geomorphological literature since the 1960 paper by Wolman and Miller. However, a step-by-step guidance on undertaking the analysis has not been made available until more recently (Soar 2000; Biedenharn et al., 2000; Thorne et al., 1998). The objective of this research was to develop a computational procedure for obtaining an objective estimate of the effective discharge and corresponding sediment yield in the Yazoo River Basin, Mississippi. However, through a detailed examination of the components of MFA, it became apparent that the type and number of discharge class intervals used in the procedure results in different estimates of the effective discharge.

Because of this finding, a program was written to further investigate the effects that the type and number of discharge classes has on the effective discharge determination. With the use of the effective discharge program, a large range of class sizes and types were analyzed to determine the most objective estimate of the effective discharge. The following section presents the conclusions that were drawn from the analysis.

5.2 Conclusions

- Nash's analytical effective discharge equation underestimates the MFA effective discharge as a result of skew in the discharge data. A better predictor for the analytical calculation when the discharge data is skewed may include the use of the Log-Pearson Type III frequency distribution, which accounts for skew in the data.
- From the analysis, fifty arithmetic and logarithmic class sizes produced the acceptable (Type II or Type III) results for determining the effective discharge using MFA for twelve sites.
- Ratio of the effective discharge to the two-year recurrence interval for the final twelve sites (Q_{eff}/Q_2) is approximately 0.8.
- A direct and reproducible MFA approach in determining the effective discharge for all twenty-three sites in this study is not currently feasible as a result of the occurrence of Type I and Type IV sediment load histograms.
- No arithmetic bin computations were successful for sites with a discharge PDF skew greater than nine.

- For sites containing a discharge skew greater than nine, it is recommended that logarithmic bins be used in determining the effective discharge for the Yazoo River Basin.
- From the results of the sediment CDF data, it appears that effective discharge in the Yazoo River Basin occurs over a range of flows that transport approximately 57% of the total sediment (μ=57%, σ=0.1). Therefore, it is recommended that this range be used to determine if the calculated effective discharge is reasonable.
- From the results of this study, the recommended method for interpreting the outputs of the arithmetic and logarithmic effective discharge calculations in order to determining effective discharge for the Yazoo Basin, Mississippi is presented in Figure 5.1.
- Finally, using the methods presented in Figure 5.1, the final determination of effective discharge for the twenty-three sites within the Yazoo River Basin, Mississippi are presented in Table 5.1.

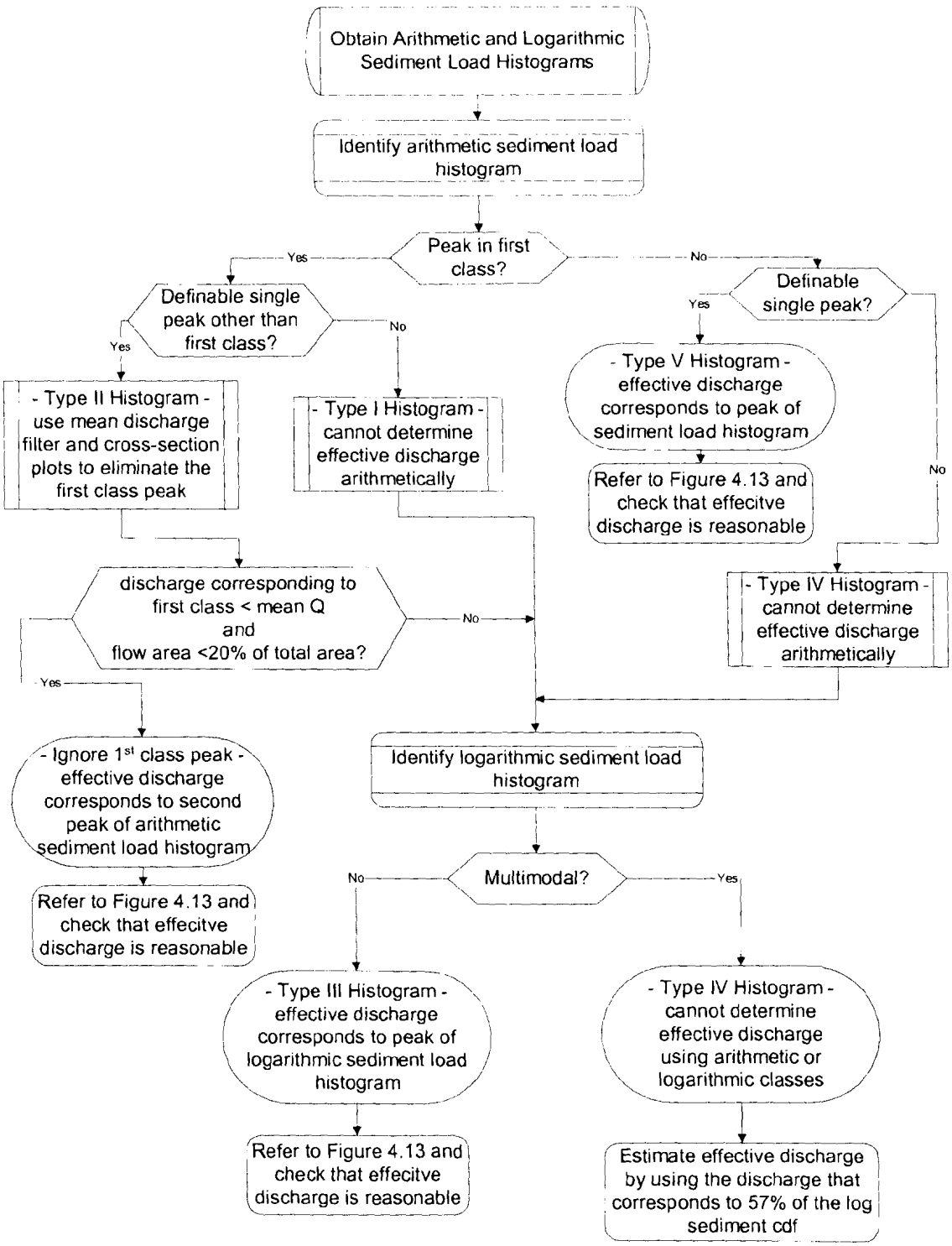

Figure 5.1 – Flow chart for interpreting the outputs of the effective discharge calculations

Table 5.1 –Effective discharge results for the Yazoo River Basin, Mississippi

	Station Name	Histogram Type	Effective Discharge	% cdf Sed	Mean Q	Q2
	DEC or USGS		(cfs)		(cfs)	(cfs)
1	Abiaca 3 (DEC)	Type II	692	58%	68	1778.65
2	Abiaca 4 (DEC)	Type II	776	60%	116	2477.43
3	Abiaca 6 (DEC)	Type II	1187	56%	116	3284.85
4	Abiaca 21 (DEC)	Type II	1244	67%	102	2350.09
5	Fannegusha (DEC)	Type III	2352	67%	68	1711.69
6	Hickahala near Senetobia	Type III	6064	58%	170	6591.32
7	Hickahala 11 (DEC)	Type III	1285	73%	36	1166.10
8	Hickahala 22 (DEC)	Type III	8708	67%	245	8553.52
9	Hotopha Creek near Batesville	Type III	552	61%	60	2660.06
10	Peters (Long) Creek near Pope	Type III	7451	69%	124	5535.07
11	Long (DEC)	Type III	1406	52%	41	967.64
12	Senetobia (DEC)	Type III	5104	70%	98	4727.63
		Discharge corresponding to 57% of log sediment cdf				
13	Batupan Bogue at Grenada	Type II	*2126	53%	774	9779.96
14	Fannegusha Creek near Howard	Type I or IV	5969	57%	172	4952.63
15	Harland Creek near Howard	Type I or IV	**22.31	57%	97	4488.90
16	Harland 1 (DEC)	Type I or IV	1743	57%	52	2009.25
17	Harland 23 (DEC)	Type I or IV	2832	57%	85	2459.85
18	Hotopha (DEC)	Type I or IV	1559	57%	50	1506.83
19	Otoucalofa (DEC)	Type I or IV	6717	57%	308	3357.62
20	Otoucalofa Canal near Water Valley	Type I or IV	19086	57%	542	5218.53
21	Topashaw Creek near Derma (DEC)	Type I or IV	4330	57%	90	4502.25
22	Yalobusha River @ Derma (DEC)	Type I or IV	4657	57%	241	7885.66
23	Yalobusha River @ Vardaman (DEC)	Type I or IV	2217	57%	141	5275.92

* Omitted from Type II results due to backwater affects, resulting in inacurrate sediment and water discharge data

** Effected by backwater resulting in inacurrate sediment and water discharge data

5.3 Recommendations for Further Research

- Additional discharge and sediment data should be collected at each location, with an emphasis on a greater range of observed sediment data with corresponding sediment gradations at low flows in order to generate sediment rating curves which better predict low flow sediment transport.
- Further analysis of Nash's analytical effective discharge equation should be conducted using the Log-Pearson Type III frequency equation in order to account for skew in the data.
- Classification of MFA computation characteristics (Type I, II, III, IV, V) outside of the Yazoo River Basin should be conducted to establish applicability.

6 REFERENCES

Andrews, C. V. (1980). Effective and bankfull discharges of streams in the Yampa River Basin, Colorado and Wyoming. *J. Hydrol.*, 46:311-333.

Ashmore, P. E., and Day, T. J. (1988). Effective discharge for suspended sediment transport in streams of the Saskatchewan River Basin. *Water Resources Research*, 24(6):864-870.

Biedenharn, D. S., Little, C. D., and Thorne, C. R. (1987). Magnitude and frequency analysis of large rivers. In: Ragan, R. M. (Ed.), *Hydraulic Engineering, Proceedings of the National Conference*, American Society of Civil Engineers, Williamsburg, pp. 782-787.

Biedenharn, D. S. and Thorne, C. R. (1994). Magnitude-frequency analysis of sediment transport in the lower Mississippi River. *Regulated Rivers: Research and Management*, 9:237-251.

Biedenharn, D. S., Copeland, R. R., Thorne, C. R., Soar, P. J., Hey, R. D., and Watson, C. C. (2000). Effective Discharge Calculation: A Practical Guide. U.S. Army Corps of Engineers, Washington, DC, Report No. ERDC/CHL TR-00-15.

Carling, P. A. (1988). The concept of dominant discharge applied to two gravel-bed streams in relation to channel stability thresholds. *Earth Surface Processes and Landforms*, 13:355-367.

Colson, B. E., and Hudson, J. W. (1976). Flood Frequency of Mississippi Streams. U.S. Geological Survey, Report No. MSHD-RD-76-014-PR.

Doyle, M. W., Boyd, K. F., and Skidmore, P. B. (1999). River restoration channel design: Back to the basics of dominant discharge. In: *Stream Corridors: Adaptive Management and Design, Proceedings of the Second International Conference on Natural Channel Systems*, Niagara Falls, Canada, March 1-4, CD ROM, Session 9.

Dubler, D. R. (1997). Effective Discharge Determination in the Yazoo River Basin, Mississippi. M.S. Thesis, Department of Civil Engineering, Colorado State University, Fort Collins, CO.

Goodwin, P., Slaughter, C. W., and Marbury, R. (1998). Dominant discharge as a design criteria in river restoration. In: Hayes, D. F. (Ed.), *Engineering Approaches to Ecosystem Restoration, Proceedings of the Wetlands Engineering and River Restoration Conference, 1998*, American Society of Civil Engineers, Denver, Colorado, March 22-26, CD ROM, Technical Session M3.

Guy, H. P., and Norman, V. W. (1970). Field methods for measurement of fluvial sediment. In: *Techniques of Water-Resources Investigations of the USGS*, Chapter C2, Book 3, 59 p.

Hendon, S. (1995). Comparison of 15-minute versus Mean Daily Flow Duration Curves from the Yazoo Basin, Mississippi. M.S. Thesis, Department of Civil Engineering, Colorado State University, Fort Collins, CO.

Hey, R. D. (1975). Design discharge for natural channels. In: Hey, R. D., and Davies, T. D. (Eds.), *Science, Technology and Environmental Management*, Saxon House, Farnborough.

Hey, R. D. (1997). Channel Response and Channel Forming Discharge. University of East Anglia, Norwich UK, Final Report, Contract No. R&D 687-EN-01. I 19.42/4:90-4087.

Johnson, P. A., and Heil, T. M. (1996). Uncertainty in estimating bankfull conditions. *Water Resources Bulletin*, American Water Resources Association, 32(6):1283-1291.

Julien, P. Y. (1995). Erosion and Sedimentation. Cambridge University Press.

Kilpatrick, F. A., and Barnes Jr., H. H. (1964). Channel Geometry of Piedmont Streams as Related to Frequency of Floods. U. S. Geological Survey, Professional Paper 422-E, 10 p.

Knighton, D. (1984). Fluvial Forms and Processes. London, UK: Edward Arnold.

Kuhnle, R., Simon, A., and Bingner, R. L. (1999). Dominant discharge of the incised channels of Goodwin Creek. In: Walton, R., and Nece, R. E. (Eds.), *Water Resources into the New Millennium: Past Accomplishments and New Challenges, Proceedings of the 1999 International Water Resources Engineering Conference*, American Society of Civil Engineers, Seattle, Washington, August 8-12, CD ROM, Technical Session RR4.

Leopold, L. B. (1994). A View of the River. Cambridge, MA: Harvard University Press, 298 pp.

Leopold, L. B., Wolman, M. G., and Miller, J. P. (1964). Fluvial Processes in Geomorphology. London, UK: W. H. Freeman and Company, 522 pp.

Lyons, J. K., Pucherelli, M. J., and Clark, R. C. (1992). Sediment transport and channel characteristics of a sand-bed portion of the Green River below Flaming Gorge Dam, Utah, USA. *Regulated Rivers: Research and Management*, 7:219-232.

Mackin, J. H. (1948). Concept of the graded river. *Bulletin of the Geological Society of America*, 59:463-512.

Nash, D. B. (1994). Effective sediment-transporting discharge from magnitude-frequency analysis. *J. Geology*, 102:79-95.

Nixon, M. (1959a). A study of bank-full discharges of rivers in England and Wales. *Proceedings of the Institution of Civil Engineers*, 12(Paper 6322):157-174.

Nixon, M. (1959b). A study of bank-full discharges of rivers in England and Wales. *Proceedings of the Institution of Civil Engineers*, 14:395-425.

Nunnally, N. R. (1967). Definition and identification of channel and overbank deposits and their respective roles in floodplain formation. *Professional Geographer*, 19:1-4.

Orndorff, R. L., and Whiting, P. J. (1999). Computing effective discharge with S-PLUS. *Computers and Geosciences*, 25:559-565.

Pickup, G., and Warner, R. F. (1976). Effects on hydrologic regime on magnitude and frequency of dominant discharge. *J. Hydrol.*, 29:51-75.

Riley, S. J. (1972). A comparison of morphometric measures of bankfull. *J. Hydrol.*, 17:23-31.

Rosgen, D. L. (1994). A classification of natural rivers. *Catena*, 22:169-199.

Salas, J. D., Smith, R. A., Tabios, G. Q., and Heo, J. (1995). Statistical Computer Techniques in Water Resources and Environmental Engineering. Department of Civil Engineering, Colorado State University, Fort Collins, CO.

Salas, J. D., Smith, R. A., Tabios, G. Q., and Heo, J. (2000). Statistical Computing Techniques in Water Resources and Environmental Engineering. Department of Civil Engineering, Colorado State University, Fort Collins, CO, pp. 4:9-4:19.

Schumm, S. A. (1960). The Shape of Alluvial Channels in Relation to Sediment Type. U.S. Geological Survey, Professional Paper 352-B, pp. 17-30.

Searcy, J. K. (1959). Flow-Duration Curves, Manual of Hydrology: Part 2. Low-flow Techniques. U.S. Geological Survey, Water-Supply Paper 1542-A.

Sichingabula, H. M. (1999). Magnitude-frequency characteristics of effective discharge for suspended sediment transport, Fraser River, British Columbia, Canada. *Hydrological Processes*, 13:1361-1380.

Soar, P. J. (2000). Channel Restoration Design for Meandering Rivers. Ph.D. Thesis, University of Nottingham, Nottingham, UK, May.

Telis, P. A. (1991). Low-flow and Flow-duration Characteristics of Mississippi Streams. U.S. Geological Survey, Water-Resources Investigations Report 90-4087, 214 p.

Thorne, C. R., Soar, P. J., Hey, R. D., and Watson, C. C. (1998). Dominant Discharge Calculation: A Practical Guide. U.S. Army Research, Development, and Standardization Group – UK, London.

Tilleard, J. (1999). Effective Discharge as an Aid to River Rehabilitation. In: Rutherford, I., and Bartley, R. (Eds.), *Second Australian Stream Management Conference: The Challenge of Rehabilitating Australia's Streams*, Adelaide, South Australia, February 8-11, pp. 629-635.

Toffaleti, F. B. (1968). A Procedure for Computation of the Total River Sand Discharge and Detailed Distribution, Bed to Surface. Committee on Channel Stabilization, USACE.

Watson, C. C., Dubler, D., and Abt, S. R. (1997). Design Hydrology Investigations. Report to U.S. Army Corps of Engineers, Waterways Experiment Station, Vicksburg, MS, August, 72 p.

Webb, B. W., and Walling, D. E. (1982). The magnitude and frequency characteristics of fluvial transport in the Devon drainage basin and some geomorphological implications. *Catena*, 9:9-23.

Williams, G. P. (1978). Bank-full discharges of rivers. *Water Resources Research*, 14:1141-1158.

Williams, G. P., and Rosgen, D. L. (1989). Measured total sediment loads (suspended loads and bedloads) for 93 US streams. U.S. Geological Survey, Open-file Report 89-67, 128 p.Wolman, M. G. (1955). The Natural Channel of Brandywine Creek, Pennsylvania. U.S. Geological Survey, Professional Paper 271, 56 p.

Wolman, M. G., and Gerson, R. (1978). Relative scales of time and effectiveness of climate and watershed geomorphology. *Earth Surface Processes and Landforms*, 3:189-208.

Wolman, M. G., and Leopold, L. B. (1957). River Floodplains - Some Observations on Their Formation. U.S. Geological Survey, Professional Paper 282C.

Wolman, M. G., and Miller, J. P. (1960). Magnitude and frequency of forces in geomorphic processes. *J. Geology*, 68:54-74.

Woodyer, K. D. (1968). Bankfull frequency in rivers. *J. Hydrol.*, 6:114-142.

Yang, C. T. (1973). Incipient motion and sediment transport. *J. Hydraulics Div.*, ASCE, 99:1679-1704.

Yevjevich, V., (1972). "Probability and Statistics in Hydrology." Water Resources Publications, Fort Collins, CO.

APPENDIX A

Sample flow frequency class size calculations

Table A.1 – Logarithmic flow frequency class size computation for Abiaca21

$$Interval\ Index = \frac{\log_e(MaxQ) - \log_e(MinQ)}{n-2}$$

$$1st\ Class\ Interval = 0$$

$$2nd\ Class\ Interval = MinQ$$

$$3rd\ Class\ Interval = e^{(\log_e(MinQ) + interval_index)}$$

$$4th\ Class\ Interval = e^{(\log_e(MinQ) + 2*interval_index)}$$

$$5th\ Class\ Interval = e^{(\log_e(MinQ) + 3*interval_index)}$$

.

.

.

$$48th\ Class\ Interval = e^{(\log_e(MinQ) + 46*interval_index)}$$

$$49th\ Class\ Interval = e^{(\log_e(MinQ) + 47*interval_index)}$$

$$50th\ Class\ Interval = MaxQ$$

	Min Q	13.60598		
	Max Q	3570		
	Number of Bins	50		
	Interval Index	0.116037739		
Class Ref#	**Bin Size (cfs)**	**Frequency**	**Bin Probability**	**CDF**
1st	0.00	0	0.00000	0.00000
2nd	13.61	2	0.00001	0.00001
3rd	15.28	18	0.00006	0.00007
4th	17.16	244	0.00088	0.00095
5th	19.27	689	0.00249	0.00344
.	.	.	.	.
.	.	.	.	.
.	.	.	.	.
48th	2830.60	234	0.00084	0.99938
49th	3178.88	135	0.00049	0.99986
50th	3570.00	38	0.00014	1.00000

Note: Class intervals can vary slightly due to rounding of the interval index.

Table A.2 – Arithmetic flow frequency class size computation for Abiaca21

$$Interval\ Index = \frac{MaxQ - MinQ}{n}$$

$$1st\ Class\ Interval = interval_index$$
$$2nd\ Class\ Interval = 2 * interval_index$$
$$3rd\ Class\ Interval = 3 * interval_index$$
$$4th\ Class\ Interval = 4 * interval_index$$
$$5th\ Class\ Interval = 5 * interval_index$$

.

.

.

$$48th\ Class\ Interval = 48 * interval_index$$
$$49th\ Class\ Interval = 49 * interval_index$$
$$50th\ Class\ Interval = 50 * inerval_index$$

	Min Q	13.60598		
	Max Q	3570		
	Number of Bins	50		
	Interval Index	71.1278804		
Class Ref#	**Bin Size (cfs)**	**Frequency**	**Bin Probability**	**CDF**
1st	71.13	190813	0.68895	0.68895
2nd	142.26	56257	0.20312	0.89207
3rd	213.38	12068	0.04357	0.93564
4th	284.51	4318	0.01559	0.95124
5th	355.64	2480	0.00895	0.96019
.	.	.	.	.
.	.	.	.	.
.	.	.	.	.
48th	3414.14	9	0.00003	0.99998
49th	3485.27	1	0.00000	0.99998
50th	3556.39	5	0.00002	1.00000

Note: Class intervals can vary slightly due to rounding of the interval index.

APPENDIX B

Sediment discharge rating curve coefficients

Table B.1 – Sediment rating coefficients for each site

			$Qs = aQ^b$ (all years)				Range of Q for Q_s Equation	
	Sediment type	**Station Name & gauge #**	**a**	**b**	**R^2**	**N**	**High Discharge**	**Low Discharge**
							cfs	**cfs**
1	Observed	Abiaca 21 near Cruger #07287160	0.0028	2.0898	0.92	77	2180	28
	Pump		0.0061	1.8926	0.89	2723	3550	21.5
	bed		0.0046	1.4923	0.31	6	2180	417
2	Observed	Abiaca 6 near Seven Pines #07287150	0.0028	2.11	0.87	75	3210	28
	Pump		0.0129	1.7502	0.91	3685	5570	3.8
	bed		0.0081	1.6067	0.98	5	3210	142
3	Observed	Batupan Bogue at Grenada #07285400	1.3458	1.1451	0.88	6	21200	1040
	Pump		0.0076	1.6146	0.76	6075	30400	17
	bed		0.2081	1.1922	0.69	6	21200	1040
4	Observed	Fannegusha Creek near Howard #07287355	0.0024	2.006	0.78	80	2200	14
	Pump		0.0032	2.01	0.95	991	7610	7
5	Observed	Harland Creek near Howard #07287404	0.0099	2.0322	0.90	82	4130	9.4
	Pump		0.0107	1.8851	0.91	5973	6490	6
	bed		1.3512	0.0073	0.59	3	4130	1060
6	Observed	Hickahala near Senetobia #07277700	0.0079	1.7557	0.94	108	16000	32
	Pump		0.0076	1.7601	0.85	5557	18000	9
	bed		0.0004	1.8405	0.72	11	16000	1910
7	Observed	Hotopha Creek near Batesville #07273100	0.0054	1.992	0.96	7	1840	14
	Pump		0.0297	1.4924	0.84	4739	9310	2
	bed		0.8178	1.0382	0.72	6	1840	260
8	Observed	Otoucalofa Canal near Water Valley #07274252	0.0031	1.8265	0.95	91	16300	25
	Pump		0.0135	1.6835	0.81	5206	20400	12
	bed		0.00001	2.3005	0.92	5	16300	219
9	Observed	Peters (Long) Creek near Pope #07275530	0.01	1.7717	0.97	10	17000	19
	Pump		0.0031	1.9597	0.95	4256	25100	4
	bed		0.0283	1.437	0.70	9	17000	656
10	Observed	Senetobia #07277730	0.1792	1.0319	0.99	8	9720	37
	Pump		0.009	1.8123	0.90	2473	11200	7.1
	bed		0.00004	1.7263	1.00	3	9720	276
11	pump	Topashaw Creek near Derma #07282090	0.0846	1.4471	0.94	304	8452	1
12	pump	Yalobusha River @ Derma #07281977	0.1078	1.2778	0.95	239	9425	1

APPENDIX C

Effective Discharge sediment histograms for fifty arithmetic and logarithmic bins

for each of the twenty-three sites

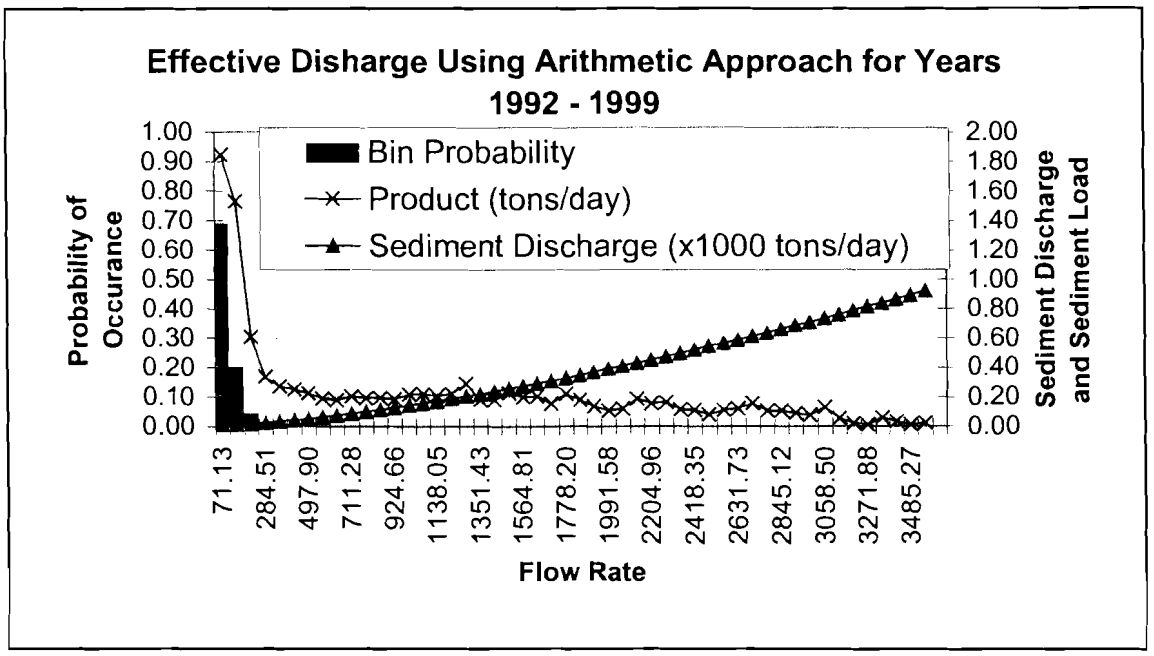

Figure C.1– Abiaca 21 near Cruger (arithmetic bins)

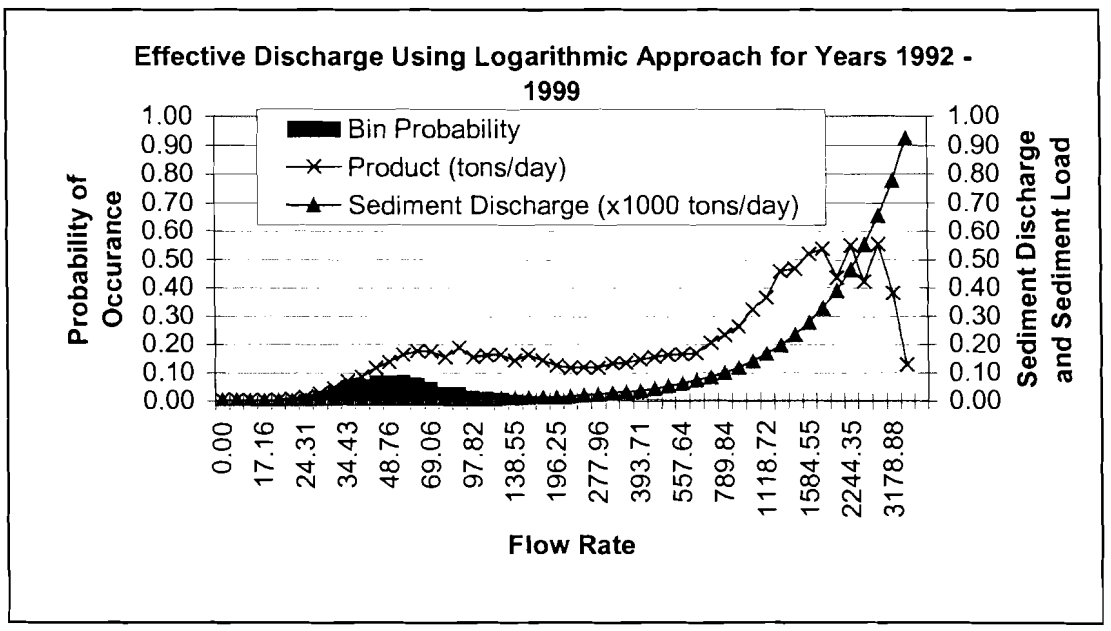

Figure C.2– Abiaca 21 near Cruger (logarithmic bins)

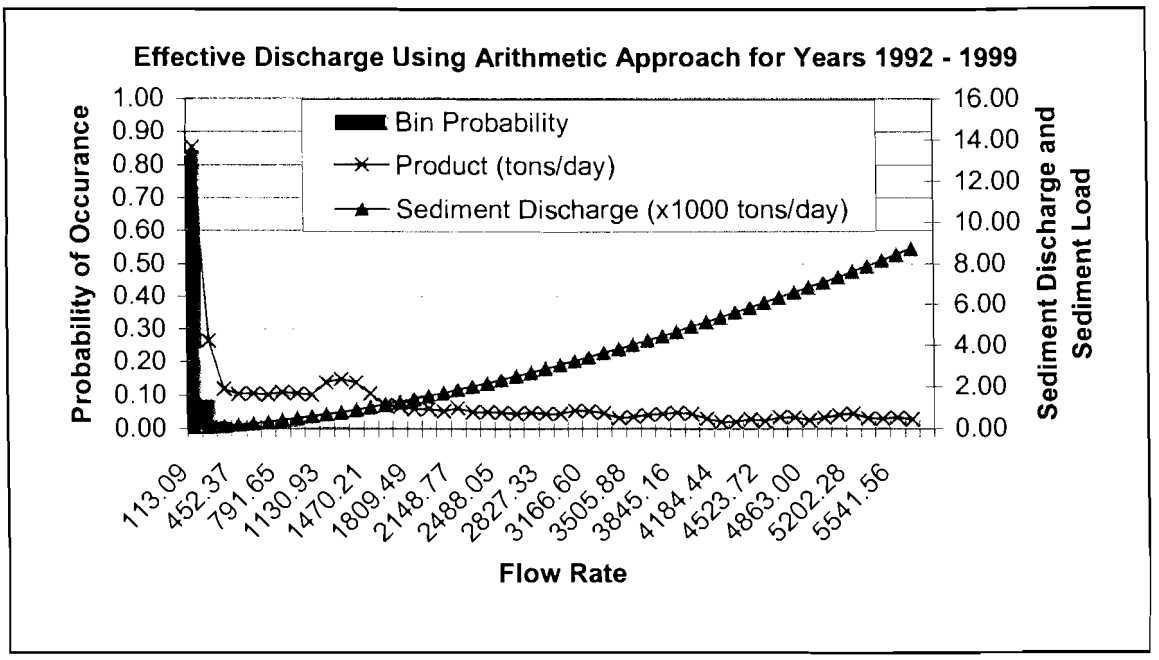

Figure C.3– Abiaca 6 near Seven Pines DEC (arithmetic bins)

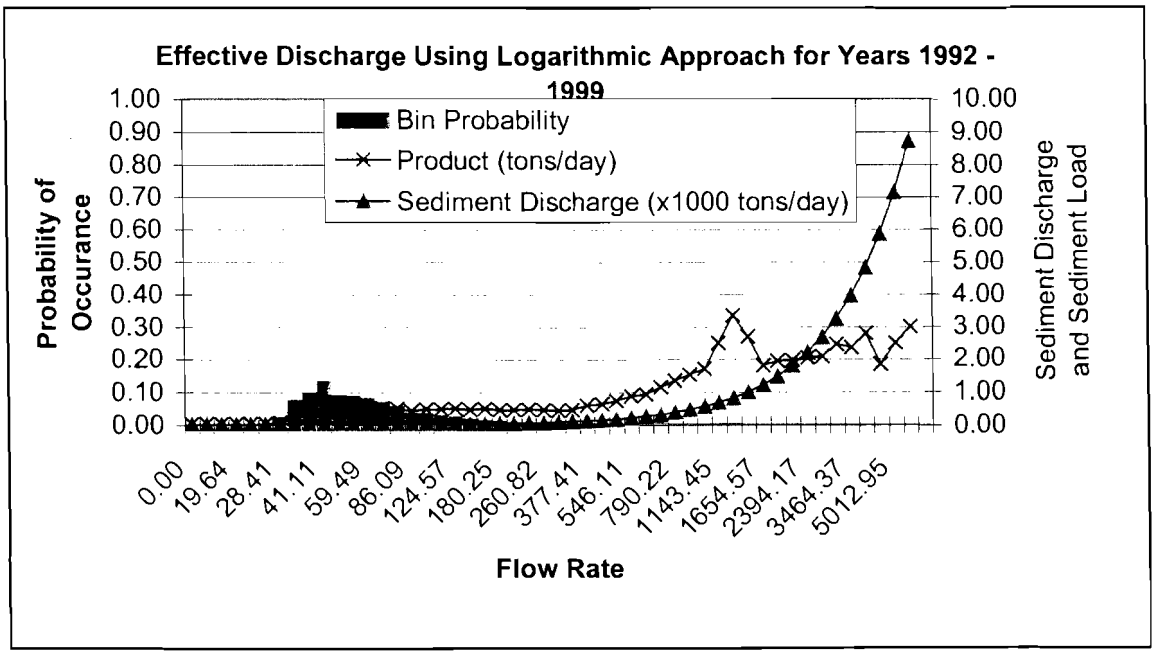

Figure C.4– Abiaca6 near Seven Pines DEC (logarithmic bins)

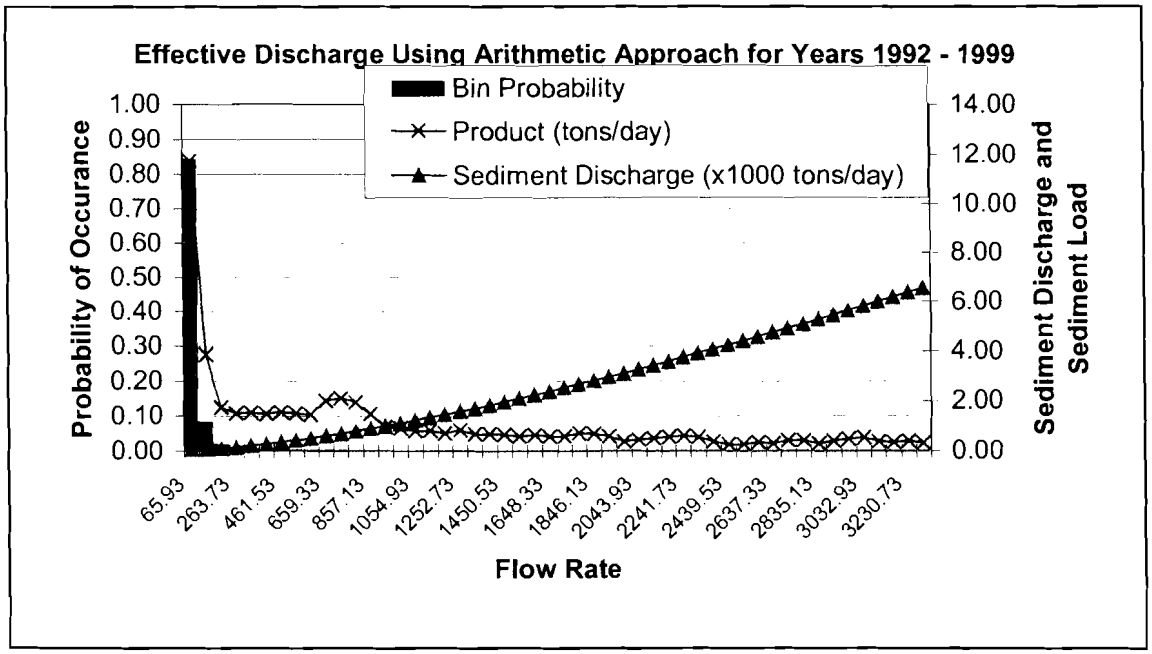

Figure C.5– Abiaca 3 DEC (arithmetic bins)

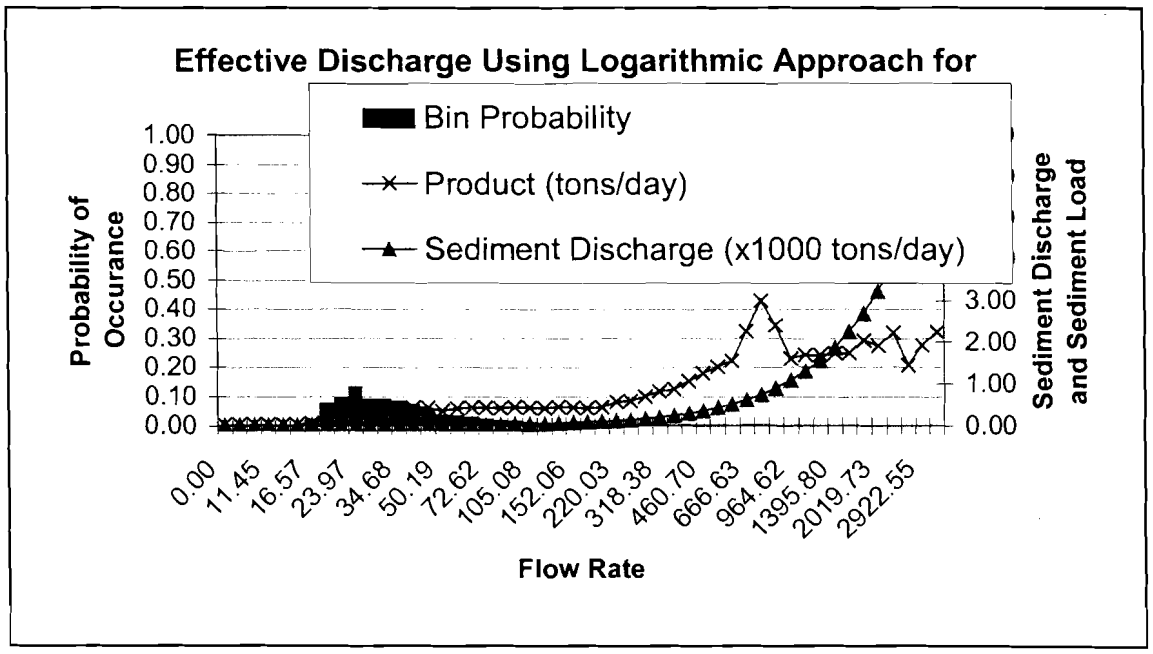

Figure C.6– Abiaca 3 DEC (logarithmic bins)

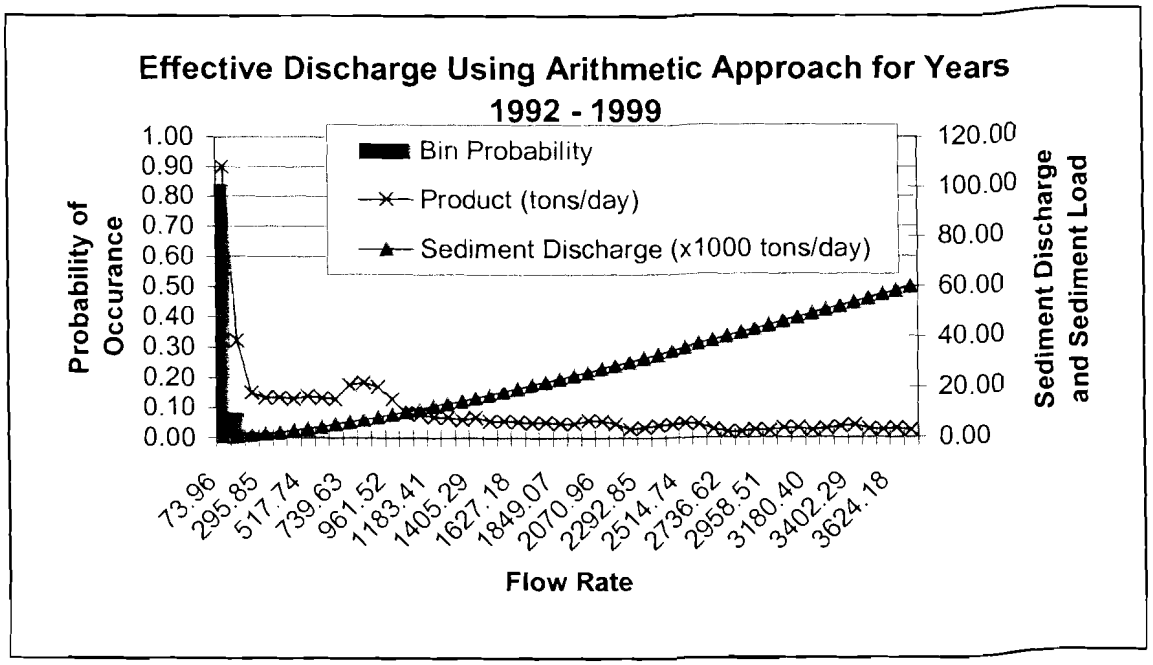

Figure C.7– Abiaca 4 DEC (arithmetic bins)

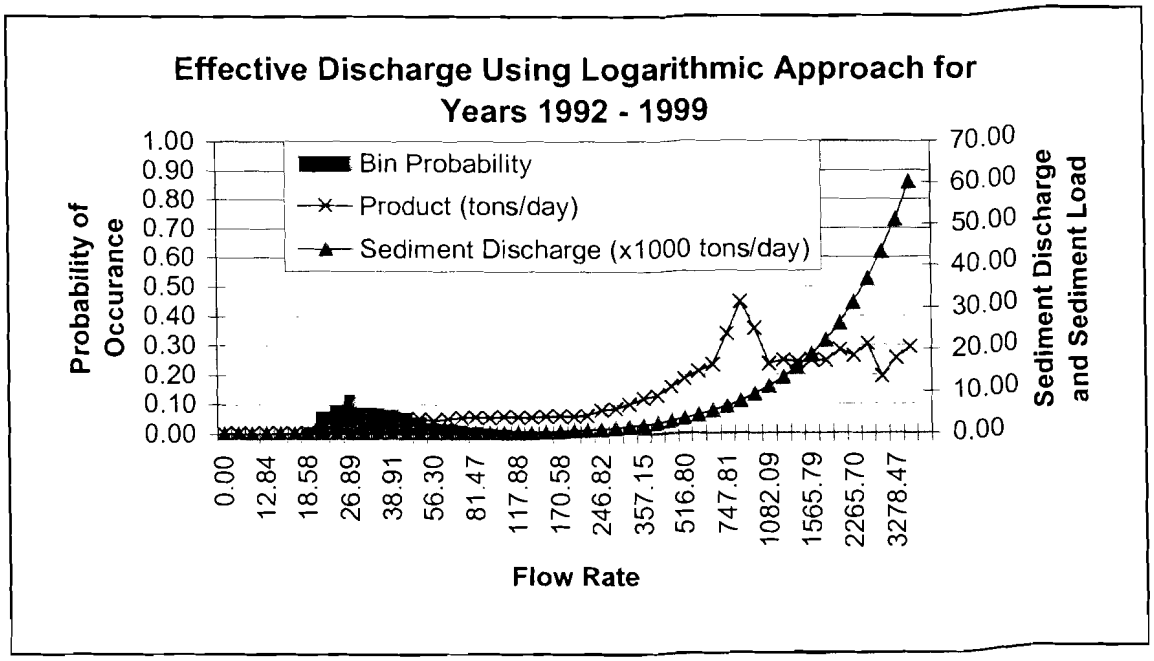

Figure C.8– Abiaca 4 DEC(logarithmic bins)

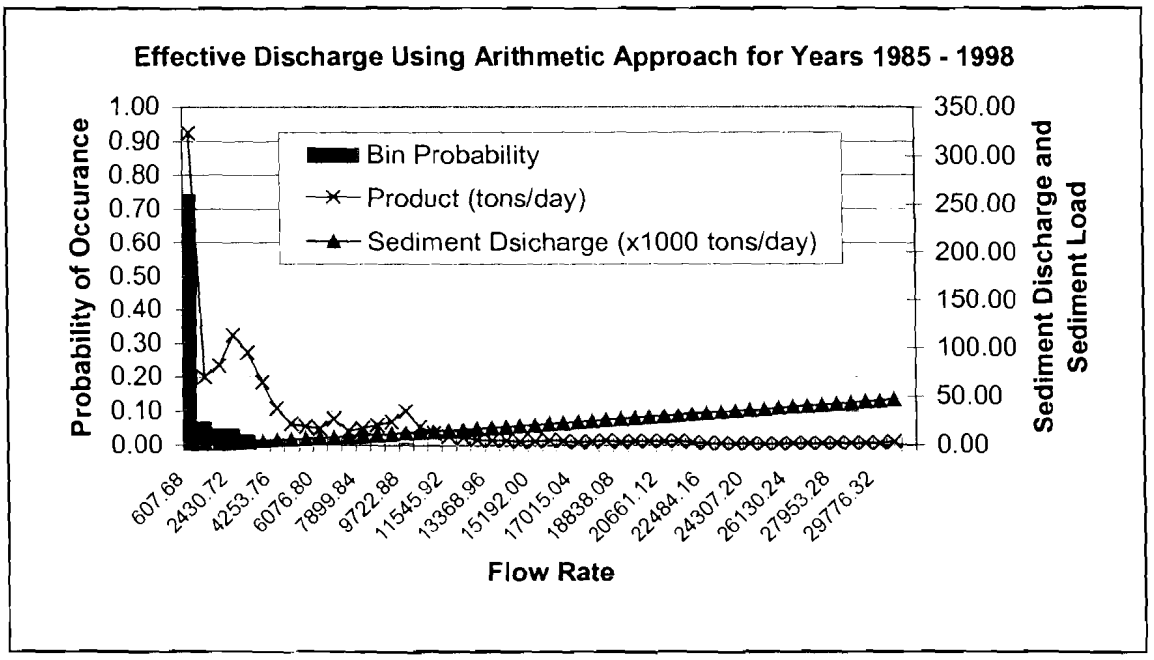

Figure C.9– Batupan Bogue at Grenada (arithmetic bins)

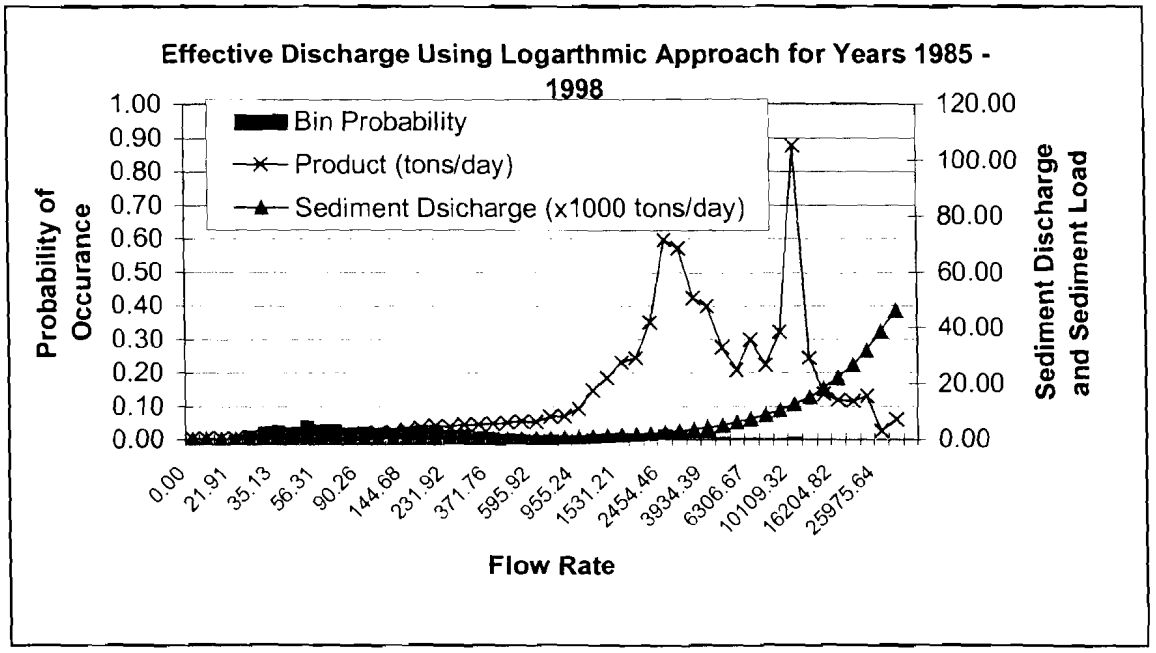

Figure C.10– Batupan Bogue at Grenada (logarithmic bins)

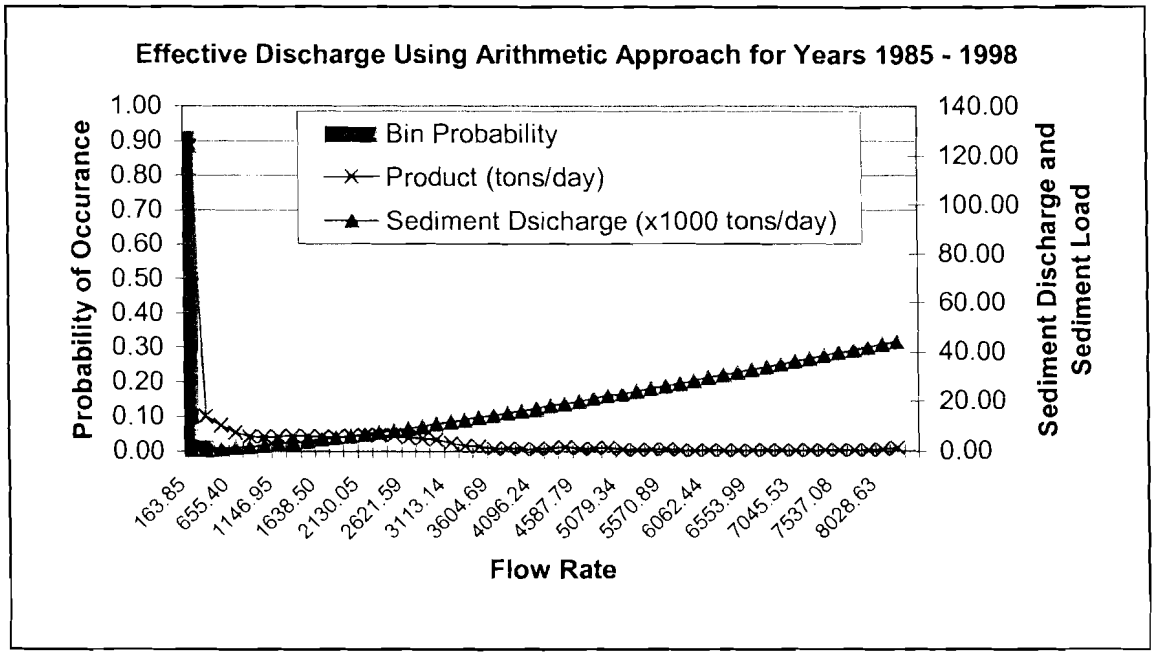

Figure C.11– Fannegusha DEC (arithmetic bins)

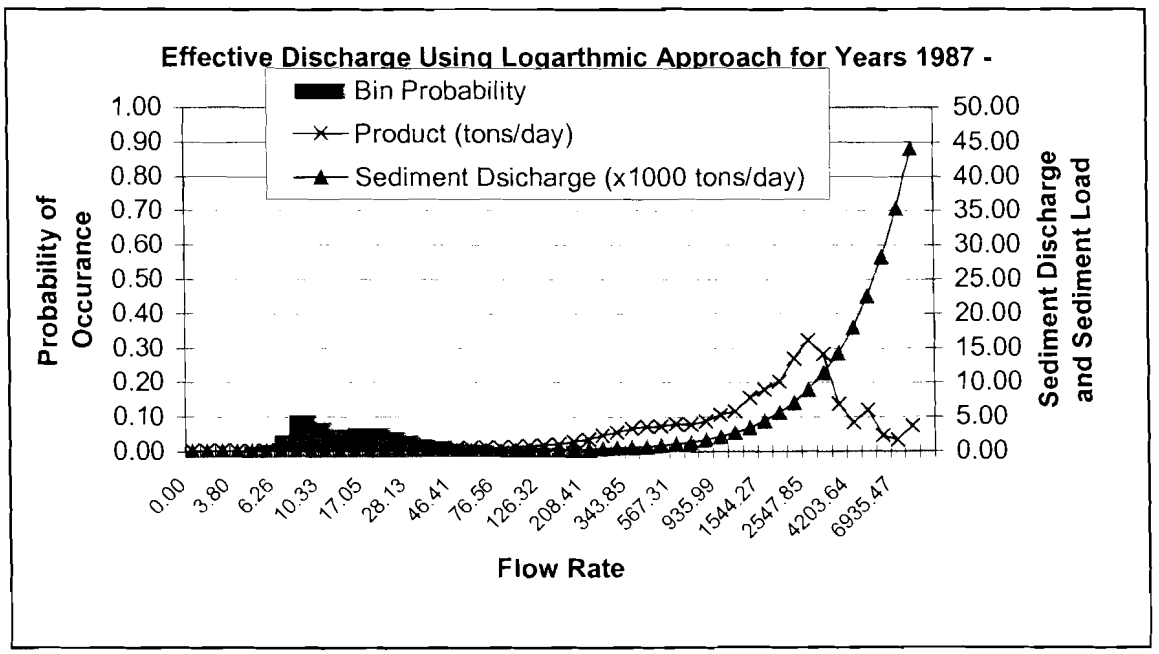

Figure C.12– Fannegusha DEC (logarithmic bins)

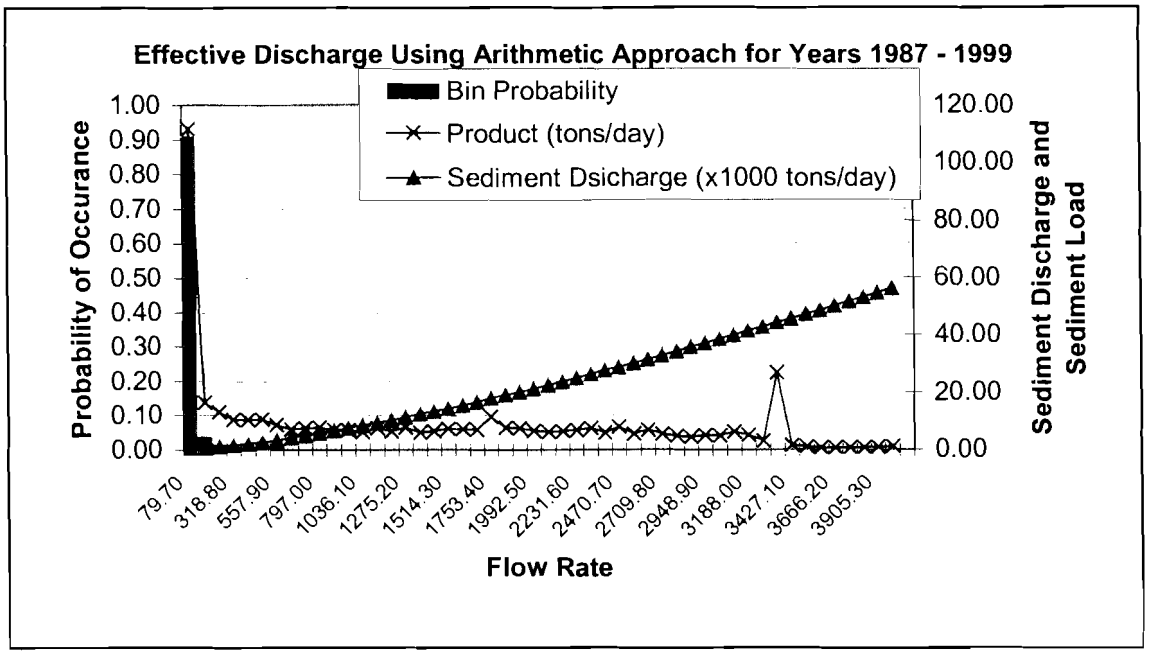

Figure C.13– Halrland 1 DEC (arithmetic bins)

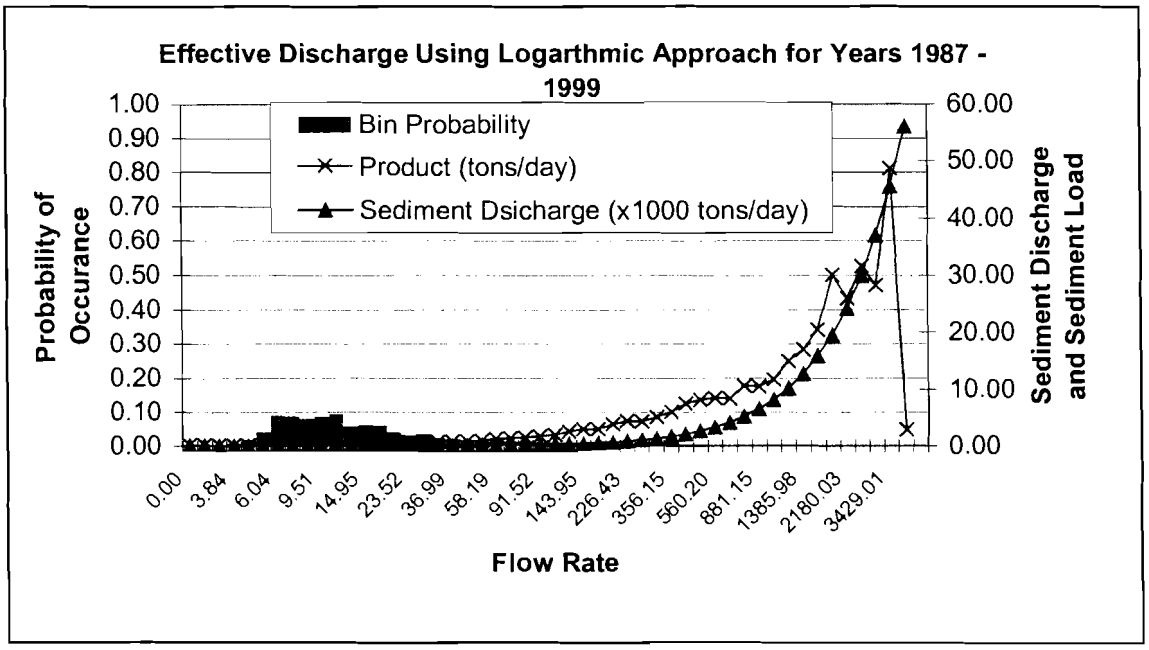

Figure C.14 – Harland 1 DEC (logarithmic bins)

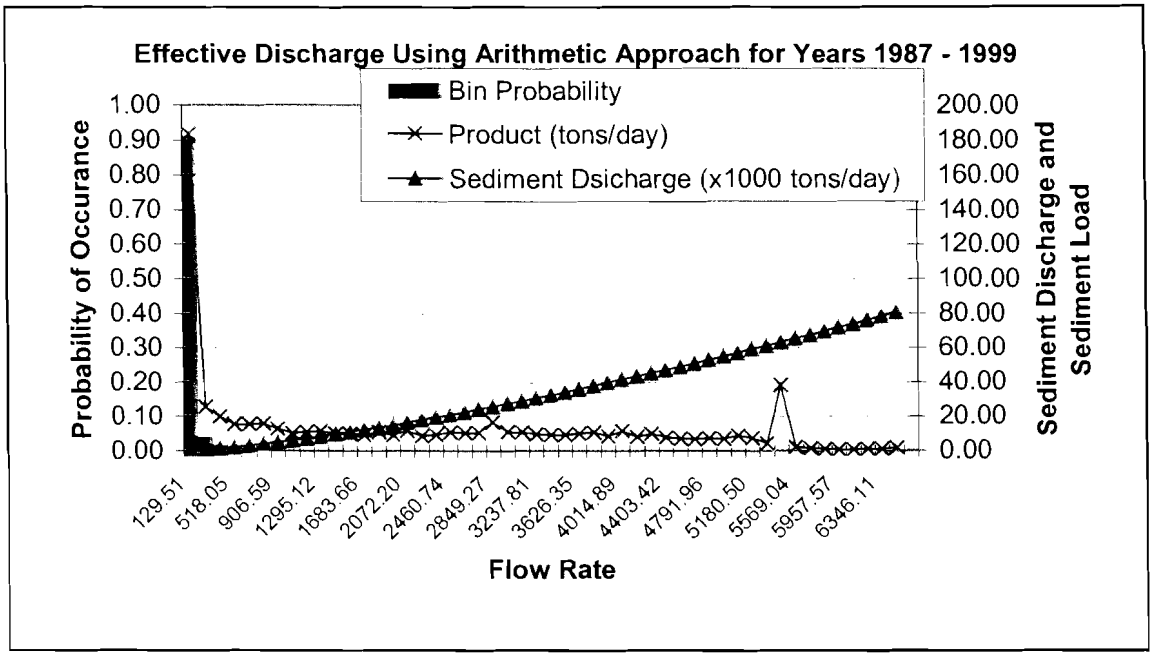

Figure C.15 – Harland 23 DEC (arithmetic bins)

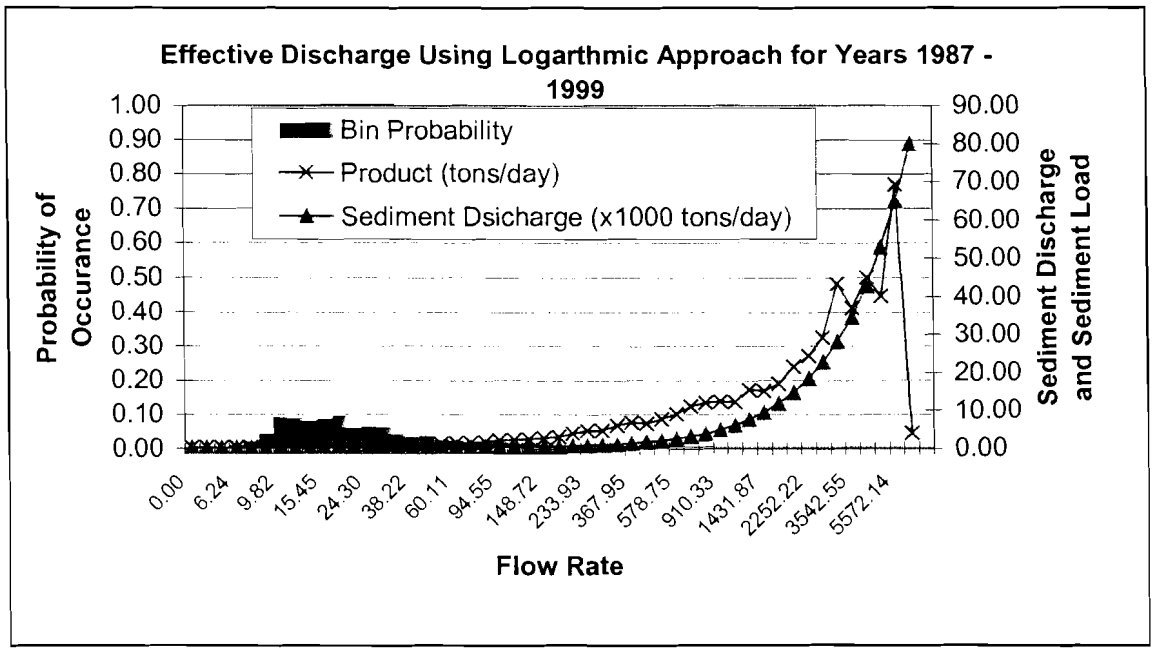

Figure C.16 – Harland 23 DEC (logarithmic bins)

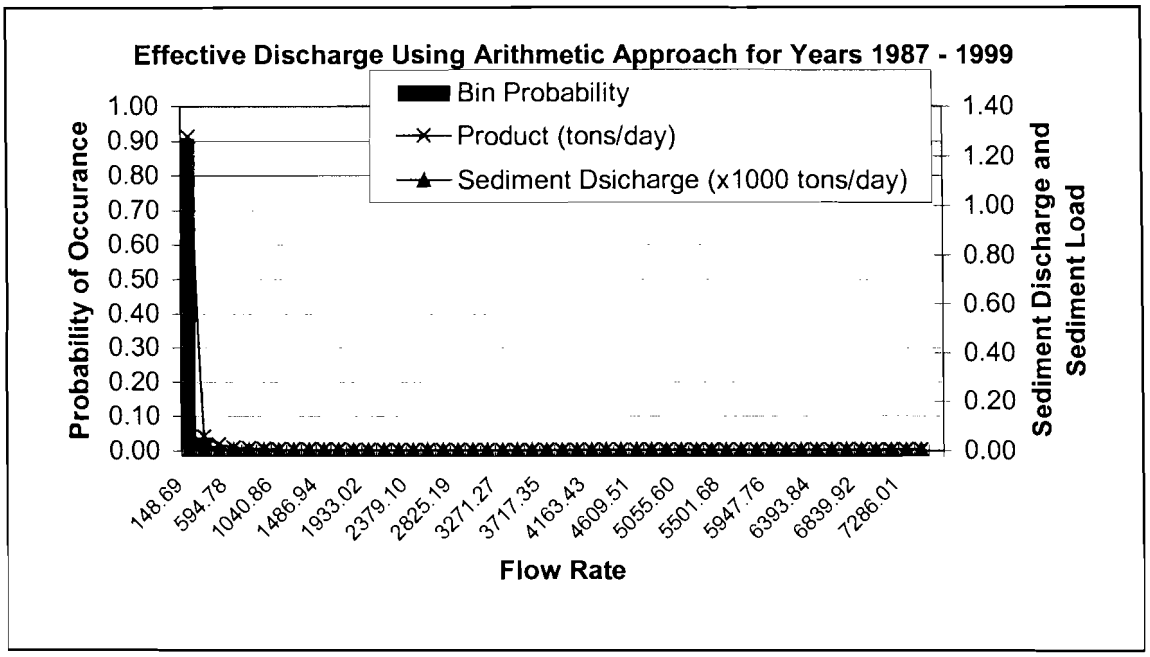

Figure C.17 – Harland near Howard (arithmetic bins)

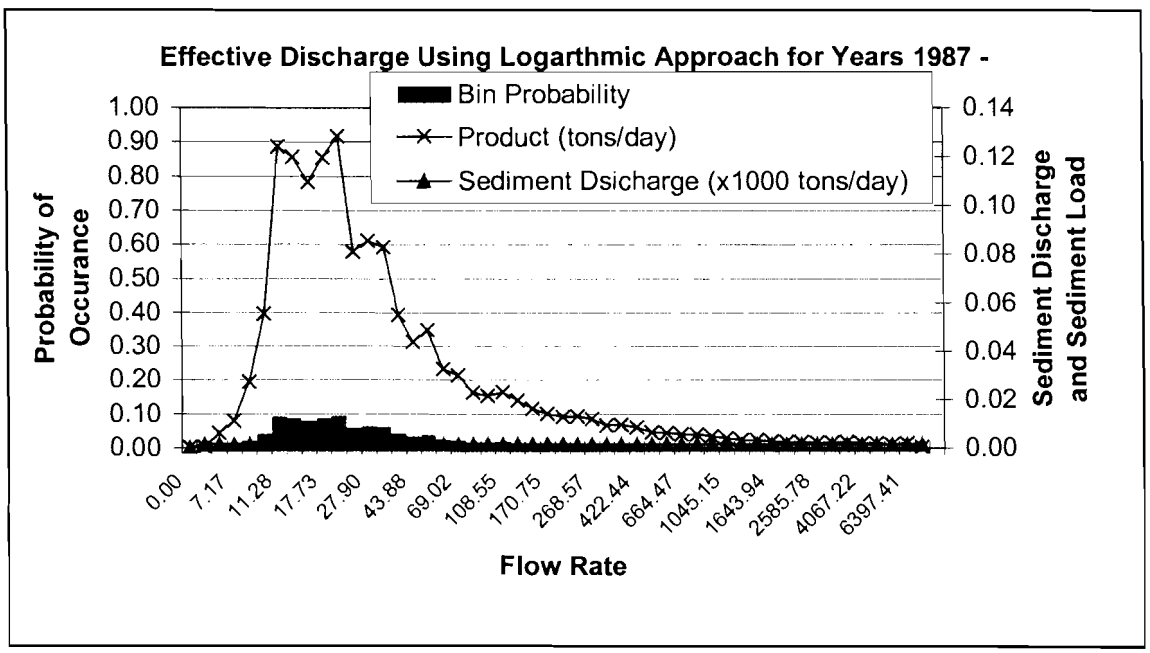

Figure C.18 – Harland near Howard (logarithmic bins)

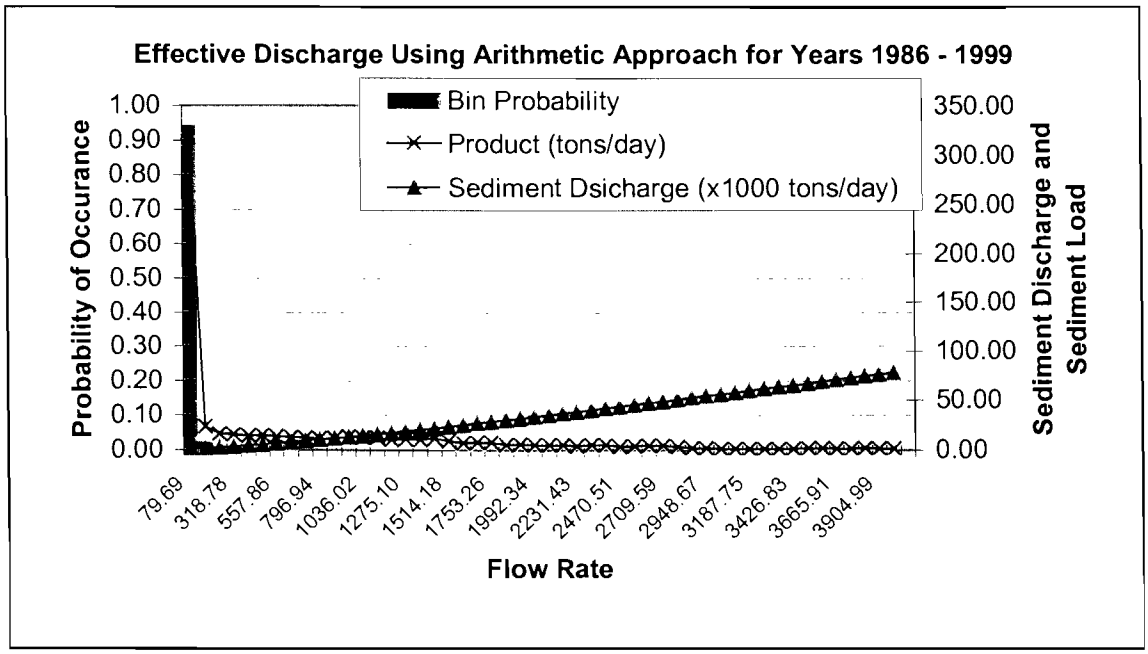

Figure C.19 – Hickahala 11 DEC (arithmetic bins)

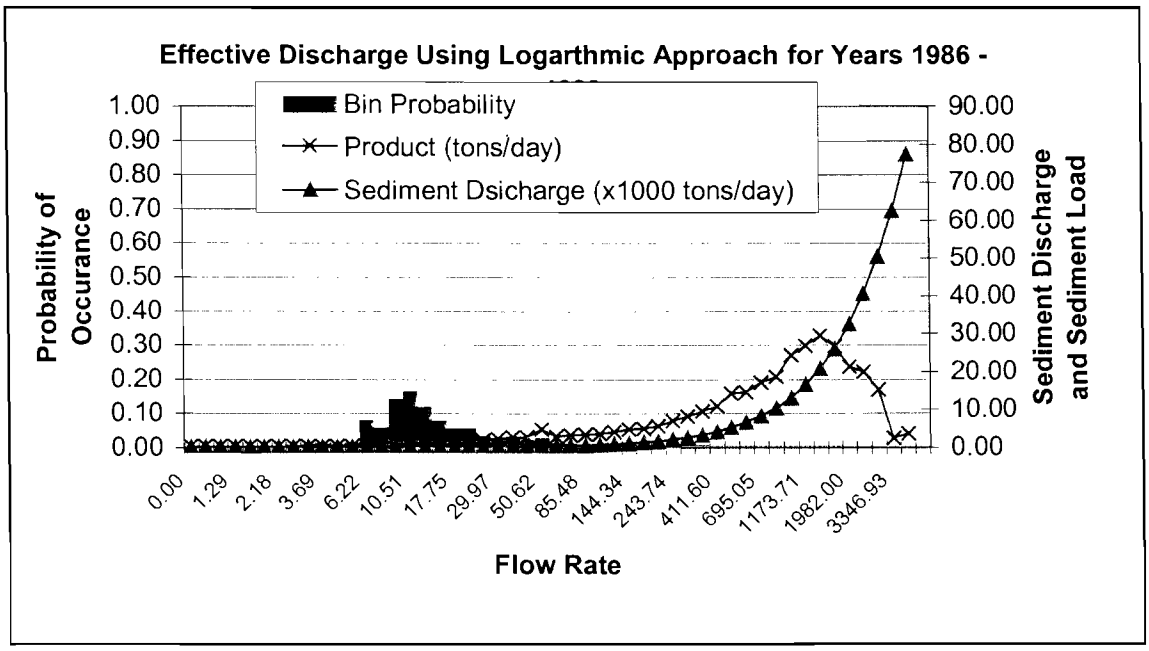

Figure C.20 – Hickahala 11 DEC (logarithmic bins)

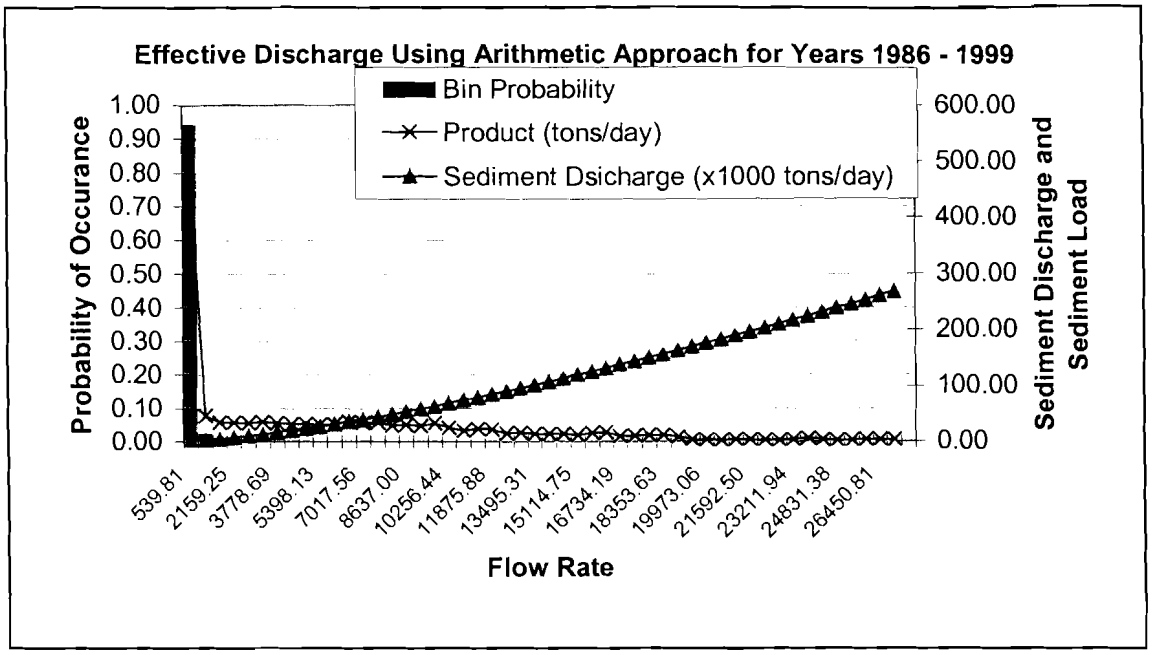

Figure C.21 – Hickahala 22 DEC (arithmetic bins)

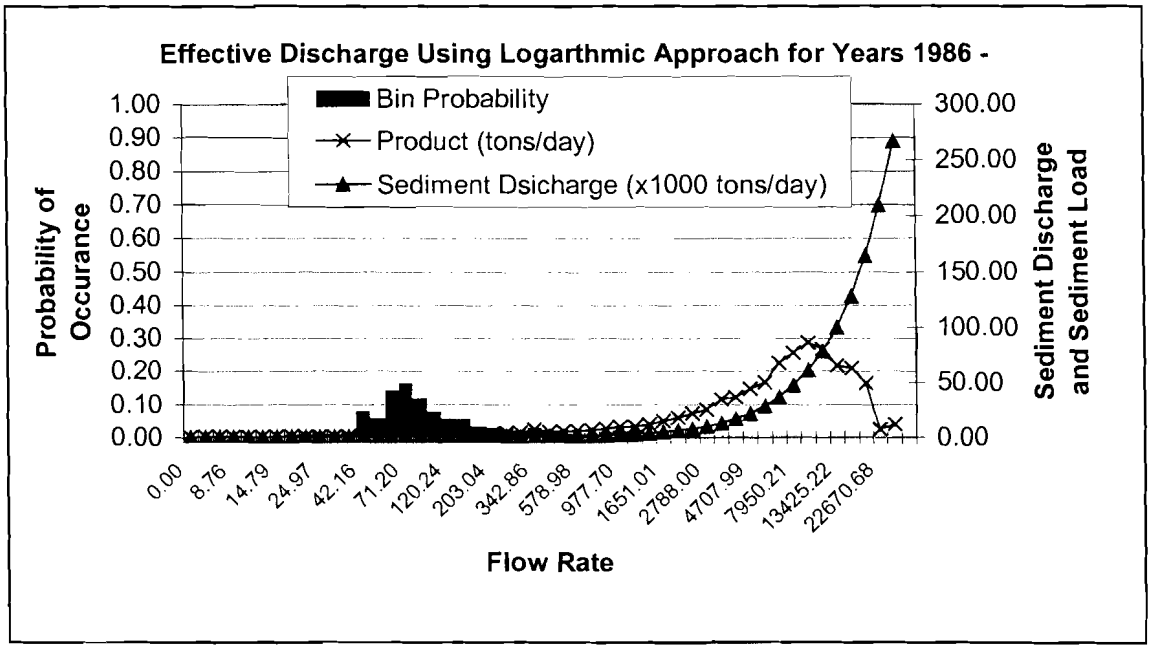

Figure C.22 – Hickahala 22 DEC(logarithmic bins)

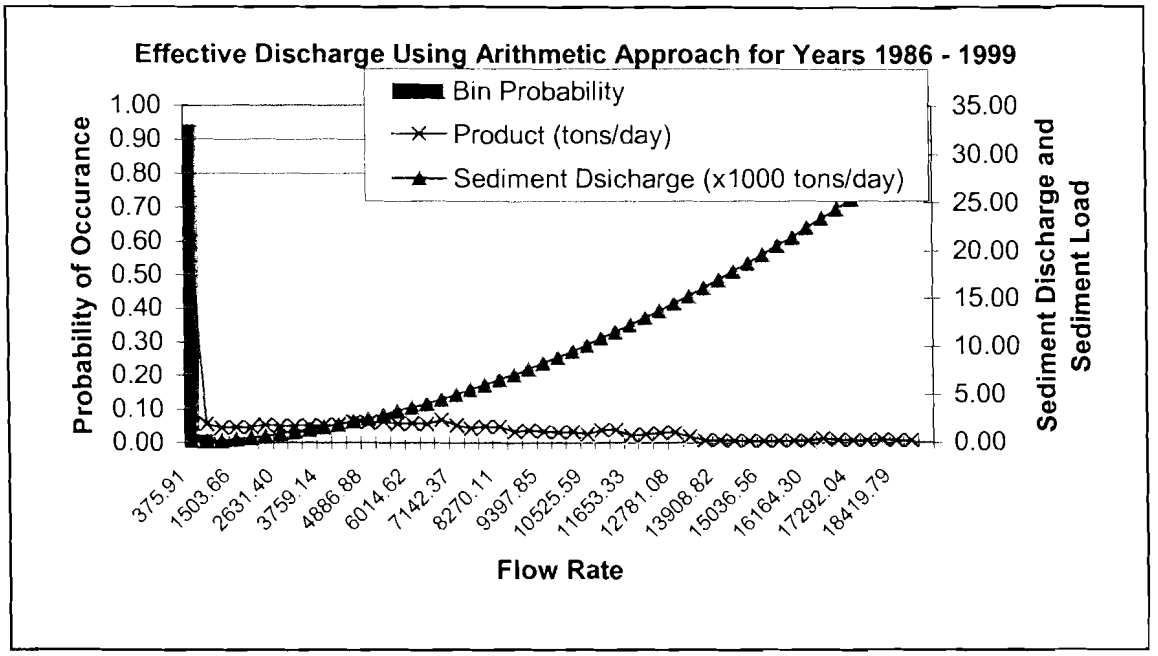

Figure C.23 – Hickahala near Senatobia (arithmetic bins)

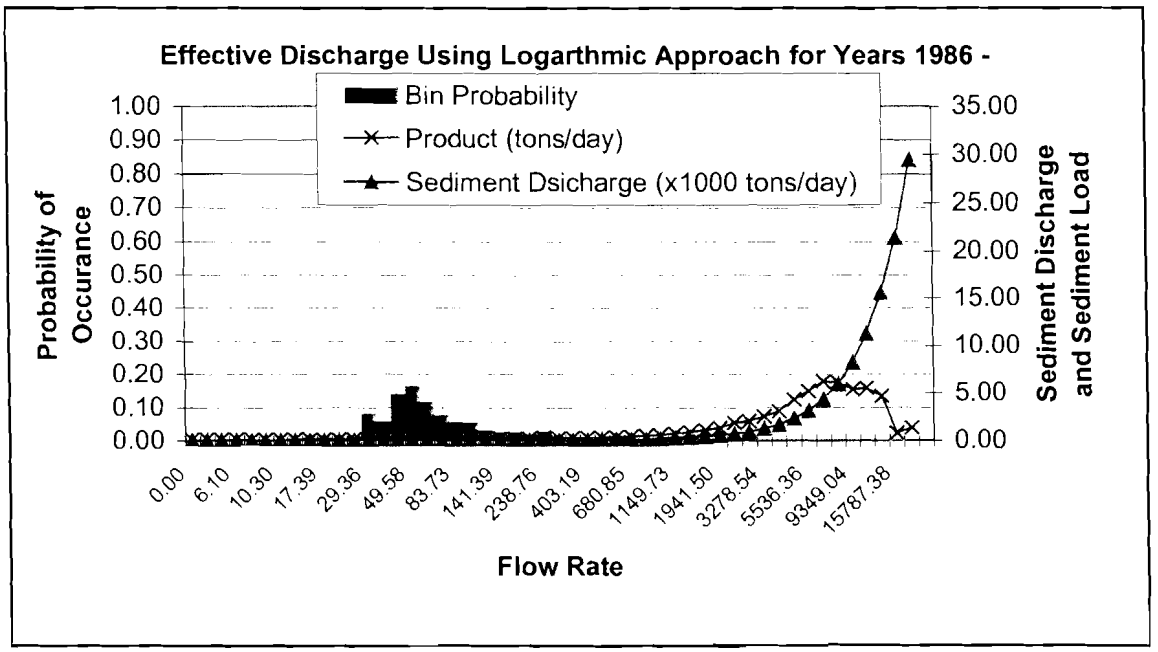

Figure C.24 – Hickahala near Senatobia (logarithmic bins)

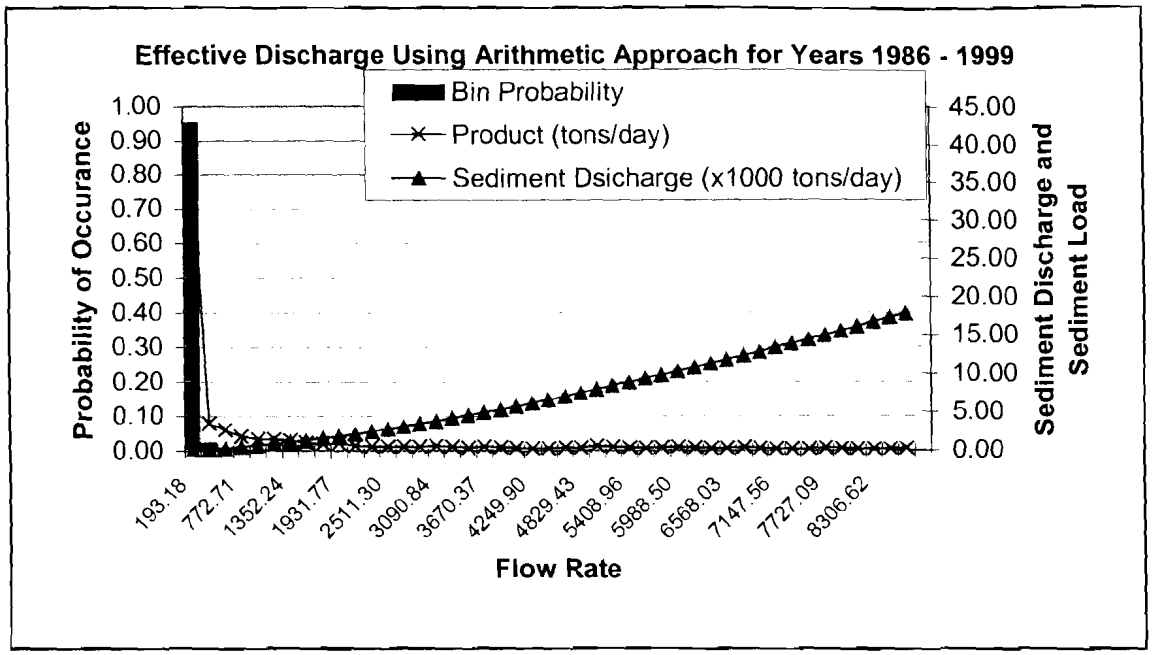

Figure C.25 – Hotopha DEC (arithmetic bins)

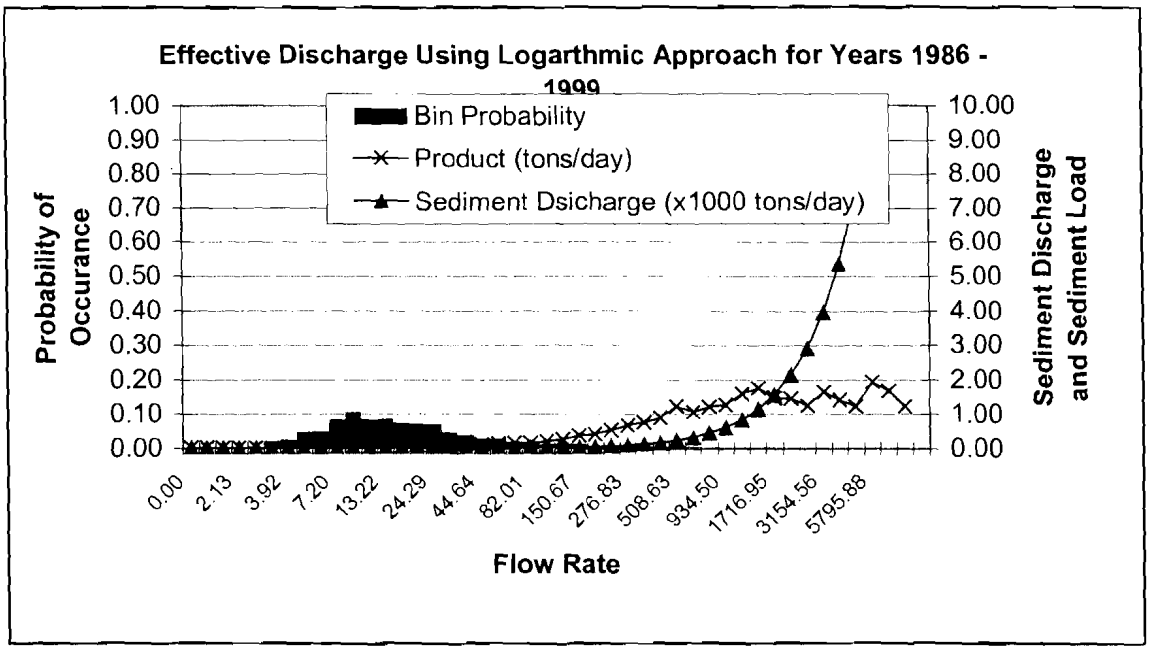

Figure C.26 – Hotopha DEC (logarithmic bins)

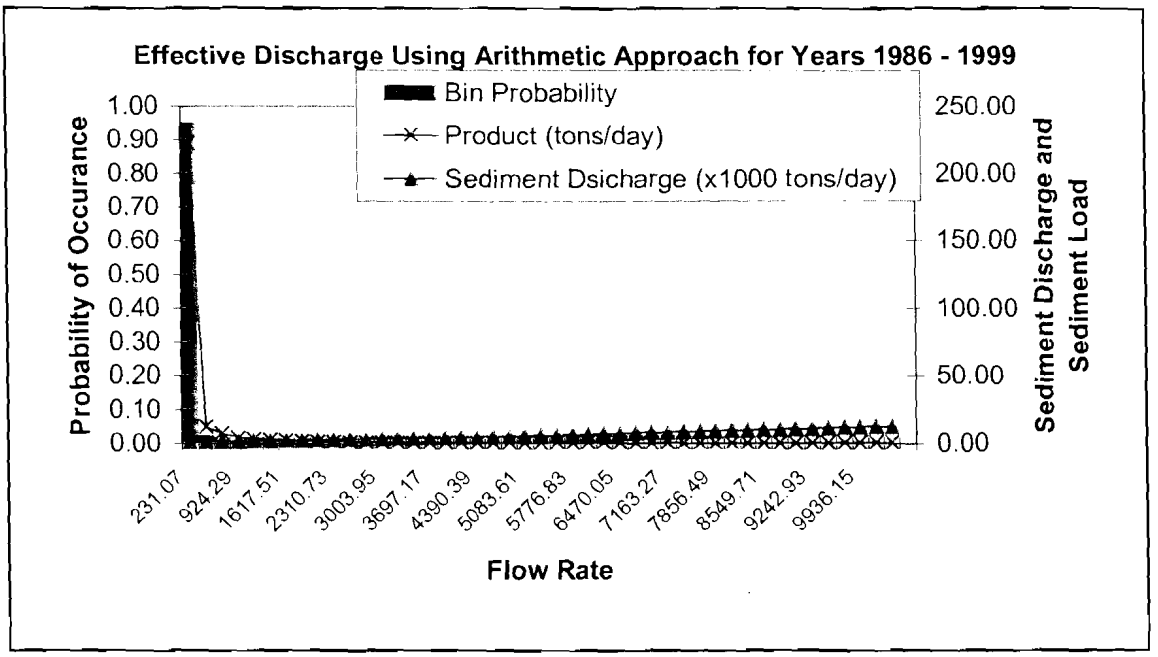

Figure C.27 – Hotopha near Batesville (arithmetic bins)

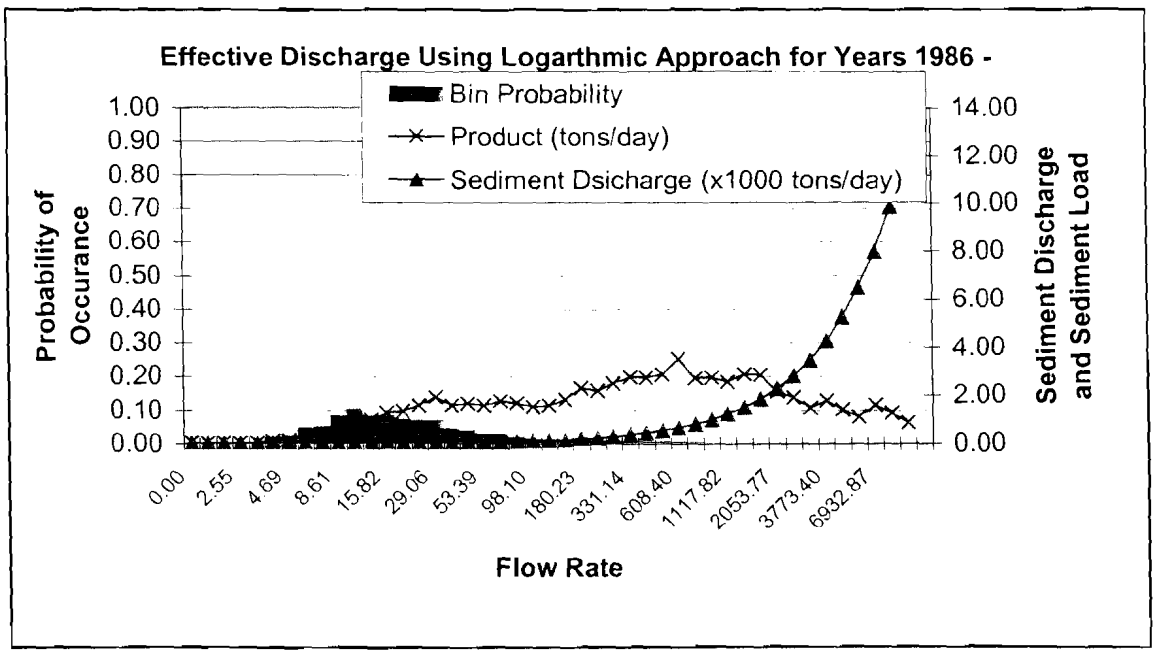

Figure C.28 – Hotopha near Batesville (logarithmic bins)

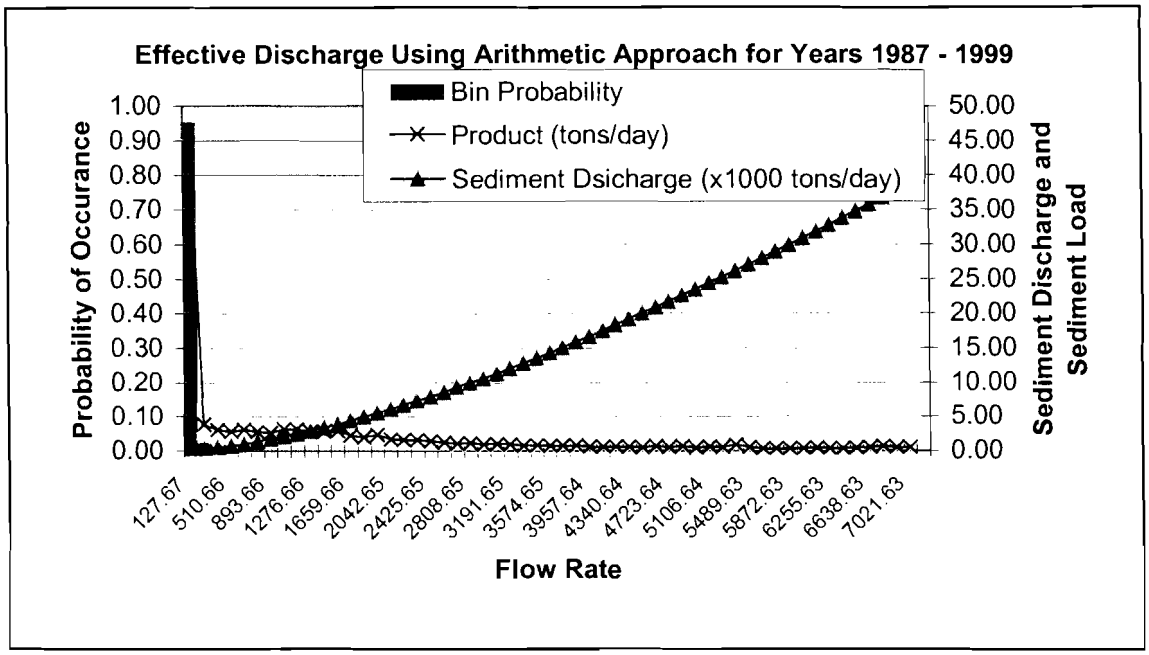

Figure C.29 – Long DEC (arithmetic bins)

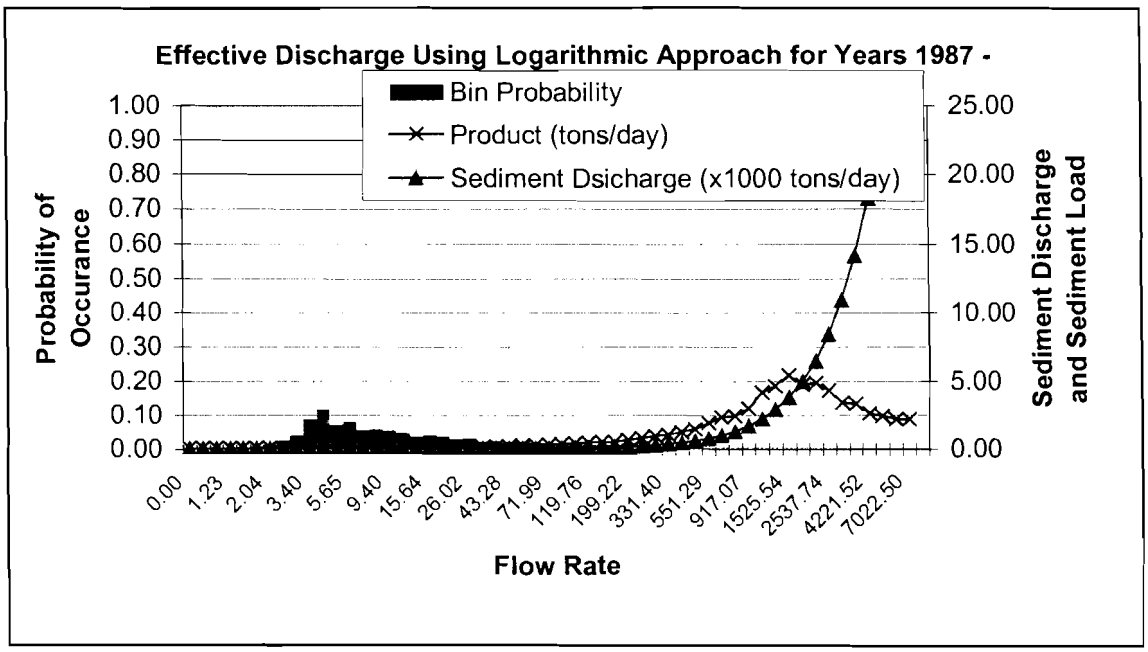

Figure C.30 – Long DEC (logarithmic bins)

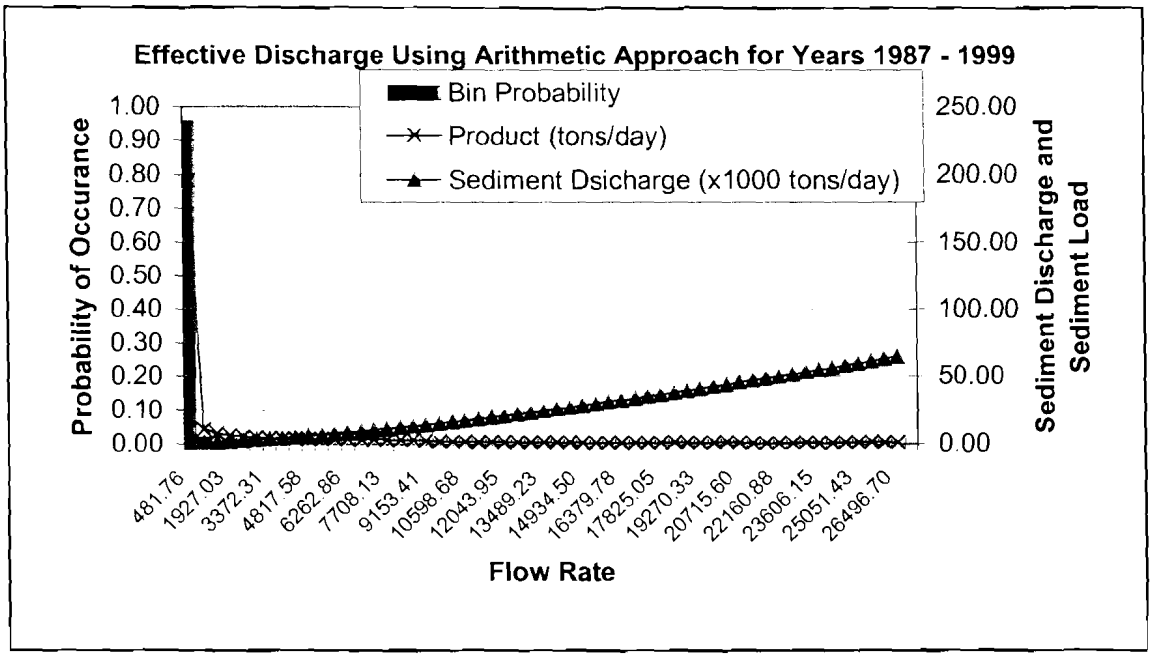

Figure C.31 – Long near Pope (arithmetic bins)

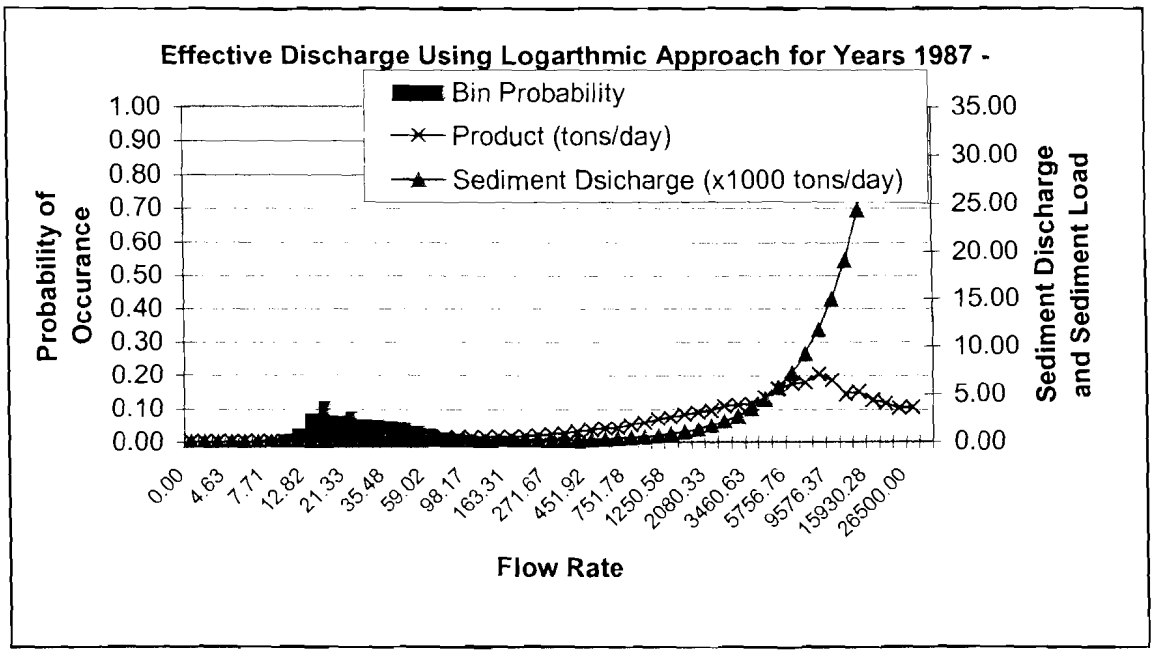

Figure C.32 – Long near Pope (logarithmic bins)

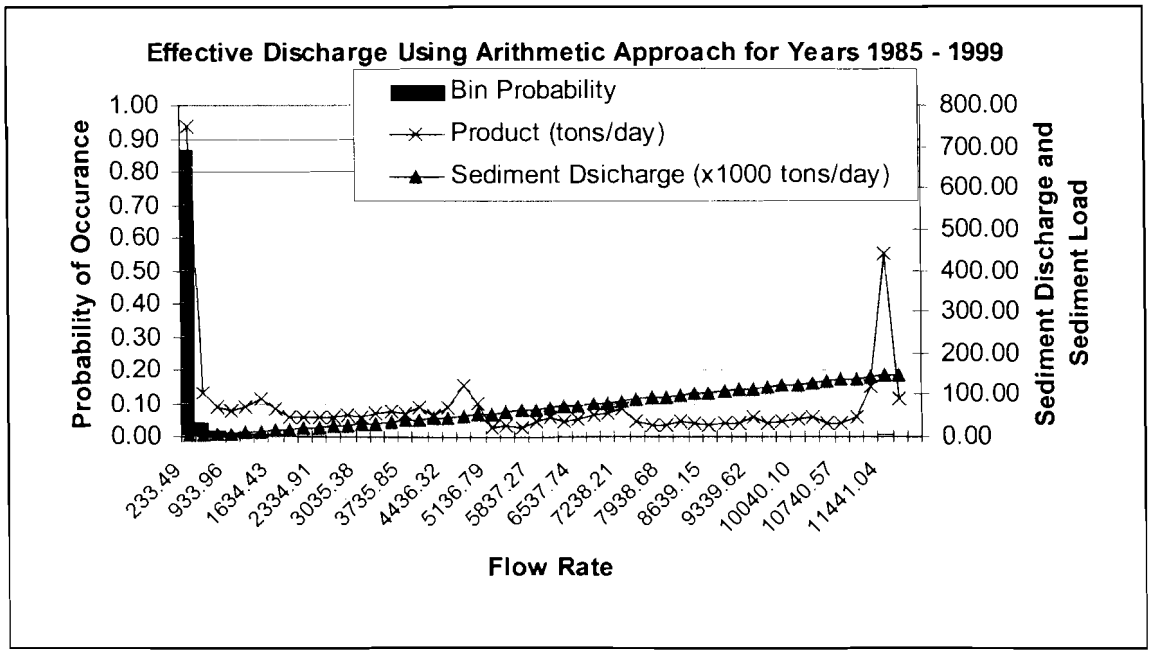

Figure C.33 – Otoucalofa DEC (arithmetic bins)

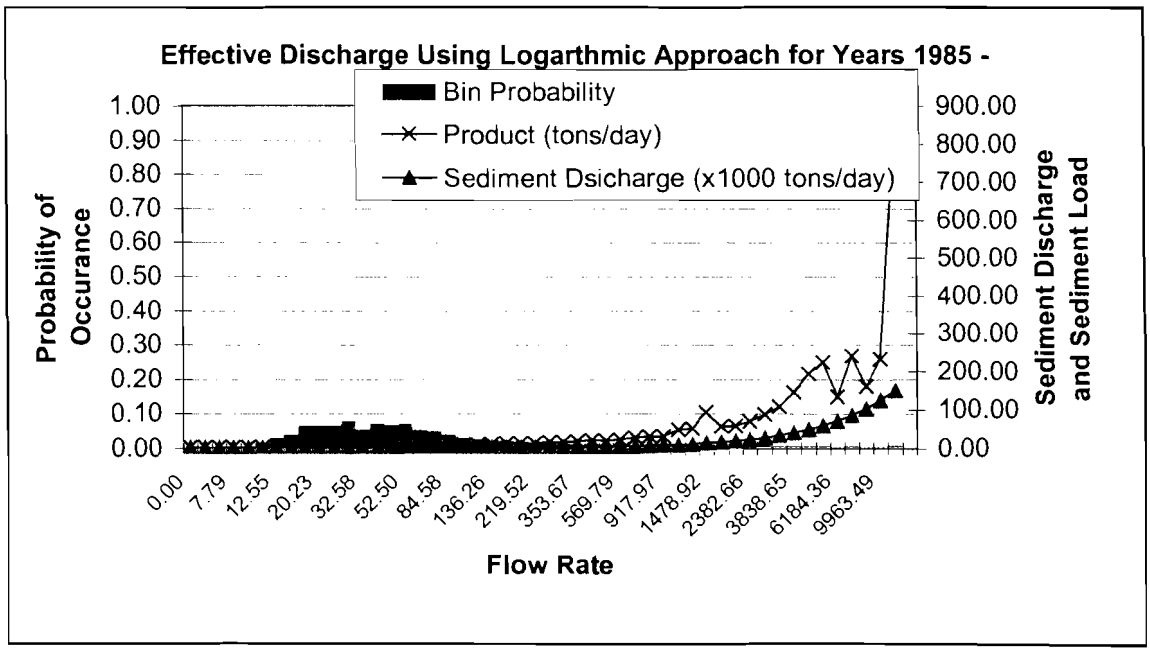

Figure C.34 – Otoucalofa DEC (logarithmic bins)

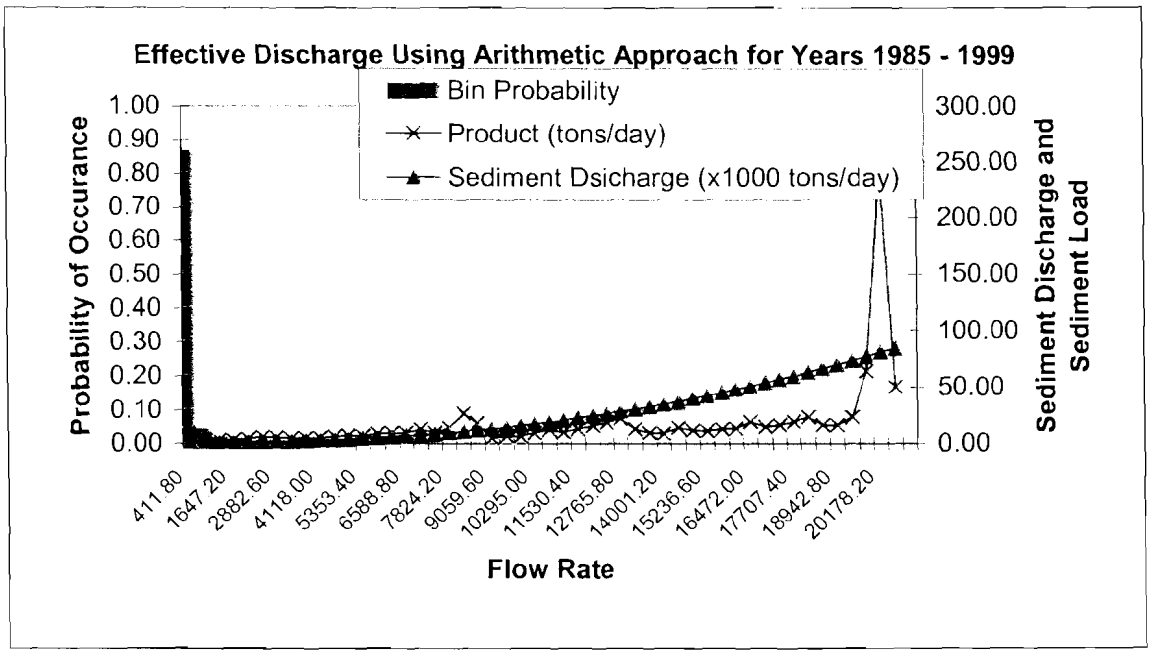

Figure C.35 – Otoucalofa near Water Valley (arithmetic bins)

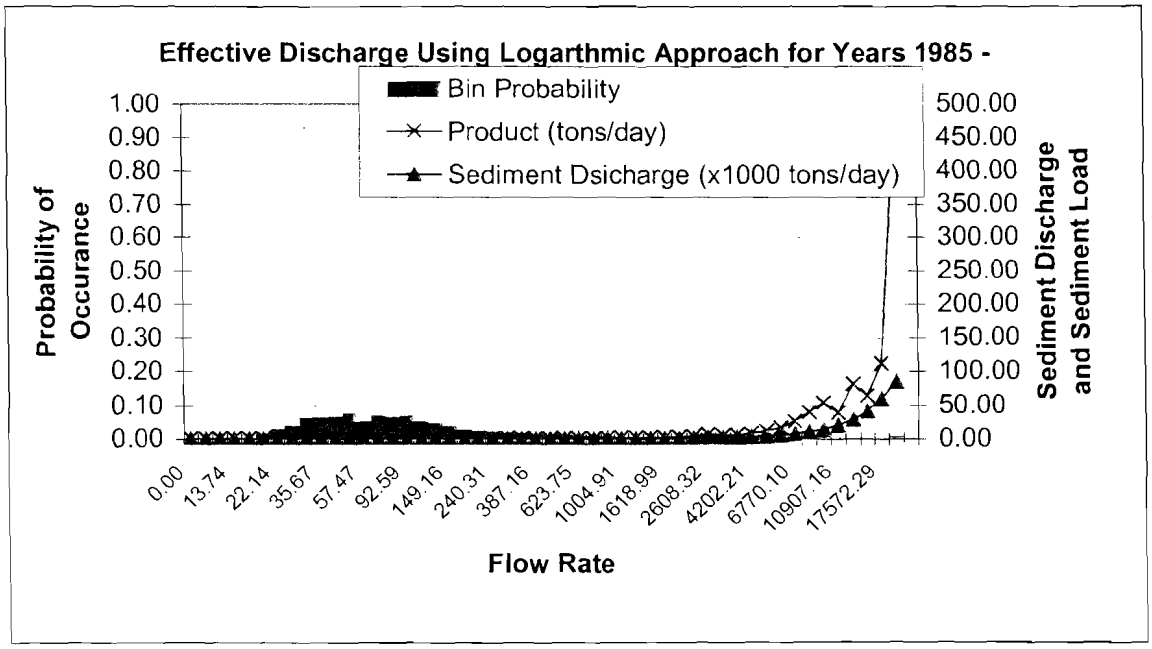

Figure C.36 – Otoucalofa near Water Valley (logarithmic bins)

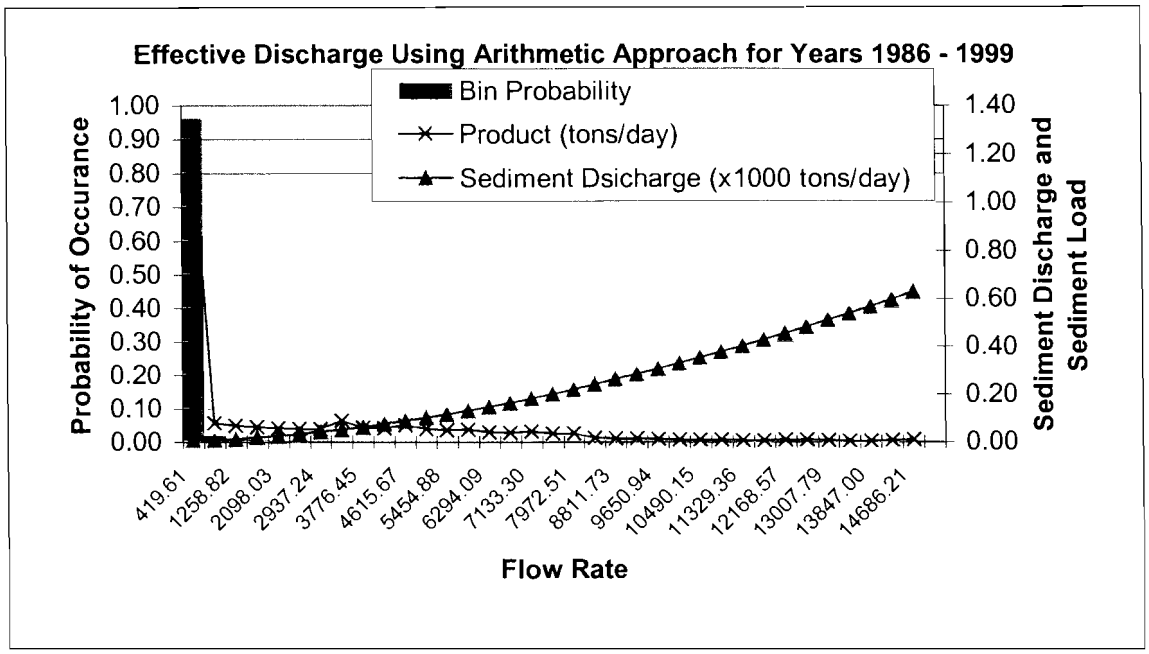

Figure C.37 – Senatobia DEC (arithmetic bins)

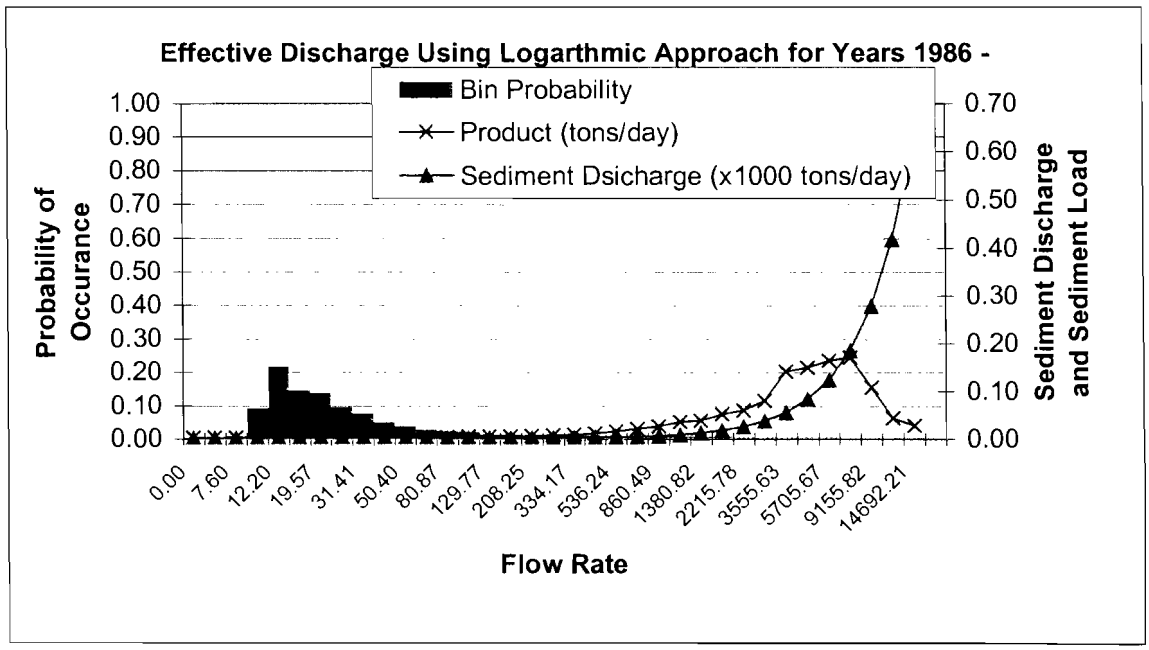

Figure C.38 – Senatobia DEC (logarithmic bins)

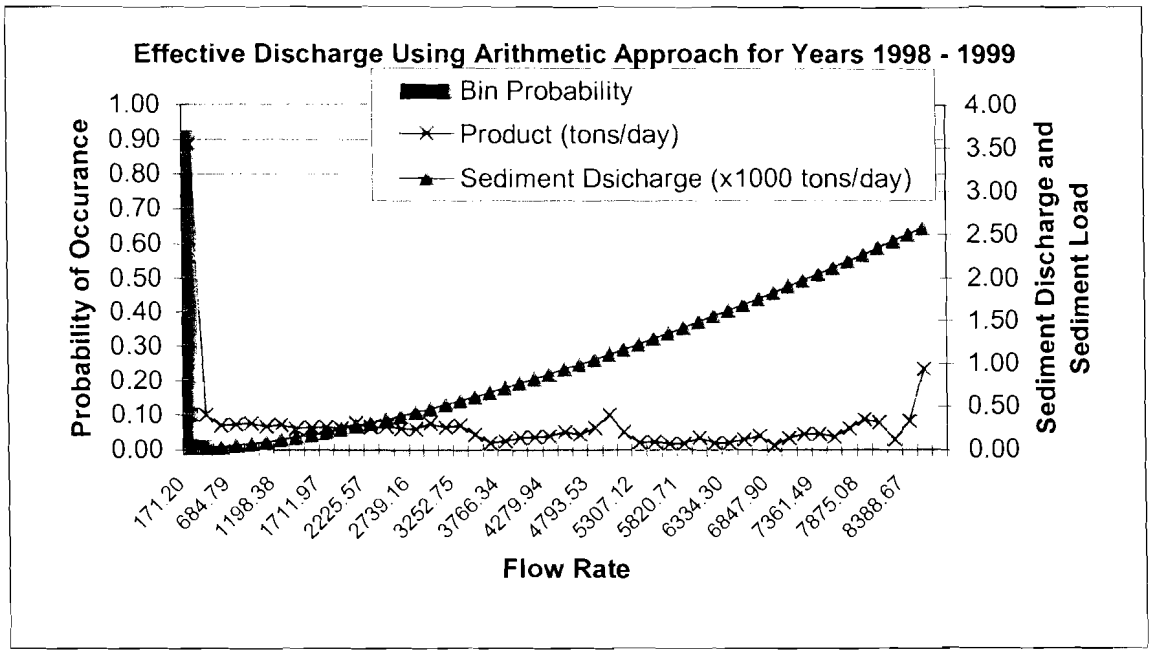

Figure C.39 – Topashaw near Derma (arithmetic bins)

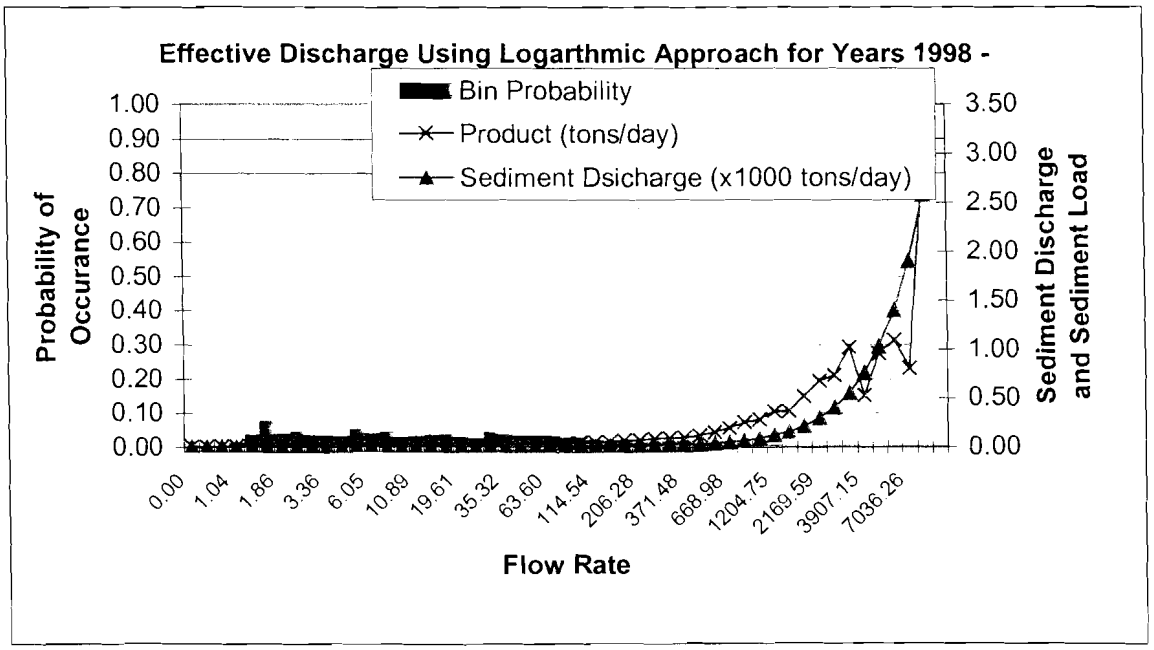

Figure C.40 – Topashaw near Derma (logarithmic bins)

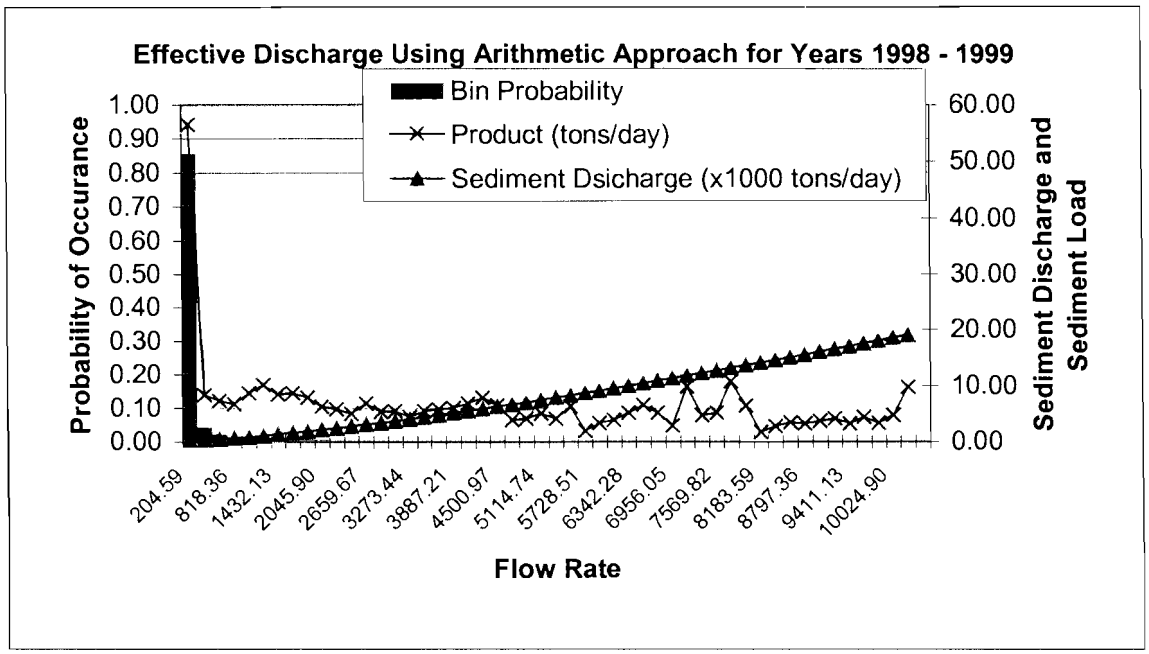

Figure C.41 – Yalobusha near Derma (arithmetic bins)

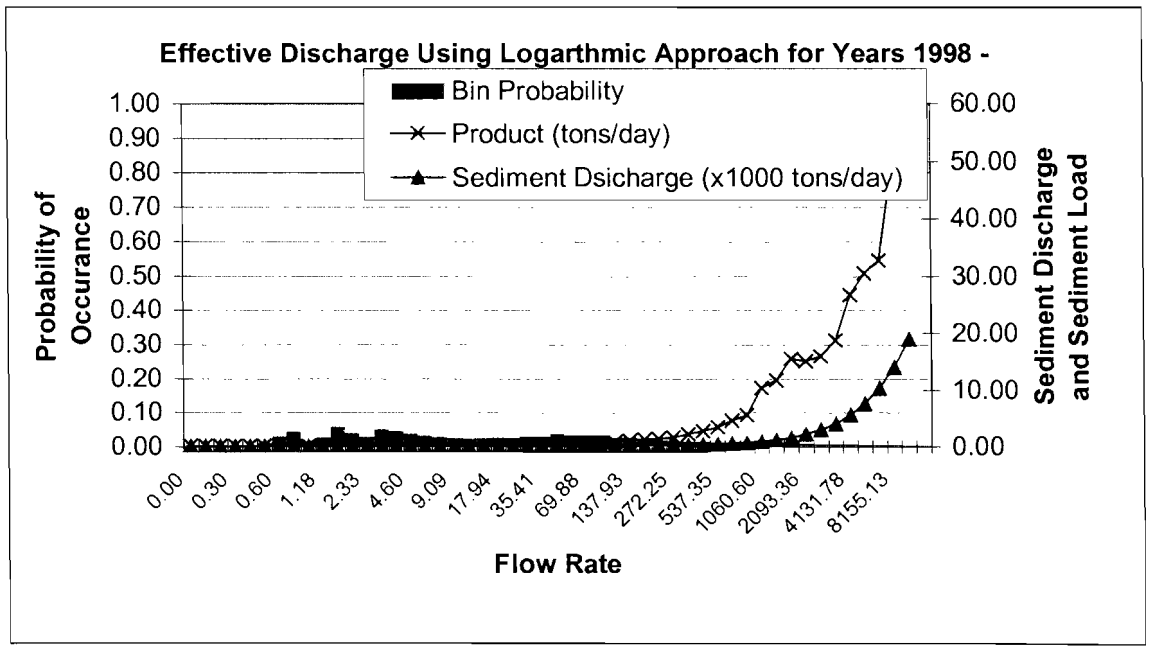

Figure C.42 – Yalobusha near Derma (logarithmic bins)

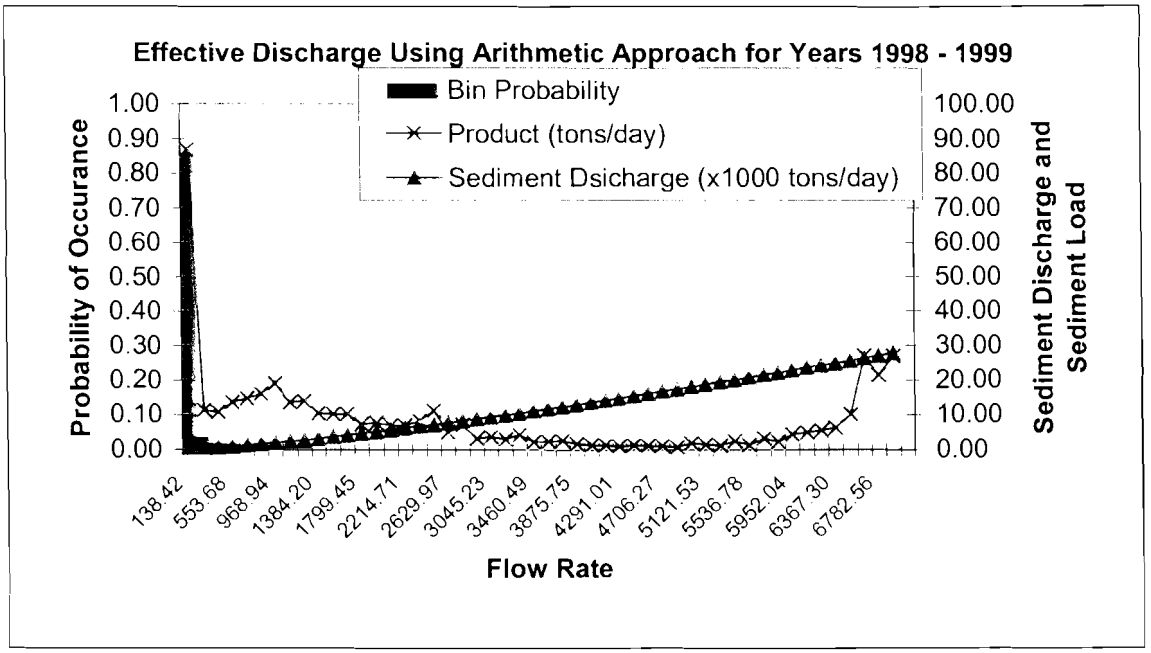

Figure C.43 – Yalobusha near Vardaman (arithmetic bins)

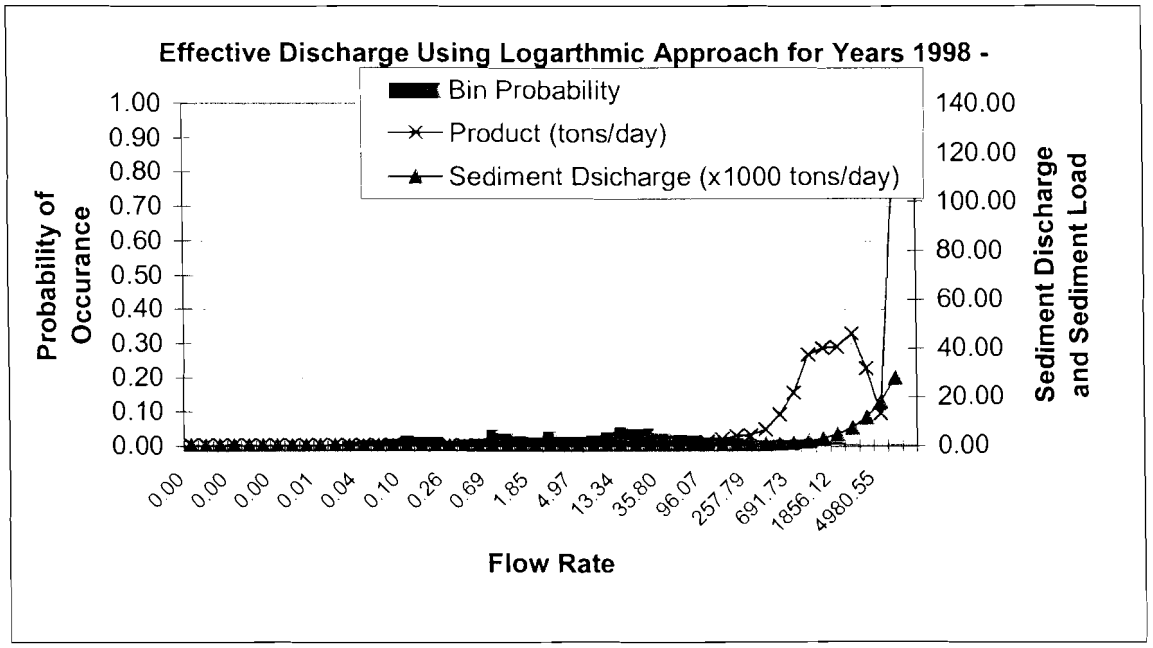

Figure C.44 – Yalobusha near Vardaman (logarithmic bins)

APPENDIX D

Effective Discharge Program Inputs

Table D.1 – Inputs for Effective Discharge Program

USGS Gage# used	Station Name	Qs = aQ^b (all years) a	b	R^2	N	Range of Q for Q_s Equation High Discharge	Low Discharge	Observed Critical Discharge	Energy Slope	Grain Size d_{50}
	DEQ or USGS location					(cfs)	(cfs)	(cfs)	(ft/ft)	(mm)
7287301 Yang	Abacus 3							75	0.00119	0.26
7287300 Yang	Abacus 4							75	0.00189	0.48
Observed	7287150	0.0028	2.11	0.8712	75	3210	28	75		
Pump	Abacus	0.0129	1.7502	0.905	3685	5570	3.8			
bed		0.0081	1.6067	0.9755	5	3210	142			
Yang									0.000697	0.5
Observed	7287100	0.0028	2.0898	0.916	77	2180	28	75		
Pump	Abacus 21	0.0061	1.8926	0.8895	2723	3550	21.5			
bed		0.0046	1.4923	0.309	6	2180	417			
Yang									0.000301	0.35
Observed	7285400	1.3458	1.1451	0.8799	6	21200	1040			
Pump	Batupan Bogue	0.0076	1.6146	0.7609	6075	30400	17			
bed		0.2081	1.1922	0.686	6	21200	1040			
Observed	7287355	0.0024	2.006	0.7849	80	2200	14	40		
Pump	Fannegusha @Howard	0.0032	2.01	0.9493	991	7610	7			
7287350 Yang	Fannegusha							40	0.001416	0.31
Observed	7287404	0.0099	2.0322	0.8964	82	4130	9.4	25		
Pump	Harland @Howard	0.0107	1.8851	0.9126	5973	6490	6			
bed		1.3512	0.0073	0.587	3	4130	1060			
7287404 Yang	Harland 1							25	0.00134	0.5
7287406 Yang	Harland 23							25	0.00102	0.5
Observed	7277700	0.0079	1.7557	0.9445	108	16000	32	35		
Pump	Hickahala @Senetobia	0.0076	1.7601	0.8536	5557	18000	9			
bed		0.0004	1.8405	0.7192	11	16000	1910			
7277700 Yang	Hickahala 11							35	0.00195	0.51
7277700 Yang	Hickahala 22							35	0.00089	0.41

Observed	7273100	0.0054	1.992	0.958	7	1840	14	7		
Pump	Hotopha @Batesville	0.0297	1.4924	0.8392	4739	9310	2			
bed		0.8178	1.0382	0.716	6	1840	260			
7273100 Yang	Hotopha							7	0.000782	0.31
Observed	7274252	0.0031	1.8265	0.9543	91	16300	25	30		
Pump	Otoucalofa @Water Valley									
bed		0.00001	2.3005	0.921	5	16300	219			
7274252 Yang	Otoucalofa							30	0.00178	0.39
Observed	7275530	0.01	1.7717	0.969	10	17000	19	30		
Pump	Long @Pope	0.0031	1.9597	0.9515	4256	25100	4			
bed		0.0283	1.437	0.698	9	17000	656			
7275530 Yang	Long							30	0.00107	0.38
Observed	7277730	0.1792	1.0319	0.9901	8	9720	37	35		
Pump	Senetobia	0.009	1.8123	0.9	2473	11200	7.1			
bed		0.00004	1.7263	0.9981	3	9720	276			
Yang									0.00144	0.41
Pump	7282090	0.0846	1.4471	0.9356	304	8452	1	40		
Yang	Topashaw @Derma								0.00055	0.17
Pump	7281977	0.1078	1.2778	0.9515	239	9425	1			
Yang	Yalobusha @Derma								0.001167	0.18
7281960 Yang	Yalobusha @Vardaman								0.001379	0.28

Table D.2 – Channel coefficients for use with SedTrans Program

Station Name	$R = cQ^d$ (reach avg) c	d	Over Bank Discharge
Abiaca 3	0.37	0.36	1375
Abiaca 4	0.10	0.51	950
Abiaca 6	0.16	0.46	1525
Abiaca 21	0.36	0.35	625
Fannegusha DEC	0.28	0.39	3500
Harland 1	0.18	0.44	3025
Harland 23	0.27	0.39	2150
Hickahala 11	0.22	0.41	2750
Hickahala 22	0.16	0.45	6000
Hotopha DEC	0.40	0.35	8000
Otoucalofa DEC	0.33	0.38	2900
Long DEC	0.17	0.44	1225
Senetobia	0.17	0.44	7750
Topashaw @ Derma	0.62	0.33	9500
Yalobusha @ Derma	0.61	0.31	10000
Yalobusha @ Vardaman DEC	0.44	0.34	3700

APPENDIX E

Effective Discharge and Q2 Cross-Section Plots

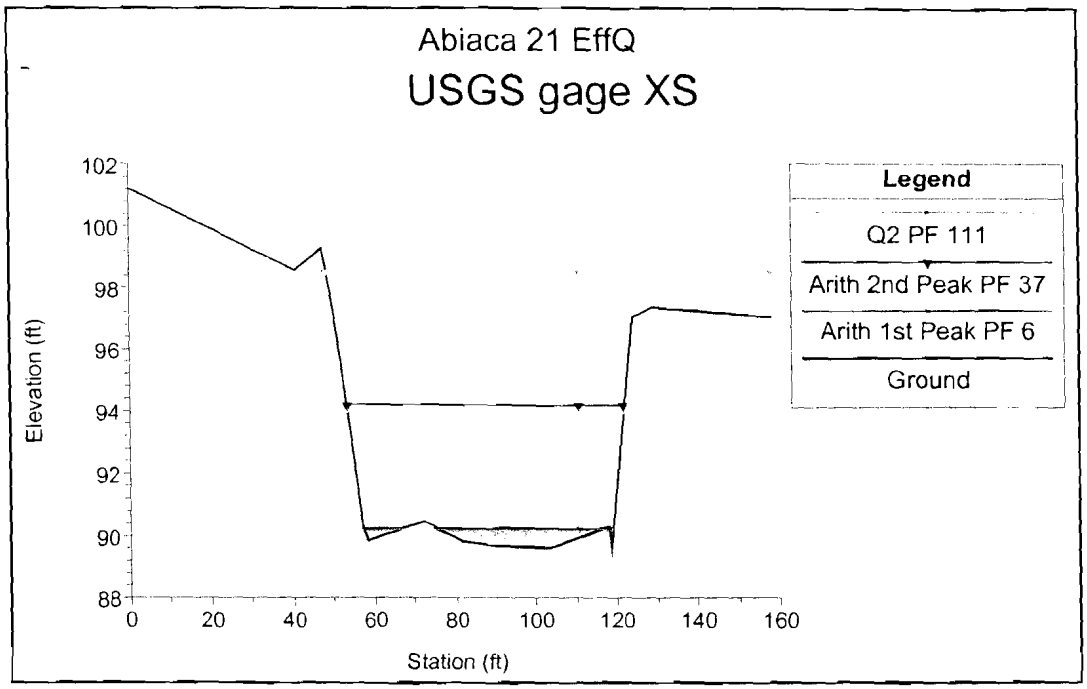

Figure E.1 – Abiaca 21 near Cruger

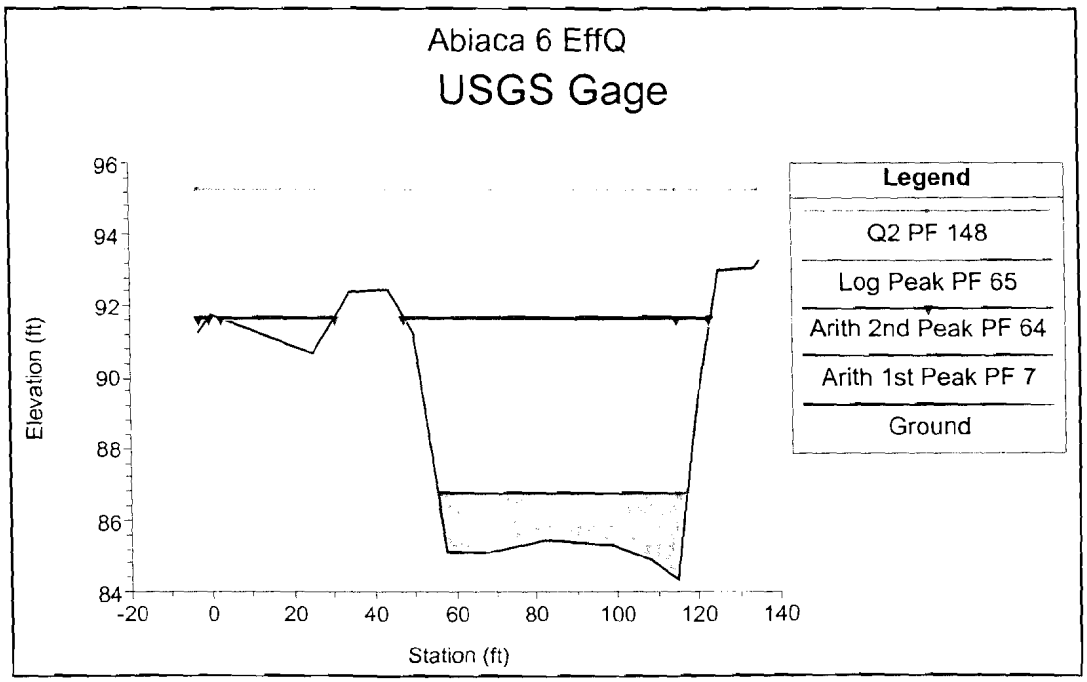

Figure E.2 – Abiaca 6 near Seven Pines

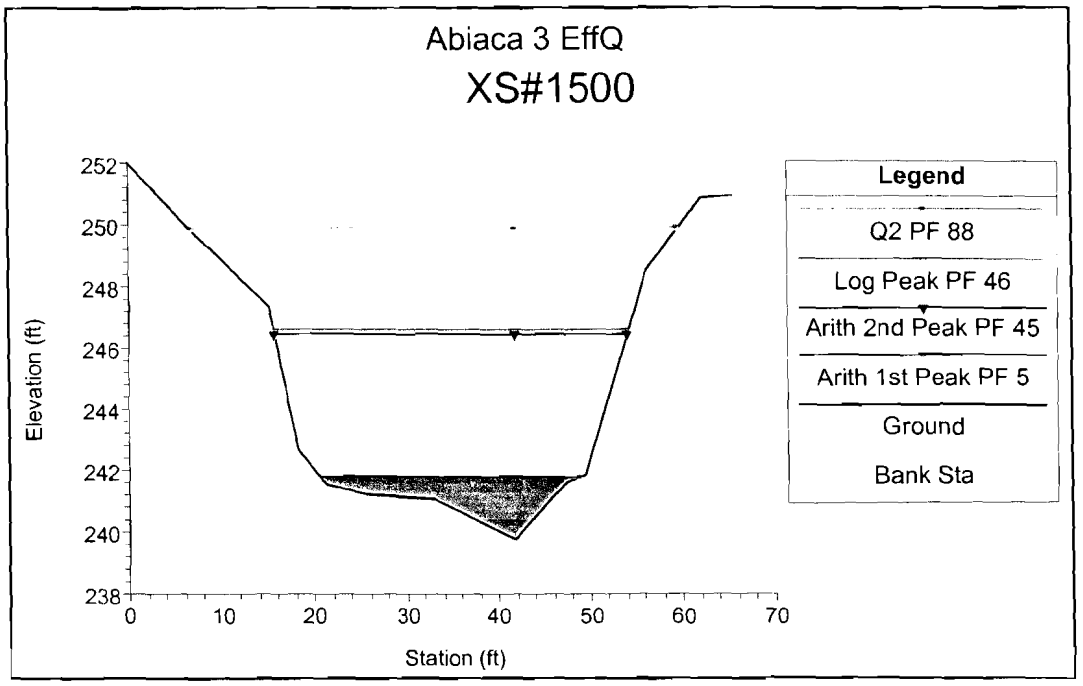

Figure E.3 – Abiaca 3

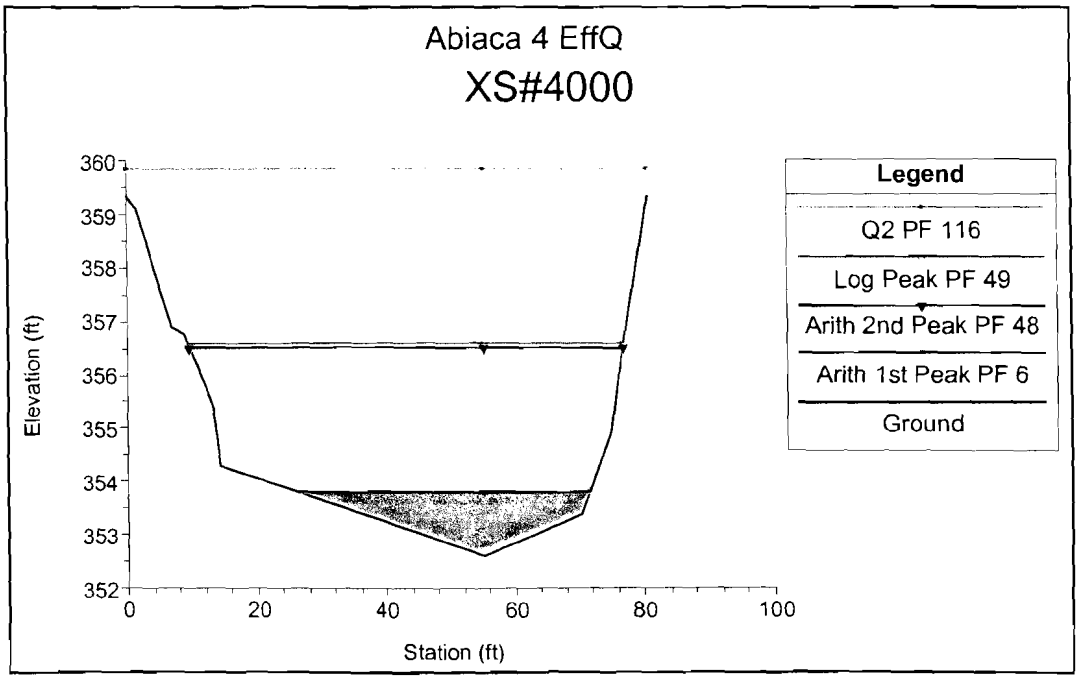

Figure E.4 – Abiaca 4

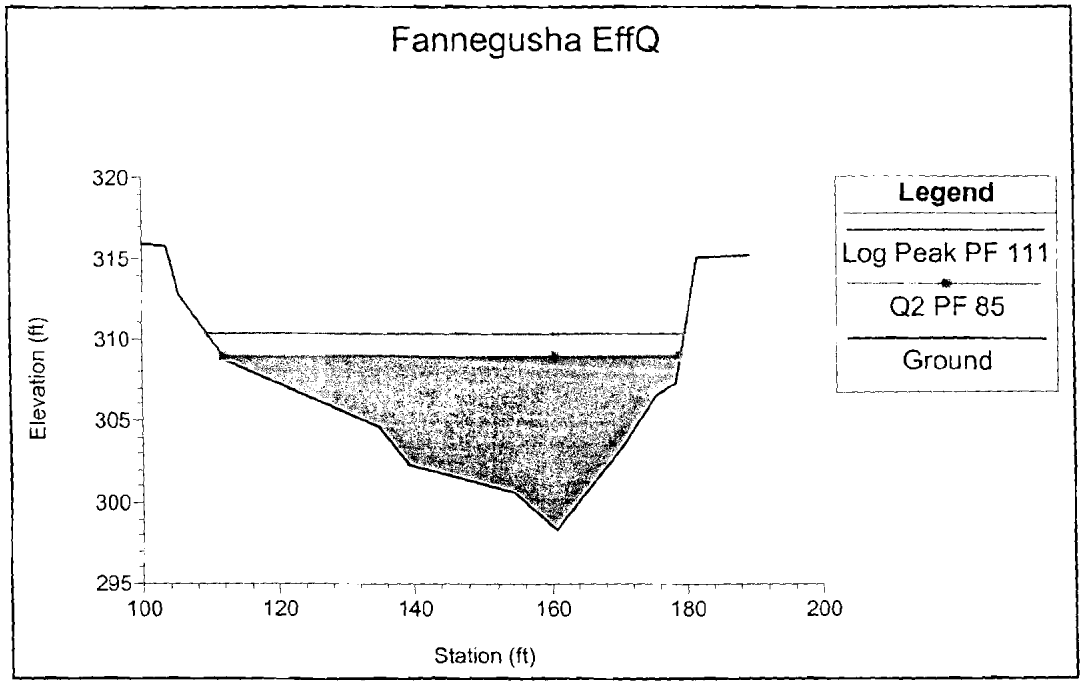

Figure E.5 – Fannegusha Dec

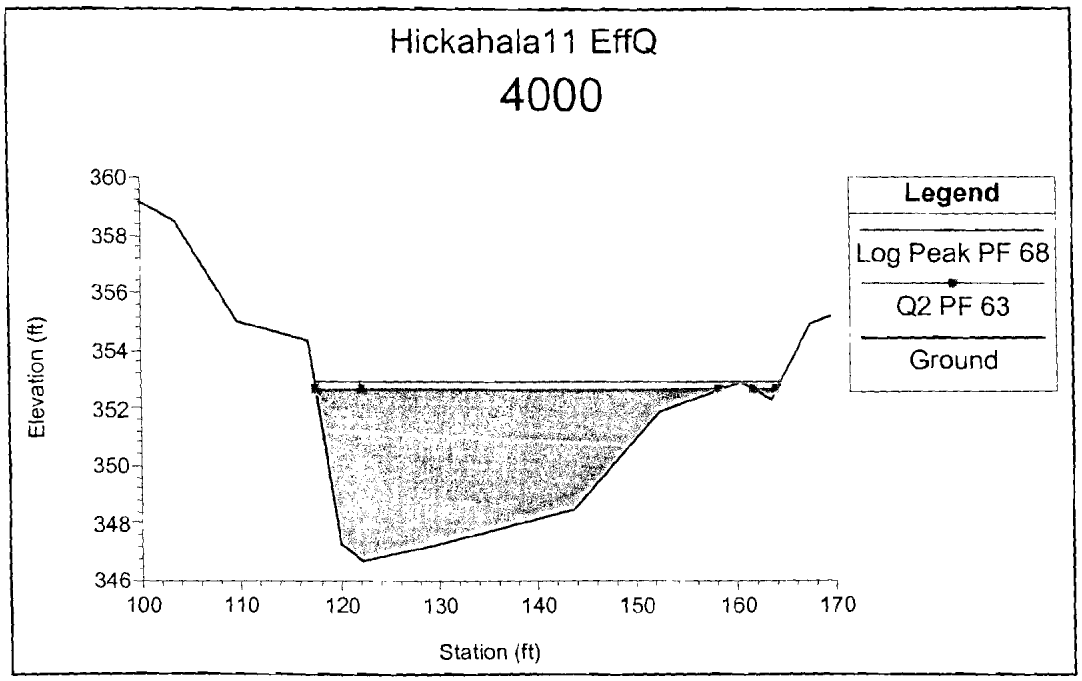

Figure E.6 – Hickahala 11

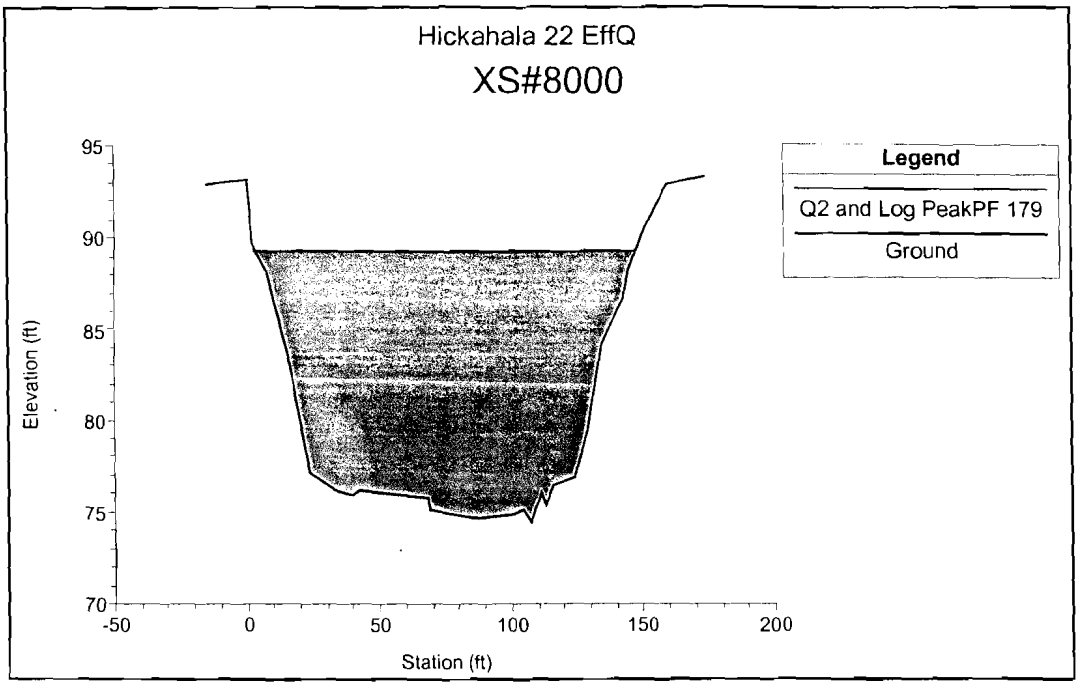

Figure E.7 – Hickahala 22

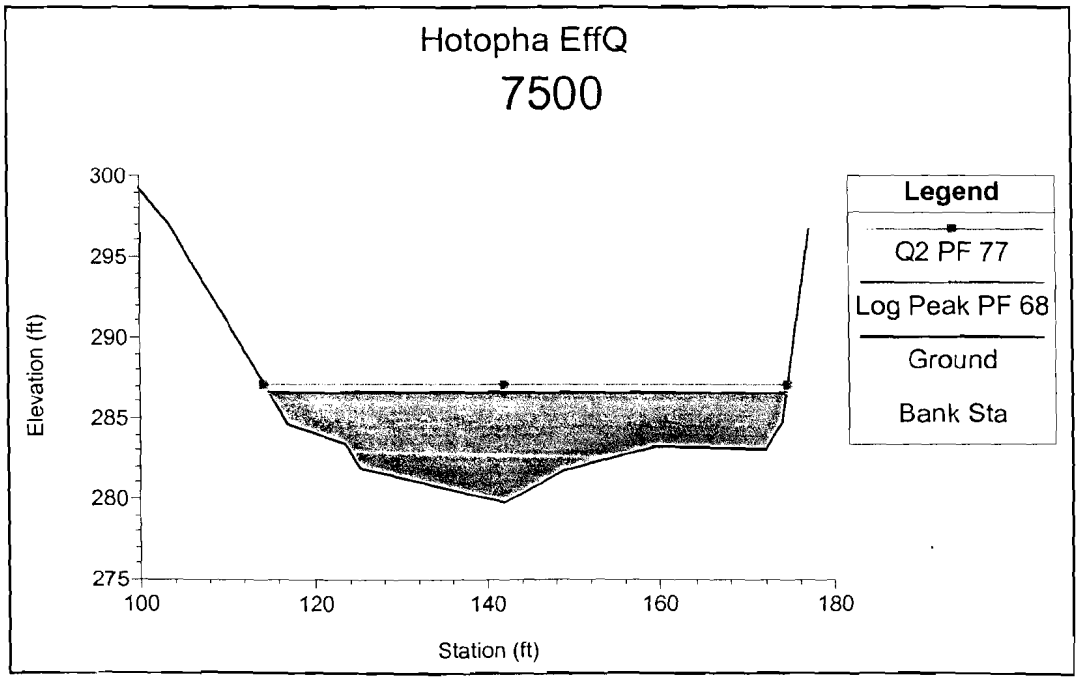

Figure E.8 – Hotopha Dec

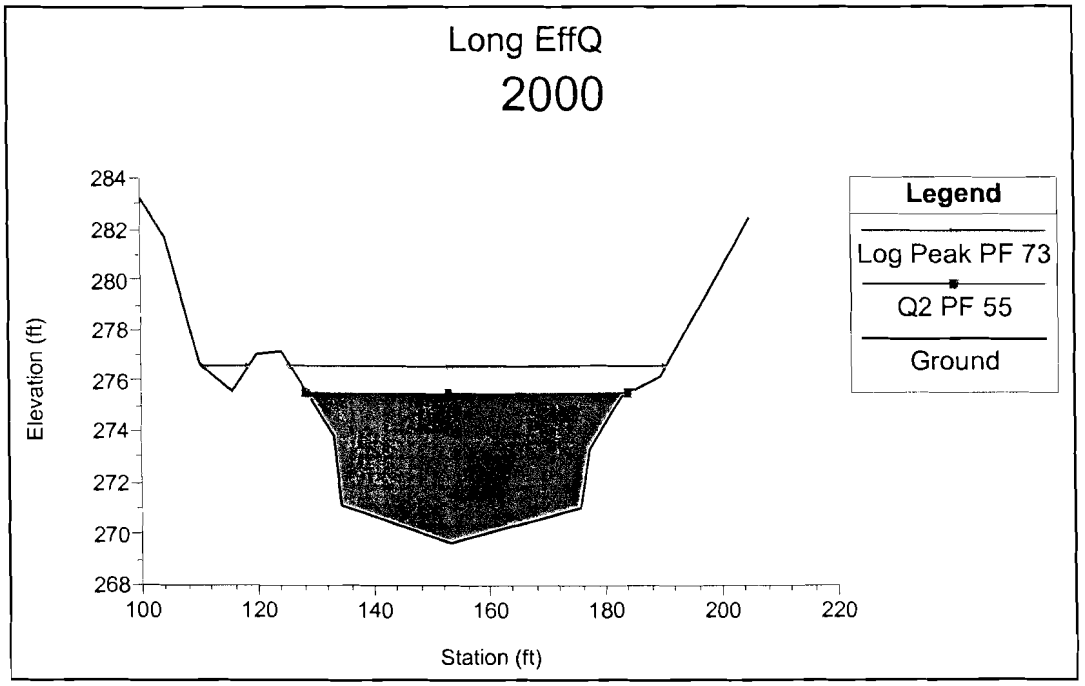

Figure E.9 – Long Dec

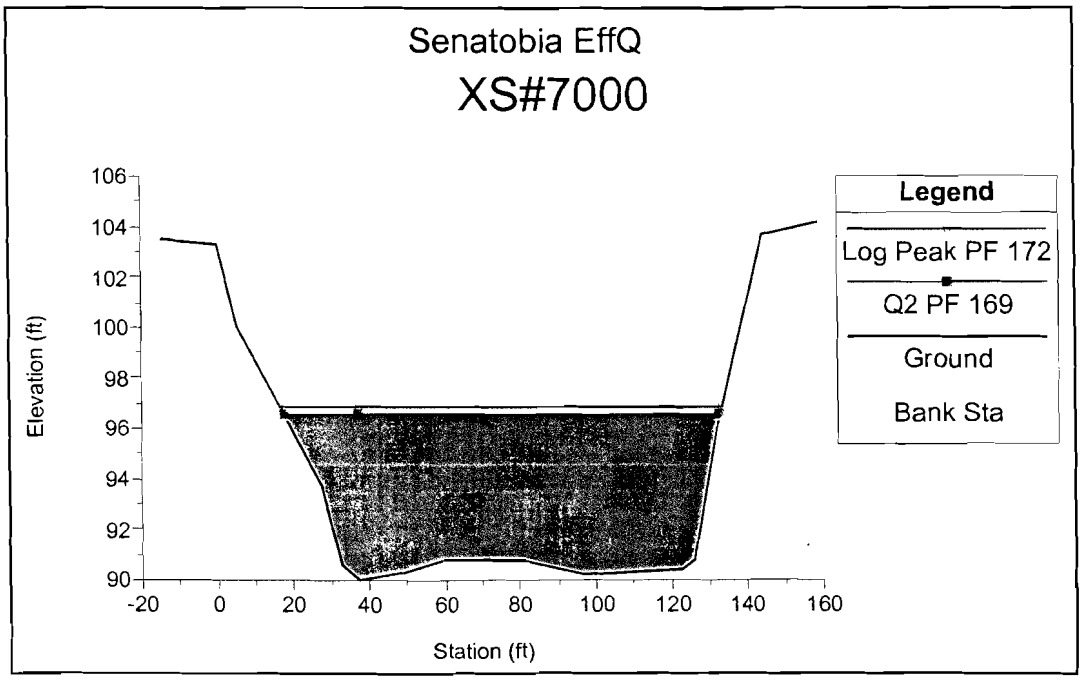

Figure E.10 – Senatobia at Senatobia